MINISTRY OF EDUCATION AND SCIENSE
AL-FARABI KAZAKH NATIONAL UNIVERSITY
DEPARTMENT OF PHYSICS AND TECHNOLOGY

PHYSICS OF NONIDEAL PLASMAS

Educational manual

T.S. Ramazanov, M.T. Gabdullin

Almaty
"Qazaq university"
2016

UDC 533.9
LBC -22.333
R 19

Reviewers:
Doctor of physical and mathematical sciences, professor K.A. Zhaksibekova
PhD E.I. Imangaliyev
PhD Ye.A. Daineko

Ramazanov T.S.
Physics of Nonideal Plasmas: educational manual / T.S. Ramazanov, M.T. Gabdullin. – Almaty: Qazaq university, 2016. – 106p.
ISBN 978-601-04-1732-8

In the course “Physics of Nonideal plasmas” many different states of plasma, such as classical and semiclassical, weakly and strongly nonideal, fully and partially ionized will be considered. The basic theoretical methods of studying structural and thermodynamic properties, optical and transport properties of nonideal plasma by the effective potentials will be studied.

В курсе "Физика неидеальной плазмы" рассматривается плазма в различных состояниях, таких как классическая и квазиклассическая, слабо и сильно неидеальная, полностью и частично ионизированная плазма. Основные теоретические методы исследования структурных и термодинамических свойств, оптических и транспортных свойств неидеальной плазмы с помощью эффективных потенциалов исследованы.

UDC 533.9
LBC 22.333

The purposes and tasks of the course are studying of properties of nonideal plasmas on the basis of different theoretical methods. Students have to solve concrete tasks in physics of plasmas and to assist in their discussions.

The tasks of study of the discipline:

- To understand the basis of theoretical methods used in investigation ionization equilibrium and properties for nonideal plasmas;
- To obtain basic knowledge about fundamental problems in nonideal plasma physics and its applications;
- To learn different types of plasma and methods of calculations;
- To choose the model of interaction between particles, taking into account different effects (screening effects, quantum mechanical effects of diffraction and symmetry, degeneration and etc.);
- To apply the obtained knowledge for the analysis of concrete physical phenomena.

The author would like to thank L.E. Strautman and T.N. Ismagambetova for their help in the process of proofreading and editing.

CONTENTS

LECTURE 1

Basic Concepts of Nonideal Plasma. Effective potentials for fully ionized plasma.

Introduction

It is well known that at low densities plasma can be considered as a mixture of ideal gases of electrons, atoms and ions. In this case the particles move along straight lines and sometimes collide with other particles. With increase of plasma density the average distances between particles decrease and particle's interacting time increases, therefore, the average potential energy increases. If this energy gets to be comparable with average kinetic energy of thermal motion, i.e. $\bar{U} \approx \bar{E}_{kinetic}$, the plasma becomes **nonideal.** It should be noted that properties of such plasma cannot be described by traditional methods of theoretical physics. The interaction between particles in fully ionized plasma can be described by long-range Coulomb potential. In the case of complex plasma consisting of electrons, ions, atoms, molecules, clusters, etc., different interaction potentials should be used.

Interparticle Interactions and Criteria of Nonideality

The ratio between the average interaction potential energy of particles and the mean thermal energy $k_B T$ is used as a criterion of nonideality of a plasma. For nondegenerate singly ionized plasma this condition can be written by coupling (nonideality) parameter Γ:

$$\Gamma = \frac{e^2}{a k_B T}, \tag{1.1}$$

where a is the average distance between particles related to the plasma density by the following simple relation:

$$(4/3)\pi n_e a^3 = 1. \tag{1.2}$$

In the case of multiple ionized plasma the different nonideality parameters for ion–ion, ion–electron, and electron–electron interactions should be used. For example, in fully ionized plasma with ions having charge number Z we have the following relations:

$$\Gamma_{ZZ} = \frac{Z^{5/3}e^2}{ak_BT} = Z^{5/3}\Gamma_{ee};$$
$$\Gamma_{Ze} = \frac{Z^{2/3}e^2}{ak_BT} = Z^{2/3}\Gamma_{ee}; \qquad (1.3)$$
$$\Gamma_{ee} = \frac{e^2}{ak_BT}.$$

It should be noted that coupling parameters (1.1) and (1.3) can be applied for semiclassical dense plasma. For description of classical plasma the following **nonideality parameter** is usually used:

$$\gamma = \frac{Z_1 Z_2 e^2}{r_D k_B T}, \qquad (1.4)$$

where r_D is the Debye screening radius. Thus, we can consider the following types of plasma using mentioned parameters:

- Ideal plasma (at $\Gamma, \gamma << 1$).
- Weakly nonideal plasma (at $\Gamma, \gamma < 1$).
- Nonideal plasma (at $\Gamma, \gamma \geq 1$).
- Strongly nonideal (coupled) plasma (at $\Gamma, \gamma >> 1$).

To determine the condition of classicality we should compare the characteristic distance between particles with the thermal electron wavelength $\lambda_e = h/(2m_e k_B T)$. Since the minimal characteristic radius of the ion–electron interaction is $r_{\min} \sim Ze^2 / k_B T$, the condition of classicality can be written as

$$\lambda_e << \frac{Ze^2}{k_B T}. \qquad (1.5)$$

The condition of classicality can be also written in terms of the degeneration parameter ξ:

$$\xi = \frac{\varepsilon_F}{k_B T} << 1, \qquad (1.6)$$

here $\varepsilon_F = \left(3\pi^2 n_e\right)^{2/3} h^2 / 2m$ is the Fermi energy. Sometimes another degeneration parameter $\theta = 1/\xi$ can be also used for describing semiclassical plasma's properties.

Notice that further compression of the plasma causes an increase of nonideality, but up to a certain value (limit) only, because at $n_e \lambda_e^3 \sim 1$ with increasing density degeneracy of electrons occurs. For example, in metals $n_e \sim 10^{23} cm^{-3}$ and electrons are degenerate at $T \le 10^5 K$, i.e. almost always. With increase of plasma density the Fermi energy can be chosen as a kinetic energy scale. Therefore, the quantum criterion of ideality has the following form:

$$\Gamma_q = e^2 n_e^{1/3} / \varepsilon_F << 1. \tag{1.7}$$

Since $\varepsilon_F \sim n_e^{2/3}$ we can conclude that $\Gamma_q \sim n_e^{1/3} / \varepsilon_F \sim n_e^{-1/3}$, i.e. the quantum criterion parameter Γ_q decreases with increasing electron density. Consequently, the degenerate electron plasma becomes more ideal with compression. Notice that at higher densities only electrons can be considered as an ideal Fermi gas, whereas the ion component is nonideal.

As a dimensionless density parameter r_S the ratio between average interparticle distance a and the Bohr radius a_B is used $r_S = a / a_B$, where $a_B = h/me^2 \approx 0{,}5 \cdot 10^{-8} cm$.

Screening of Charged Particle's Field in Plasma

Due to the long–range character of the Coulomb potential the many-particle interactions at large distances are important. The potential created by the selected test particle and its plasma environment is the well known Debye potential [1]:

$$\varphi = \frac{e^2}{r} e^{-r/r_D}, \tag{1.8}$$

where k corresponds to different charged plasma species and r_D is the Debye screening radius:

$$r_D = \left(4\pi e^2 \sum_k Z_k^2 n_k \Big/ k_B T \right)^{-1/2}. \tag{1.9}$$

According to (1.4) the criterion of ideality for singly charged plasma can be written as:

$$\gamma = \frac{e^2}{r_D k_B T} \sim > 1. \qquad (1.10)$$

Let us introduce the number of electrons in the Debye sphere $N_D = (4/3)\pi n_e r_D^3$. Then the criterion (1.10) can be expressed in terms of N_D as $\gamma = (3\Gamma^3)^{1/2} = (3N_D)^{-1}$. For ideal plasma we have condition $N_D \sim 1$.

If the electrons of plasma are degenerate, i.e. $n_e \lambda_e^3 \sim 1$, the screening length by degenerate electrons is defined by the Thomas–Fermi radius:

$$r_{TF} = (\pi / 3n_e)\sqrt{h^2 / 4me^2}\ . \qquad (1.11)$$

In two–component electron–ion plasma, in which the electrons are degenerate but ions are classical, the screening radius of the test charge is defined by the following expression:

$$r^{-2} = (r_{TF}^e)^{-2} + (r_D^i)^{-2} \approx (r_D^i)^{-2}. \qquad (1.12)$$

Quantum Effects in Interparticle Interactions

At small distances (when average distance between particles is approximately equal to the thermal wave-length, i.e. $a \sim \lambda_e$) we have to take into account quantum effects (for instance, diffraction and symmetry effects). These effects lead to the formation of atoms and molecules and play an important role. Taking into account these effects eliminates the divergencies at small distances between particles.

For adequate taking into account of quantum effects at small distances the Slater sum and the Boltzmann factor should be jointly applied. It is known that the probability density of finding two particles at a distance r in classical statistics is proportional to the Boltzmann factor $\exp\left(-\Phi(r)/k_B T\right)$, here $\Phi(r)$ is the interaction potential between two particles. In quantum physics such probability is defined by the Slater sum [2]:

$$S_2(r,T) = 2\lambda_e^3 \sum_n \Psi_n^* \exp\left(-E_n / k_B T\right) \Psi_n\,, \qquad (1.13)$$

where Ψ_n and E_n are the wave functions and the corresponding eigenvalues of the energy of two particles, respectively, and the summation in (1.13) is performed over all states of discrete and continuous spectra.

Let us define the pseudopotential $\tilde{\Phi}(r,T)$ as a potential giving in the classical case the same particle distribution in space as the potential $\Phi(r)$ gives in the quantum case, i.e.

$$\tilde{\Phi}(r,T) = -k_B T \ln S_2(r,T)\,. \qquad (1.14)$$

Notice that the pseudopotential $\tilde{\Phi}(r,T)$ has the limiting value at $r=0$ and coincides with $\Phi(r)$ in the limit $T \to \infty$. At large distances ($r \to \infty$) $\tilde{\Phi}(r,T)$ has a Coulomb-like asymptotic dependence.

From equation (1.14) at $T \to \infty$ and $n_e, n_i \to \infty$ the following expression for effective potential is obtained [3]:

$$\Phi_{\alpha\beta}(r) = \frac{e^2}{r}\left(1-\exp\left(-\frac{r}{\lambda_{\alpha\beta}}\right)\right) + \delta_{\alpha\beta}\delta_{e\alpha}\ln(2)k_B T \exp\left(-\frac{r^2}{\pi\ln(2)\lambda_{ee}^2}\right). \qquad (1.15)$$

Taking into Account both Quantum and Screening Effects

It should be noted that even in a rarefied plasma, when $\gamma \sim 1$, one cannot directly apply the formulas of ideal gas theory for describing the thermodynamic and transport properties of the plasma. Some quantities such as the second virial coefficient or the mean free path are diverging due to the specific character of the Coulomb interaction. It is known that the Coulomb potential has a long range character at large distances and an infinite divergence at small distances.

The divergence at small distances is eliminated by taking into account the quantum diffraction and symmetry effects. The divergencies of physical quantities at large distances can be eliminated by taking into account the effect of charge screening in plasma.

Notice that diffraction effect is related to the de Broglie waves of microparticles and symmetry effect corresponds to the Pauli exclusion principle.

Consequently, in dense semiclassical plasma the collective (screening) and quantum-mechanical effects play an important role in the studies of thermodynamic and kinetic properties of the system. In general case these potentials contain quantum diffraction effects at short distances, as well as screening effects for large distances [4:

$$\Phi_{\alpha\beta}(r) = \frac{Z_\alpha Z_\beta e^2}{\sqrt{1-4\lambda_{\alpha\beta}^2 / r_D^2}} \left(\frac{e^{-Ar}}{r} - \frac{e^{-Br}}{r} \right) \qquad (1.16)$$

for electron-electron and electron-ion interactions and here

$$A^2 = \frac{1}{2\lambda_{\alpha\beta}^2}\left(1-\sqrt{1-\lambda_{\alpha\beta}^2 / r_D^2}\right);\ B^2 = \frac{1}{2\lambda_{\alpha\beta}^2}\left(1+\sqrt{1-\lambda_{\alpha\beta}^2 / r_D^2}\right).$$

For describing of ion-ion interactions we have the following expression [5]:

$$\Phi_{ii}(r) = \frac{Z_i Z_i e^2}{\sqrt{1-4\lambda_{ei}^2 / r_D^2}} \left(\lambda_{ei}^2 B^2 \frac{e^{-Ar}}{r} - \lambda_{ei}^2 A^2 \frac{e^{-Br}}{r} \right). \qquad (1.17)$$

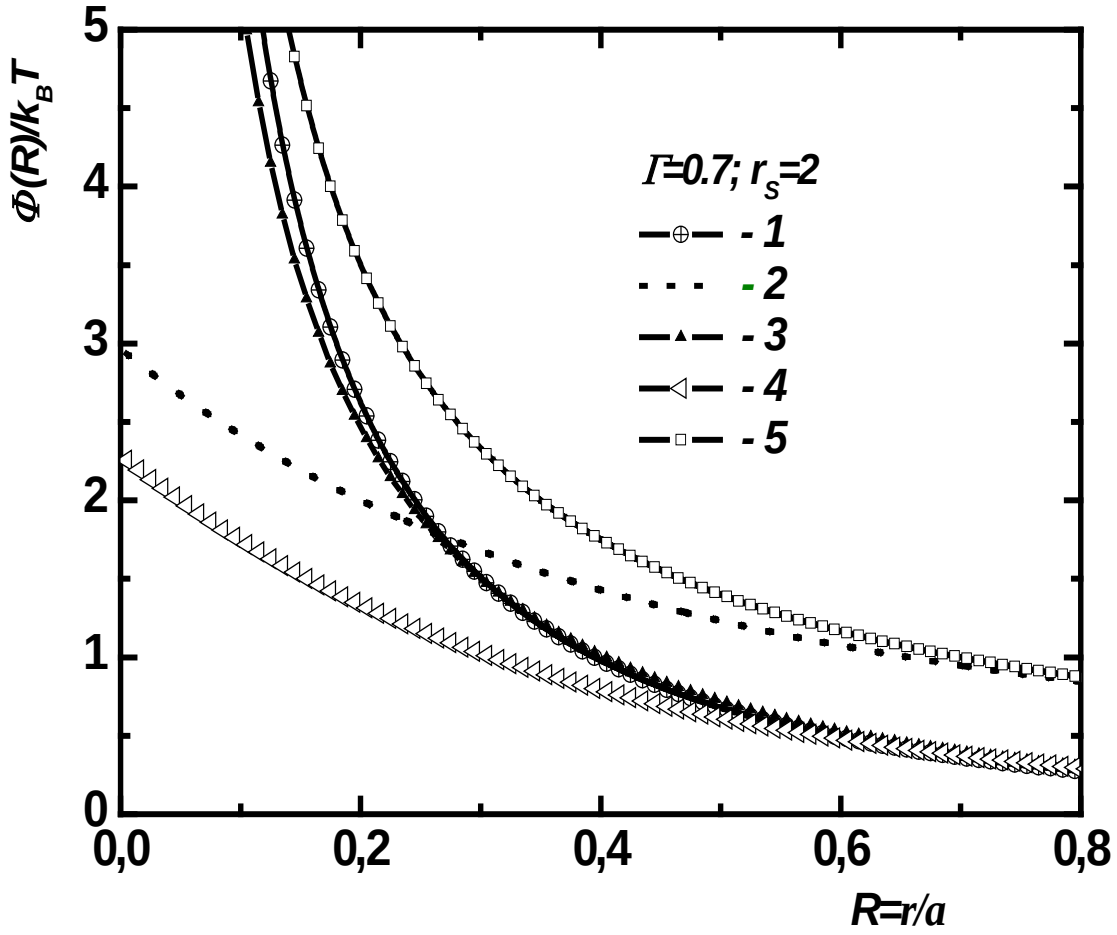

Figure 1.1 - Effective potentials for fully ionized semiclassical plasma.
1 – The Debye potential; 2 – The Deutsch potential;
3 – (T.Ramazanov et al., ion-ion)
4 – (T.Ramazanov et al., e-e, e-i)
5 – The Deutsch potential for i-i interaction.

Questions:

1. The definition of nonideal plasma.
2. Criteria of nonideality.
3. Existence of nonideal plasmas.
4. Screening effects.
5. Quantum effects.

LECTURE 2

Basic Concepts of Nonideal Plasma

Charge-Atom Interactions in Nonideal Plasma

In the previous lecture we considered interaction models between charged particles only. Notice that in partially ionized plasma (at high densities and low temperatures) the interactions between charged and neutral particles are dominant and cannot be described in an ideal–gas approximation. The effects of nonideality due to charge–neutral interaction are important for such properties as the electrical conductivity, thermal conductivity, thermoelectromotive force, etc.

The interaction between isolated classical atoms and charges. Let us consider the potential produced by atoms (molecules) at the ion (electron) location. It is known that the full ion–atom (electron–atom) interaction consists of the exchange, electric and polarization interactions. The polarization force is appreciable even at low densities due to its long range character. An atom polarized by microfields of ions (electrons) creates at the ion (electron) location the polarization potential, thus, we obtain the following polarization interaction potential for isolated classical atoms and ions (electrons):

$$\varphi(r) = -\frac{\alpha e^2}{2r^4}, \tag{2.1}$$

where $r > r_a$ is the distance between particles; α is the polarizability of the atom and r_a is the atomic radius. The total potential created by all atoms at the ion location is:

$$\varphi = 4\pi \int_{r_a}^{\infty} \varphi(r) n_a(r) r^2 dr, \tag{2.2}$$

here $n_a(r)$ is the atomic number density which depends on the distance from the ion. If the ion-atom interaction is not so strong the dependence $n_a(r)$ can be neglected, i.e. $n_a \neq n_a(r)$. Then

$$\varphi = -2\pi e^2 n_a \alpha / r_a. \tag{2.3}$$

The ideality criterion can be written in the following form:

$$\Gamma_{ia} = \frac{2\pi e^2 n_a \alpha}{r_a k_B T} << 1, \qquad (2.4)$$

where r_a is the "cut-off" radius of the polarization interaction (this radius is approximately equal to the atomic linear size). It should be noted that the effects of nonideality caused by charge–neutral interaction can occur in highly polarizable gases such as metal vapors. For instance, in the case of cesium plasma $\alpha = 400 a_B^3$; $r_a = 4a_B$ and at $T = 2000\,K$ we have $\Gamma_{ia} \le 0{,}1$ as long as $n_a < 10^{19} cm^{-3}$.

Notice that the electron–atom interaction potential has the same polarization asymptote $\varphi(r)$ but it cannot be adequately determined in wide range of temperatures because in this case we have to calculate the electron-atom scattering phases. It is the separate and complicated problem. However, the electron–atom interaction at low temperatures can be described by a single parameter, namely, the electron–atom scattering length L (as long as $n_a |L|^3 \sim 1$). Then the real potential $\Phi(r)$ can be replaced by a δ-like potential:

$$\Phi(r) = 2\pi h^2 L \delta(r)/m. \qquad (2.5)$$

The electron–atom interaction energy is calculated by following relation:

$$U = \int n_a(\vec{r}\,')\Phi(\vec{r} - \vec{r}\,')\left|\Psi(\vec{r})\right|^2 d\vec{r} d\vec{r}\,', \qquad (2.6)$$

where $\Psi(\vec{r})$ is the electron wave function. For weakly coupled plasma the electron–atom correlations can be neglected and using Eq. (2.5) we obtain:

$$U = 2\pi h^2 L n_a / m. \qquad (2.7)$$

Finally, the criterion of plasma ideality corresponding to the electron–atom interaction has the following form:

$$\Gamma_{ea} = \frac{2\pi |L| h^2 n_a}{m k_B T} << 1. \qquad (2.8)$$

The screening and quantum effects in "charge-atom" interactions. Let us introduce the different effective potentials for the interactions between neutral atoms and charged particles in plasma. We will focus on the polarization potential describing the interaction between charged particles (electrons) and neutrals. In

particular, we consider the inclusion of screening and quantum-mechanical effects into the polarization potential.

As mentioned above at large distances the interaction between an isolated atom and a charged particle is given by Eq. (2.1). However, this potential is not appropriate for dense (nonideal) plasmas. At short distances it becomes singular. It has to be modified if r is of the order of the extension of the atom as given by the Bohr radius a_B. According to Buckingham, a cutoff radius r_1 can be introduced as follows:

$$\Phi(r) = -\frac{e^2\alpha}{2(r^2 + r_1^2)^2}, \tag{2.9}$$

where $r_1^4 = \alpha a_B / 2$ and we obtain the finite value of this potential $\Phi(0) = -e^2 / a_B$.

At large distances modification is also necessary. It is known that in dense plasmas the Coulomb interaction between charged particles is screened. We have to take into account also the screening effects in the polarization potential [6]:

$$\Phi(r) = -\frac{e^2\alpha}{2(r^2 + r_1^2)^2} \exp\left(-\frac{2r}{r_D}\right)\left(1 + \frac{r}{r_D}\right)^2, \tag{2.10}$$

where r_D is the Debye radius.

Notice that both screening and quantum effects should be taken into account in nonideal partially ionized plasma. In general case the neutral atom is polarized in an external electric field generated by charges of plasma. Thus, we can consider atoms as dipoles. Let us consider semiclassical partially ionized plasma consisting of electrons, ions and atoms. In this case the following effective potential for electron-atom interaction is obtained [7]:

$$\Phi(r) = -\frac{e^2\alpha}{2r^4\left(1 - 4\lambda\!\!\!^{-2} / r_D^{\,2}\right)}\left(e^{-Br}(1+Br)(1-B^2\lambda\!\!\!^{-2}) - e^{-Ar}(1+Ar)(1-A^2\lambda\!\!\!^{-2})\right)^2, \tag{2.11}$$

where

$$A^2 = \frac{1}{2\lambda\!\!\!^{-2}}\left(1 + \sqrt{1 - 4\lambda\!\!\!^{-2} / r_D^{\,2}}\right),$$
$$B^2 = \frac{1}{2\lambda\!\!\!^{-2}}\left(1 - \sqrt{1 - 4\lambda\!\!\!^{-2} / r_D^{\,2}}\right), \tag{2.12}$$

In (2.11) we take into account quantum diffraction effects only in interactions between electrons. In the limiting case $\lambda\!\!\!^{-} << r_D$ this potential takes the form of a well-known interaction potential (2.1) for isolated classical atoms and electrons.

At high densities the quantum diffraction effects must be also taken into account in considerations of atom-electron interactions. Then in this case we have the following potential for electron-atom interaction [7]:

$$\Phi(r) = -\frac{e^2\alpha}{2r^4(1-4\lambda\!\!\!^{-2}/r_D{}^2)}\left(e^{-Br}(1+Br)-e^{-Ar}(1+Ar)\right)^2. \quad (2.13)$$

Notice that at small distances between particles ($r \to 0$) this potential has the finite value $\Phi(0) = -\alpha e^2/8\lambda\!\!\!^{-2}$.

Neutral and compound particles in plasma. Firstly, we will shortly discuss here influence of atom-atom interactions in plasma. Usually the plasma interactions (Coulomb and polarization) have high intensity and long–range character and the interaction between neutral particles are weak. In order to estimate the intensity of atom-atom interactions the van der Waals type equation of state can be used:

$$(p + n_a^2 a) = \frac{n_a k_B T}{1 - n_a b}. \quad (2.14)$$

Then, the ideality criteria can be written as:

$$n_a b << 1, \qquad n_a a / k_B T << 1, \quad (2.15)$$

where a and b are the parameters in the van der Waals equation. These parameters can be expressed in terms of the critical temperature and density:

$$T_c = 8a/27b, \qquad n_c = (3b)^{-1}. \quad (2.16)$$

It should be noted that interatomic interactions in plasma are important at densities close to and higher than the critical values.

The range of existence and the classification of states of nonideal plasma. Let us consider the fully ionized two–component hydrogen plasma and the corresponding existence diagram, the (n_e, T) plane in logarithmic coordinates, for such plasma (see Figure 2.1). In this figure the lines corresponding to the conditions $(\gamma = 1, \gamma_q = 1, \xi = 1)$ are also shown. These lines divide the (n_e, T) diagram into several characteristic regions.

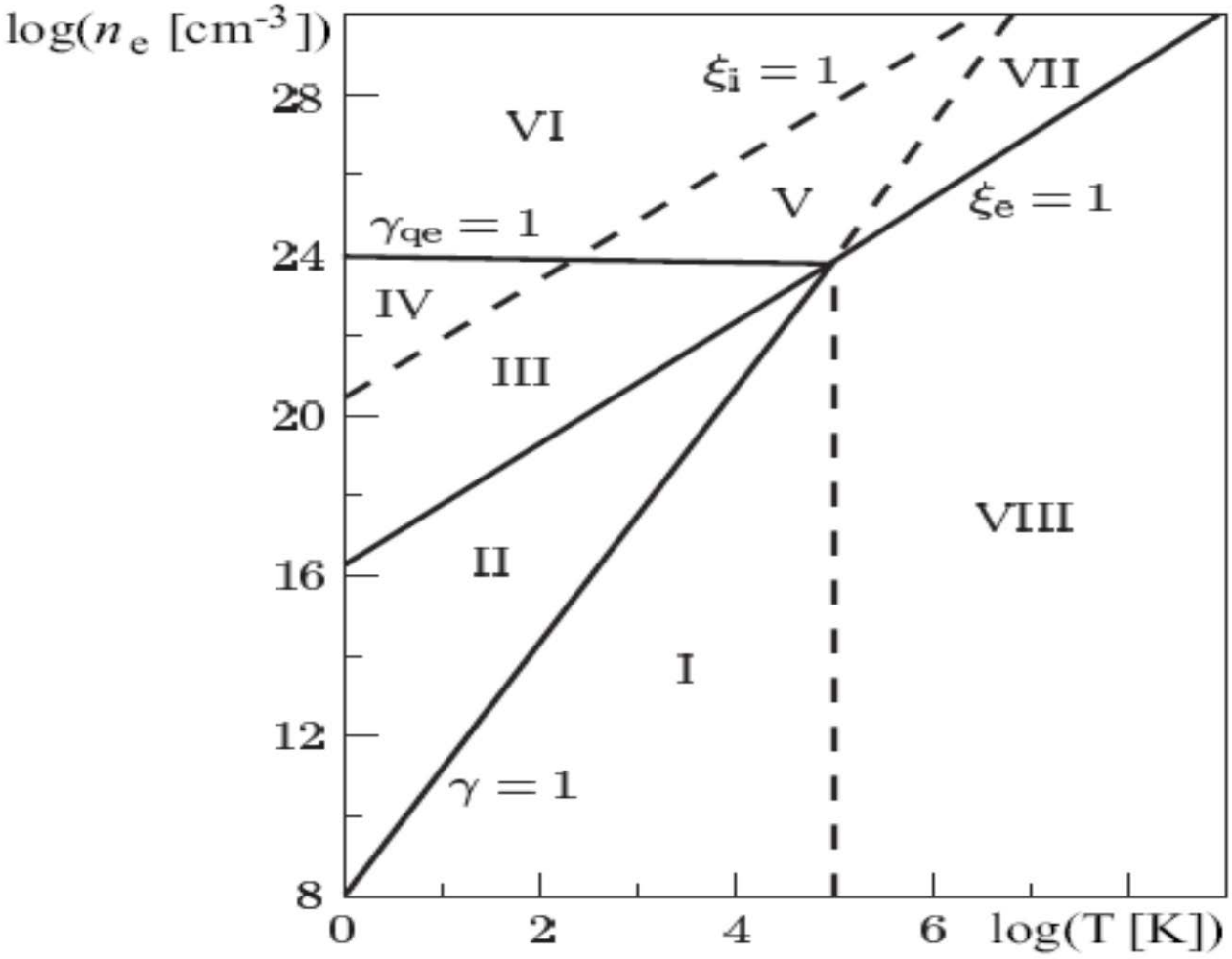

Figure 2.1. The range of existence for nonideal hydrogen plasma.

Let us analyze separate regions on (n_e, T) diagram:

- Region I: $\xi_e < 1, \xi_i < 1, \gamma < 1$: classical plasma with weak interaction of the electrons and ions.
- Region II: $\xi_e < 1, \xi_i < 1, \gamma > 1$: classical plasma with strong interaction of the electrons and ions.
- Region III: $\xi_e > 1, \xi_i < 1, \gamma_{qe} > 1, \gamma > 1$: the electrons form a degenerate system with strong interaction while the ions form a classical system with strong interaction.
- Region IV: $\xi_e > 1, \xi_i > 1, \gamma_{qe} > 1, \gamma_{qi} > 1$: quantum plasma with strong interaction of the electrons and ions.
- Region V: $\xi_e > 1, \xi_i < 1, \gamma_{qe} < 1, \gamma > 1$: the electrons form a degenerate system with weak interaction while the ions form a classical system with strong interaction.

- Region VI: $\xi_e > 1, \xi_i > 1, \gamma_{qe} < 1, \gamma_{qi} > 1$: the electrons are degenerate and interact weakly; the ions are degenerate and interact strongly.
- Region VII: $\xi_e > 1, \xi_i < 1, \gamma_{qe} < 1, \gamma < 1$: electron/ion plasma with weak interactions, in which the electron component is degenerate.
- Region VIII: $\xi_e < 1, \xi_i < 1, \gamma < 1$: classical plasma with weak interaction of the electrons and ions.

It should be noted that regions I, VII, and VIII represent gaseous plasmas at various temperatures and densities, regions V and VI correspond to a solid state. Regions III and IV also correspond to a condensed matter. Region I represents a weakly nonideal low–temperature gas discharge plasma. Region VIII corresponds to high–temperature almost ideal plasma.

Nonideal plasma in nature and its scientific and technical applications. In Figure 2.2 the plasma parameters realized in nature and in various technical devices are shown [3].

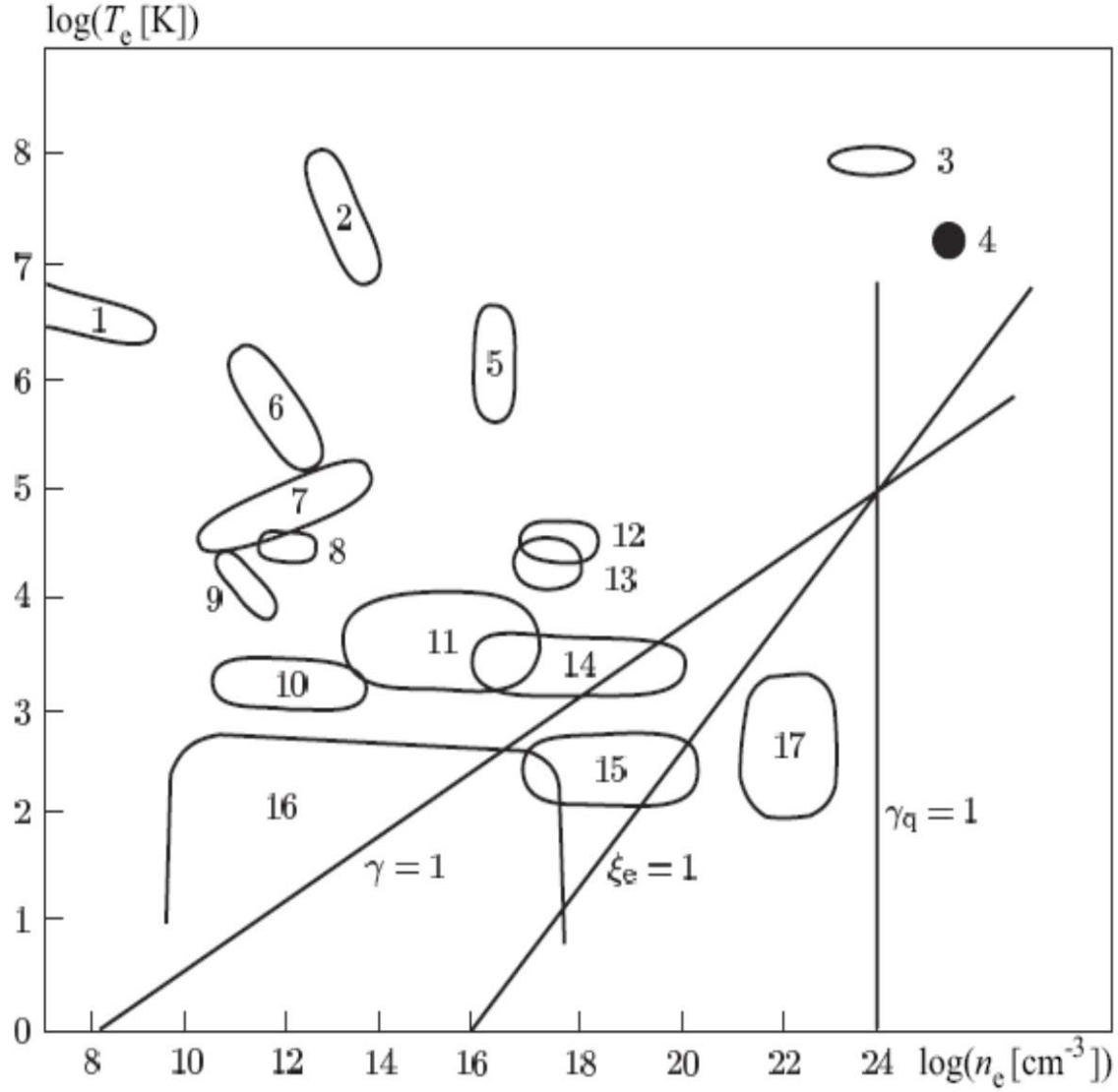

Figure 2.2 - The plasma parameters realized in nature and in various technical devices. 1 - solar corona; 2 - tokamak; 3 - laser–induced fusion; 4 - core of Sun; 5 - Z–pinch; 6 - stellarator; 7 - gas lasers; 8 - plasmotron; 9 - chromosphere of Sun; 10 - plasma of hydrocarbon fuel combustion products; 11 - electric arcs; 12 - cathode spot; 13 - spark; 14 - MHD generator; 15 - semiconductor plasma; 16 - metal–ammonia solutions; 17 - metals.

Questions:

1. Describe polarization interaction potential for isolated classical atoms and ions (electrons).
2. Inclusion of screening and quantum-mechanical effects into the polarization potential.
3. The screening and quantum effects in “charge-atom” interactions.
4. Classification of states of nonideal plasma.
5. Nonideal plasma in nature and its applications.

LECTURE 3

Experimental Methods of Nonideal Plasma Generation

Electrical Methods of Nonideal Plasma Generation

Introduction. There are two principally different techniques, namely:

- heating of ampoules containing the investigated material in resistance furnaces;
- Joule heating of the investigated material by an electric current.

Plasma heating in furnaces. The stationary methods of plasma generation are based on heating an ampoule containing the material under investigation (measuring cell) in electric furnaces of various designs. In the Figure 1 the schematic diagram of such a setup for investigating of alkali metals at high temperatures and pressures is shown (Alekseev, 1968). Argon from the cylinder (1) was fed via a system of valves to the chamber (3) for purification. Purified argon was delivered into a nitrogen thermo compressor (4) with the pressure up to 600 bar, and from the thermo compressor to the measuring chamber (5) containing a heater and a measuring cell. The pressure was monitored by gauges (2). The temperature was determined using a standard thermocouple.

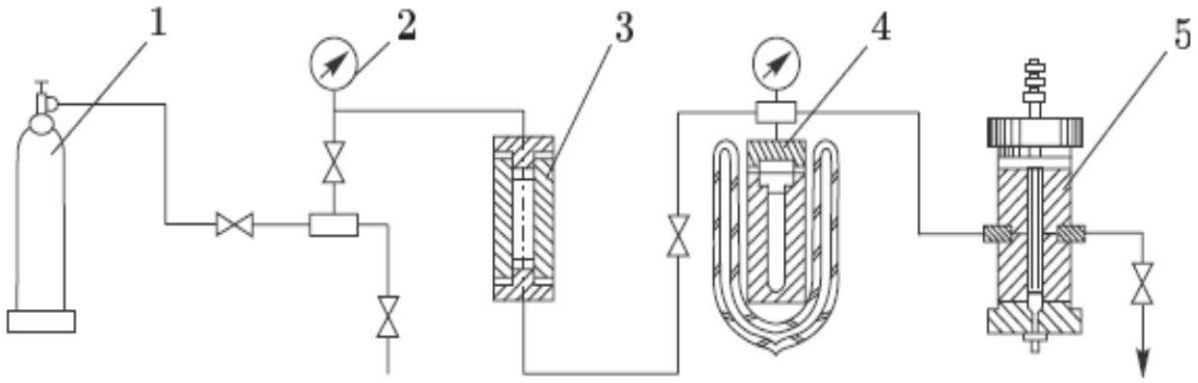

Figure 3.1. The schematic diagram of the experimental setup for generation and investigation of nonideal plasma of metals.
1 - cylinder with argon; 2 - pressure gauges; 3 - argon cleaning system; 4 – thermo compressor; 5 - high–pressure chamber.

The most convenient object for investigations of the nonideality effect is cesium which has a low ionization potential ($I = 3{,}89\,eV$), low critical pressure (about $110\,bar$), and a critical temperature that is quite accessible to static experiments (about $2000\,K$). In the such experiments plasma has the following value of the nonideality parameter $\gamma \leq 1$.

The isobaric Joule heating in a capillary. This method was developed by Kulik et al. (1984) [10] to investigate the properties of nonideal plasma of cesium, sodium, potassium and lithium. A schematic diagram of such experimental setup is shown in Fig. 3.2.

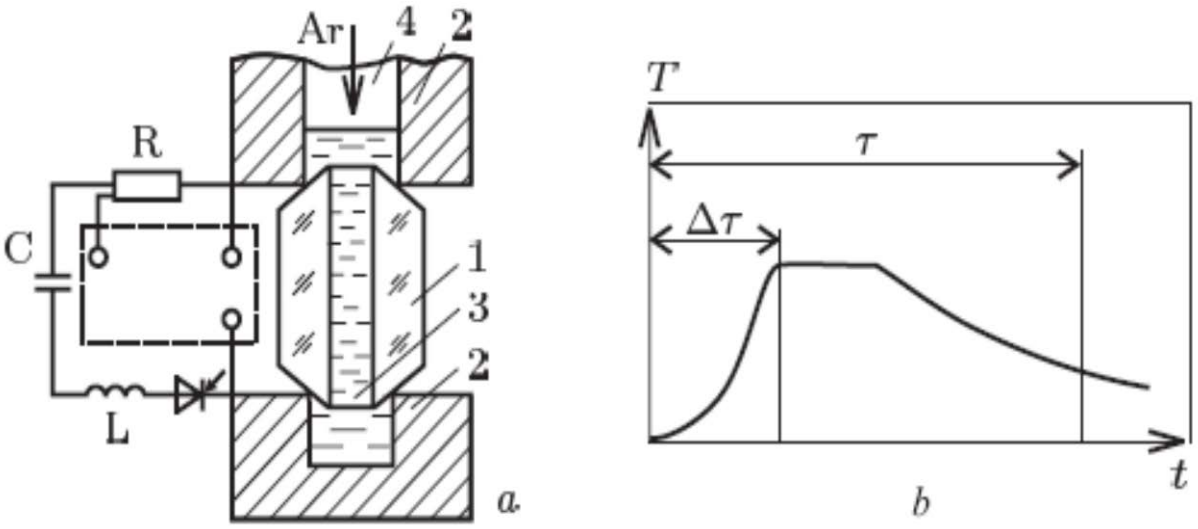

Figure 3.2. A schematic diagram of setup for isobaric heating in a transparent capillary.
(a): 1 - capillary; 2 - electrodes; 3 - liquid cesium; 4 - argon purge. (b) The time dependence of plasma temperature.

In this apparatus transparent quartz (or glass) capillary $0{,}7\,mm$ in diameter and $20\,mm$ long is filled with liquid cesium (or other metals) under constant pressure of argon. The cesium in the capillary is heated by a current pulse shaped by an electric circuit consisting of a capacitor, an inductor and a control thyristor (see, Fig.2). In the experiment, the current–voltage characteristic $U(i)$ is measured (from the oscillogram). Then, the isobars of electrical conductivity $\sigma(T)$ and thermal conductivity $\kappa(T)$ are calculated on the basis of the dependence $U(i)$ using the following relations:

$$\begin{cases} \dfrac{1}{r}\dfrac{d}{dr}\left(r\kappa\dfrac{dT}{dr}\right)+\sigma U^2=0; \\ i=2\pi U\displaystyle\int_0^R \sigma r dr \end{cases}, \qquad (3.1)$$

where the first equation is the equation of thermal balance and the second one is the Ohm's law; r is the distance from the capillary axis and R is its radius. Some

boundary conditions for equation (3.1) such as $dT/dr=0$ at $r=0$ and $T=T_S$ at $r=R$ should be added, here T_S is the temperature of the outer surface of the plasma measured by pyrometer. The typical plasma parameters in such experiments are as follows: the maximum pressure is $0{,}1 GPa$ and the temperature range is $(4\div 20)\cdot 10^3 K$.

Exploding wire method. The schematic diagram of the exploding wire method is shown in Figure 3.3 (Dikhter and Zeigarnik, 1981). A cesium (or lithium) wire 6 is placed in a high–pressure chamber 5. An electric current with a density of $(1\div 5)\cdot 10^6 A\cdot cm^{-2}$ is passed through the wire and metallic plasma is generated.

Such plasma contained by a high–pressure inert gas is heated and expands at constant pressure. In the experiment the pressure in the chamber, the oscillography of current in the circuit and the voltage drop across the plasma column are measured. The plasma column expansion process is registered by photo recording. Finally, one can use the measured values to calculate the enthalpy, density and electrical conductivity. The typical plasma parameters in the experiment with an exploding wire are as follows: the maximum pressure is $0{,}5 GPa$ and the temperature range is $(5\div 9)\cdot 10^3 K$.

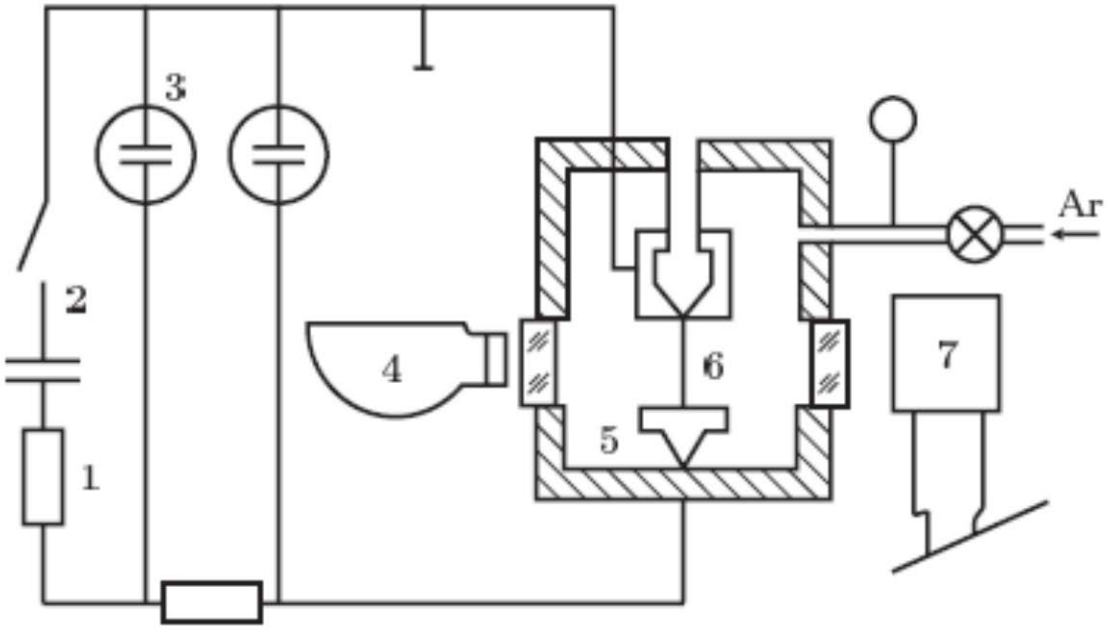

Figure 3.3 - A schematic diagram of the experimental setup for exploding wire method.

1 - ballast resistor; 2 - capacitor bank; 3 - oscillograph; 4 - high–speed photorecorder; 5 - high–pressure chamber; 6 - heated wire; 7 - spectrograph.

High–pressure electric discharges. Due to the high density of material and high level of temperature, the charged particle concentration in a plasma of high–pressure electric arcs and discharges is equal to $10^{18} \div 10^{21} cm^{-3}$ at pressures $\geq 1 MPa$. It should be noted that in such a plasma, the nonideality parameter may reach substantial values. Pulsed discharges in gases are generated upon discharging a battery of capacitors through an inter-electrode gap. One of the possible designs for a discharge tube is shown in Figure 3.4 (Radtke, Guenter, 1976).

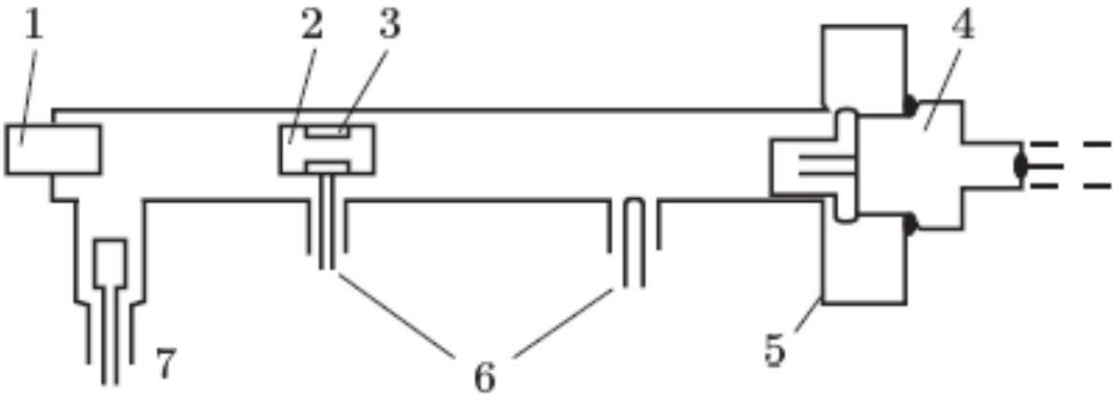

Figure 3.4 - A schematic diagram of high pressure discharge tube.

1 - quartz window; 2 - auxiliary electrode; 3 - steel ring; 4 - pressure sensor; 5 - cathode; 6 - tungsten probes; 7 - anode.

It consists of a quartz tube with four electric leads: anode, cathode (with a pressure sensor), and two measuring probes. Inside the tube, a movable auxiliary electrode for ignition is mounted. The tube has a length of $10 cm$ and a diameter of $1 cm$. It is filled with an inert gas at an initial pressure of up to $0{,}1 MPa$. The typical plasma parameters are as follows: $p = 0{,}1 GPa$; $T = 18 \cdot 10^3 K$; $n_e = 10^{18} \div 10^{19} cm^{-3}$; $\Gamma = (1 \div 2{,}3)$.

Conclusion. In the first method (plasma heating in furnaces) homogeneous volumes of plasma are obtained but the plasma temperature is restricted to $3000 K$ due to the thermal resistance of structural materials. The methods of the Joule heating include high–pressure gas discharges, the explosion of conductors, discharges in liquids and some other techniques. By these methods the plasma can be generated at considerably higher temperatures up to $10^5 K$ but there are some difficulties concerning the homogeneity of plasma volumes caused by various plasma instabilities.

Dynamic Methods of Nonideal Plasma Generation

Here we consider the principally different dynamic methods of nonideal plasma generation. Notice that by these methods the highest plasma parameters can be obtained. These methods are based on the accumulation of energy in the investigated material, or on the viscous dissipation in the front of shock waves, which propagate throughout the material causing its compression, acceleration and irreversible heating, or on adiabatic variation of pressure in the material.

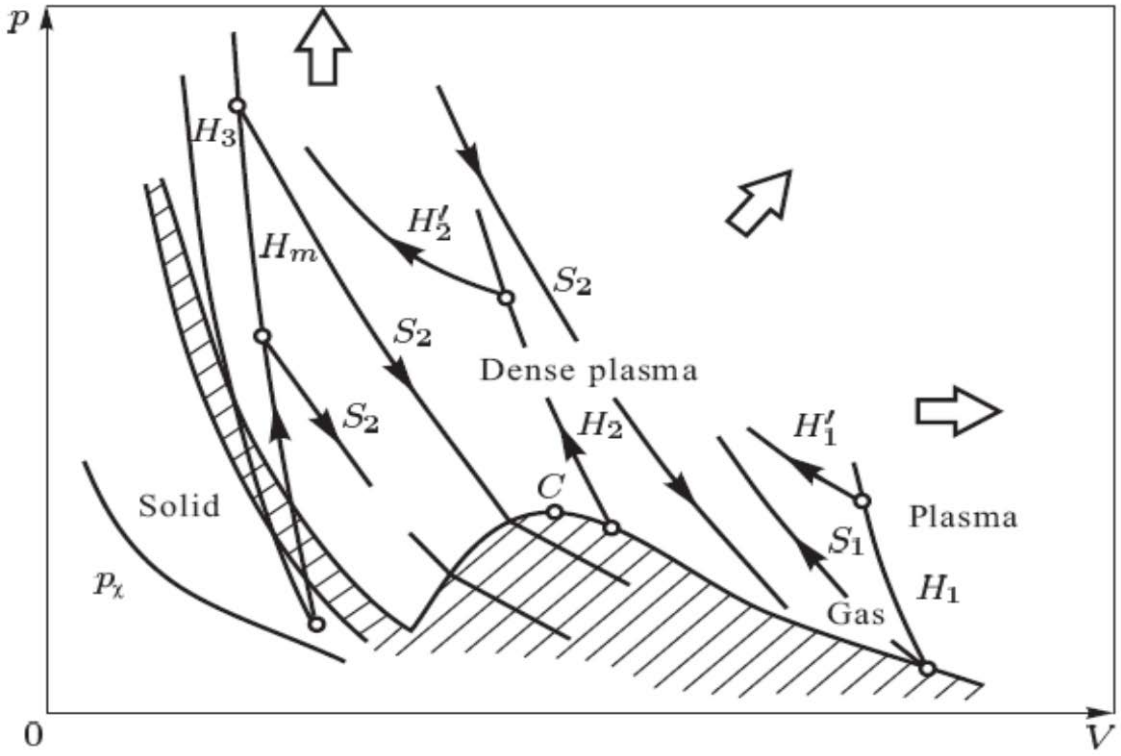

Figure 3.5 - Schematic presentation of the principles of dynamic generation of plasma. p_x is the boundary of maximum compressions of the material, i.e., the "cold" (T = 0 K) compression curve. The shaded areas show two–phase regions of melting and evaporation. C is the critical point. Circles indicate the initial states of the medium. H_1 and H_2 are the curves of cesium and inert gas compression by incident and reflected (H_1' and H_2') shock waves. H_3 and H_m are the curves of shock-wave compression of solid and porous metals. S_1 is the curve of adiabatic compression of cesium. S_2 is the unload adiabat of shock–compressed metals.

The technique of dynamic generation of plasma consists of the following methods:

- the adiabatic compression of gases (curve S_1);
- the shock–wave compression of gases (curves H_1 and H_2);
- the shock–wave compression of solid matter (curves H_3 and H_m);
- the adiabatic expansion of shock–compressed matter (S_2).

The main advantages of these methods are

- the high purity and homogeneity of the investigated volume;
- the absence of electric and magnetic fields (hampering the diagnostics and causing the development of various instabilities in the plasma);
- the possibility of obtaining extremely high parameters of plasma;
- using the general laws of conservation of mass, momentum and energy we can obtain the thermodynamic characteristics of plasma by the registration of the kinematic parameters of the shock waves (i.e. by the measurement of times and distances).

The adiabatic and shock-wave compression of gases. As an example we consider the dynamic compression of the cesium plasma because cesium has the lowest ionization potential $3{,}89eV$ and we have high charge concentration n_e at moderate temperatures and a substantial value of the nonideality parameter. Therefore, cesium is the most popular element in nonideal plasma experiments.

Figure 3.6 shows a schematic diagram of the experimental setup on the basis of the pneumatic, diaphragm shock tube for dynamic compression of cesium vapors (V. Fortov, e.a) [9]. The experimental apparatus with a length of $4m$ and an inside diameter of $4{,}5cm$ was heated to $700C$. An ionizing shock wave emerged upon expansion into saturated cesium vapor of helium, argon or their mixtures pre-compressed to about $0{,}1GPa$.

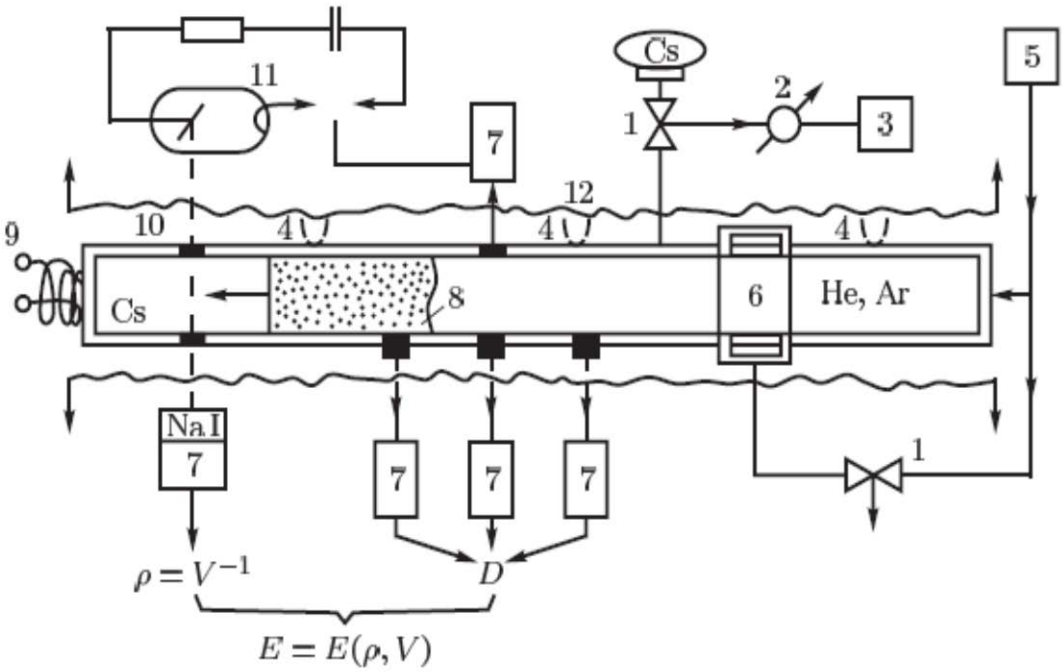

Figure 3.6 - A schematic diagram of the heated cesium shock tube. 1 - air–operated valves; 2 - a system for measuring the initial cesium pressure; 3 - a liquid cesium vessel; 4 - thermocouples; 5 - propelling gas; 6 - a diaphragm unit; 7 - photomultipliers; 8 - shock– compressed plasma; 9 - electrical conductivity measuring coil; 10 - beryllium windows; 11 - X–ray tube; 12 - an electric heater.

To determine physical characteristics of plasma the corresponding diagnostic methods should be developed. The dynamic diagnostic methods are based on the using of the relationship between the thermodynamic properties of the investigated medium and the experimentally observed hydrodynamic phenomena. (Zel'dovich and Raizer, 1988) [11-13]. It is known that the laws of conservation of mass, momentum and energy are satisfied in the front of the shock wave upon propagation of a stationary shock–wave through the material:

$$\begin{cases} \upsilon/\upsilon_0 = (D-u)/D; \\ p = p_0 + Du/\upsilon_0; \\ E - E_0 = (1/2)(p+p_0)(\upsilon_0 - \upsilon) \end{cases}, \qquad (3.2)$$

where the subscripts "0" denote the parameters of material before the front of the shock wave; D is the shock velocity; u is the mass velocity in the front of the shock wave; E, p, υ are the specific internal energy, the pressure and the specific volume, respectively. It is seen that the hydrodynamic and thermodynamic characteristics of the material can be derived from the recording of any two out of five parameters characterizing the shock wave E, p, υ, D, u. Usually the shock velocity D is measured most readily and accurately using the well known techniques. The choice of the second measured parameter depends on the actual experimental conditions.

The typical plasma parameters are as follows: $p = (0{,}1 \div 20)GPa$; $T = (0{,}1 \div 2)\cdot 10^5 K$; $n_e = 5\cdot 10^{15} \div 5\cdot 10^{22} cm^{-3}$; $\Gamma = (0{,}2 \div 3{,}2)$.

The adiabatic expansion of shock–compressed matter. In such experiments the isentropic expansion curves for shock–compressed matter (curve S_2, see Figure 3.5) are described by the Riemann integrals:

$$\begin{cases} \upsilon = \upsilon_H + \int_p^{p_H} \left(\frac{du}{dp}\right)^2 dp; \\ E = E_H - \int_p^{p_H} p\left(\frac{du}{dp}\right)^2 dp \end{cases}. \qquad (3.3)$$

These quantities are calculated along the measured isentrope $p_S = p_S(u)$. By recording under different initial conditions and shock–wave intensities, one can determine the caloric equation of state $E = E(p,\upsilon)$ in the region of the $p-\upsilon$ diagram. The experimental results for cooper demonstrate that the adiabatic

expansion from the states on the shock adiabat with $p \sim 1410\,GPa$, $T \sim 5 \cdot 10^4\,K$, $\upsilon \sim 0,052\,cm^3 g^{-1}$ leads to a weakly nonideal plasma with the following parameters $p \sim 0,73\,GPa$; $T \sim 9200K$; $\upsilon \sim 1,3\,cm^3 g^{-1}$ and $\Gamma \sim 0,1$.

Questions:
1. Electrical methods of nonideal plasma generation.
2. Plasma heating in resistance furnaces.
3. Joule heating by an electric current.
4. Dynamical methods of nonideal plasma generation.
5. Adiabatic and shock-compression methods of generating plasma.

LECTURE 4

Thermodynamic Properties of Nonideal Plasmas

Introduction

There are several methods for investigation of the thermodynamic properties of nonideal plasma. A perturbation theory can be applied at $\Gamma << 1$ for weakly nonideal plasma. For strongly coupled plasma ($\Gamma > 1$) we use a computer simulation by the Monte Carlo method. In order to apply the Monte Carlo method we have to know the interaction potential between particles in plasma. The thermodynamic properties of nonideal plasma at intermediate values of the coupling parameter can be investigated by integral equation methods (BBGKI, Ornstein-Zernike etc.) [14].

One Component Plasma (OCP)

Let us consider the simple and well-studied model of one component plasma (OCP). The one–component plasma (OCP) means a system of point-like ions placed in a homogeneous medium of charges of the opposite sign. The OCP-model is a good approximation for describing the plasma at high pressures. Such a plasma occurs in an inertial thermonuclear fusion and astrophysical objects (in the center of white dwarfs and giant planets). In these cases, matter is ionized under the effect of pressure and degenerate electrons have sufficient kinetic energy, i.e.

$$\overline{E}_{kin} \approx \left(3\pi^2 n_e\right)^{2/3} h^2 / 2m , \qquad (4.1)$$

which means the degenerate electrons produce an almost uniform background density distribution. It should be noted that the kinetic energy of electrons is $\varepsilon_F >> k_B T$ due to the small electron mass at high density ($r_S \to 0$) and the pressure of electron component is much higher than the corresponding pressure of the ion subsystem. Consequently, we have two systems: the Coulomb system of point-like nuclei described by the Boltzmann statistics and the quantum electron fluid (see the regions V, VI and VII in the Lecture No. 2). Notice that the interaction between these components is weak and most attention is concentrated on the analysis of the Coulomb internuclear (interionic) interaction. According to this OCP model there are no bound states (of molecules, atoms and ions). As the OCP model is the simplest, it has been studied in detail by theoretical and computer simulation methods for a wide range of the coupling parameter.

Table 1.1

One–component plasma of astrophysical objects

Parameter	Jupiter	White dwarf	Neutron star
Z	1 (H)	6 (C)	26 (Fe)
n_i, cm^{-3}	$6 \cdot 10^{24}$	$5 \cdot 10^{30}$	10^{32}
T, K	10^4	10^8	10^8
γ	50	10–200	870
r_s, a_0	0.65	$0.4 \cdot 10^{-2}$	$0.8 \cdot 10^{-3}$

Discussion of calculation results. The radial distribution functions are shown in the Figure 4.1. Figure 4.2 represents the results for static structure factors.

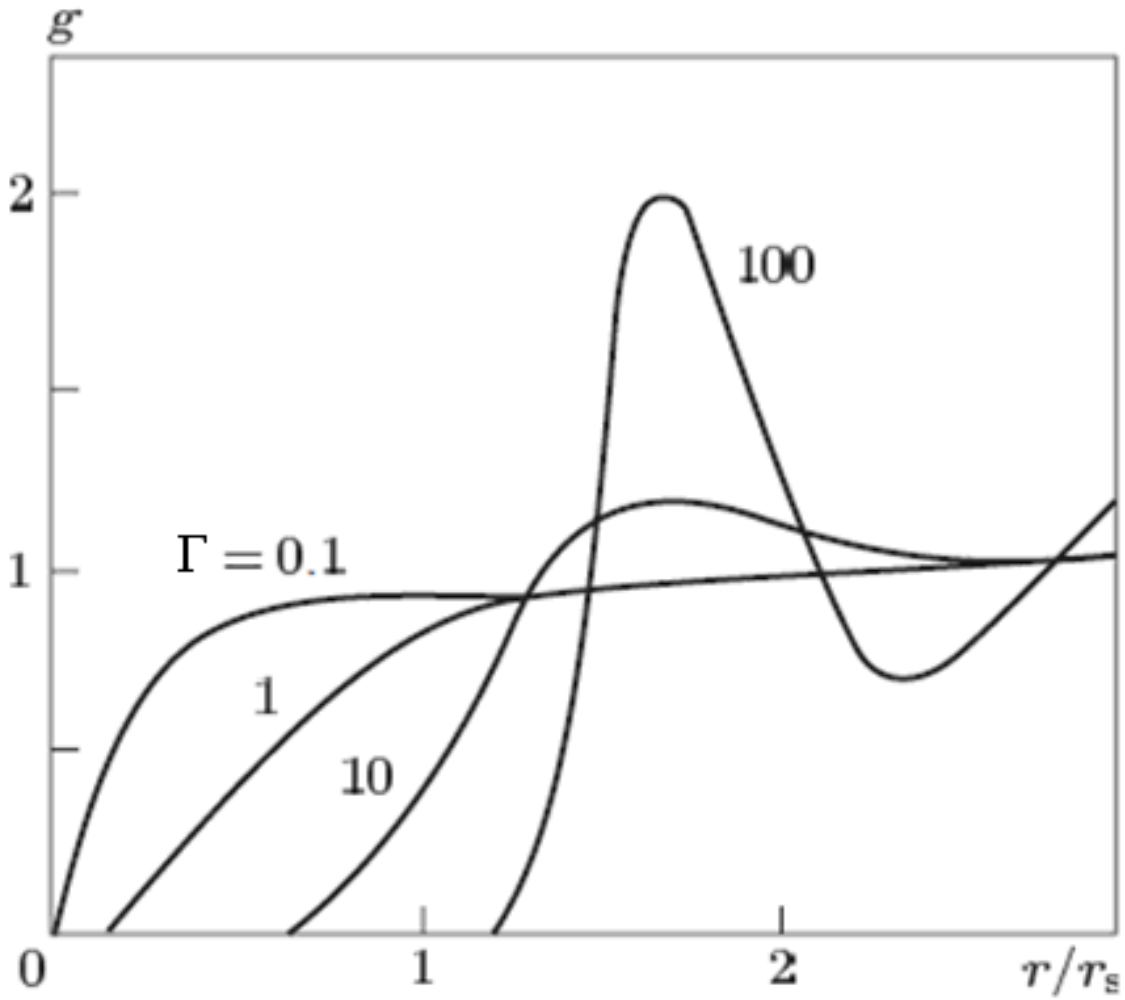

Figure 4.1 - The OCP radial distribution functions for different values of the coupling parameter Γ.

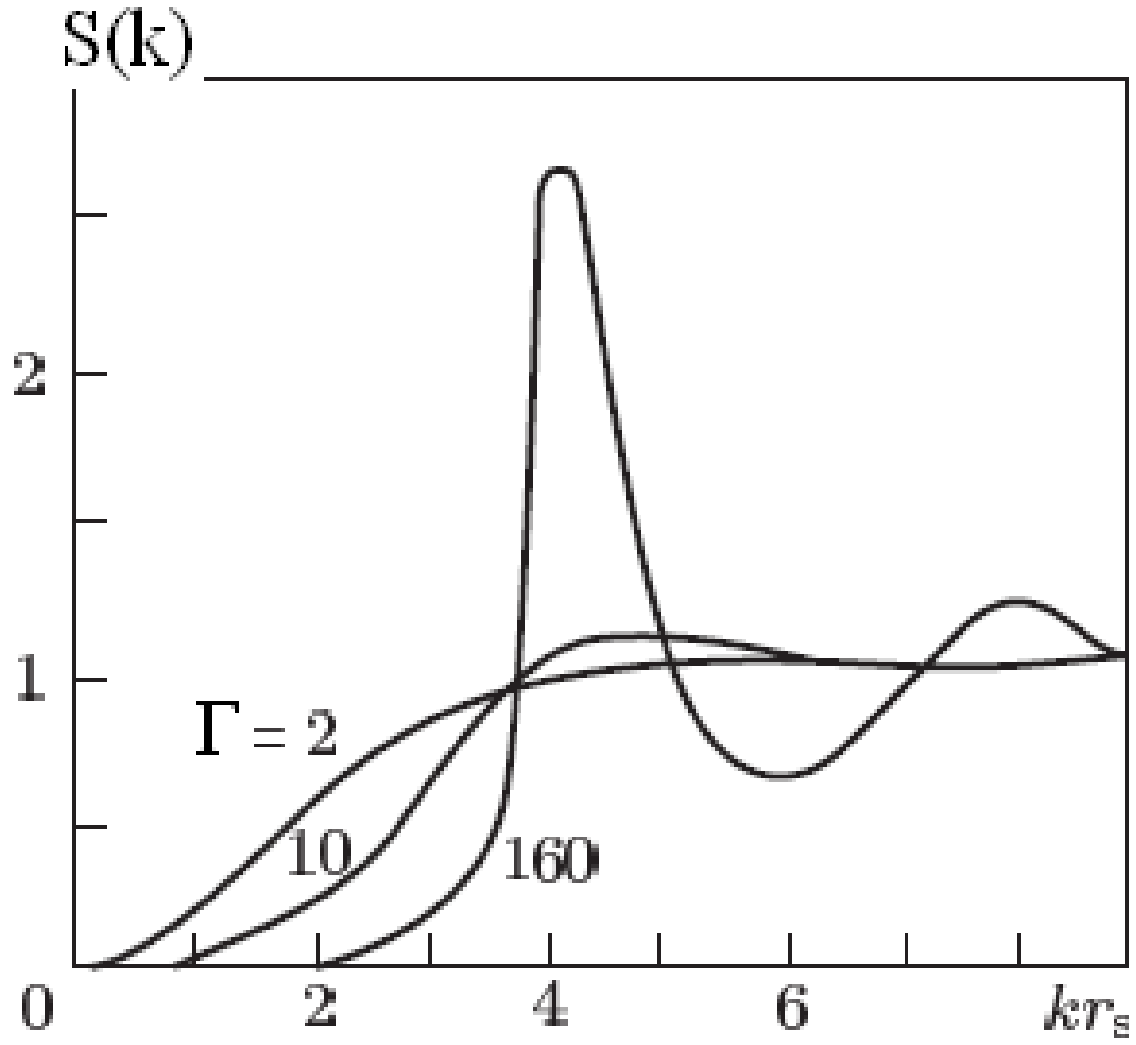

Figure 4.2 - The OCP static structure factors for different values of the coupling parameter Γ.

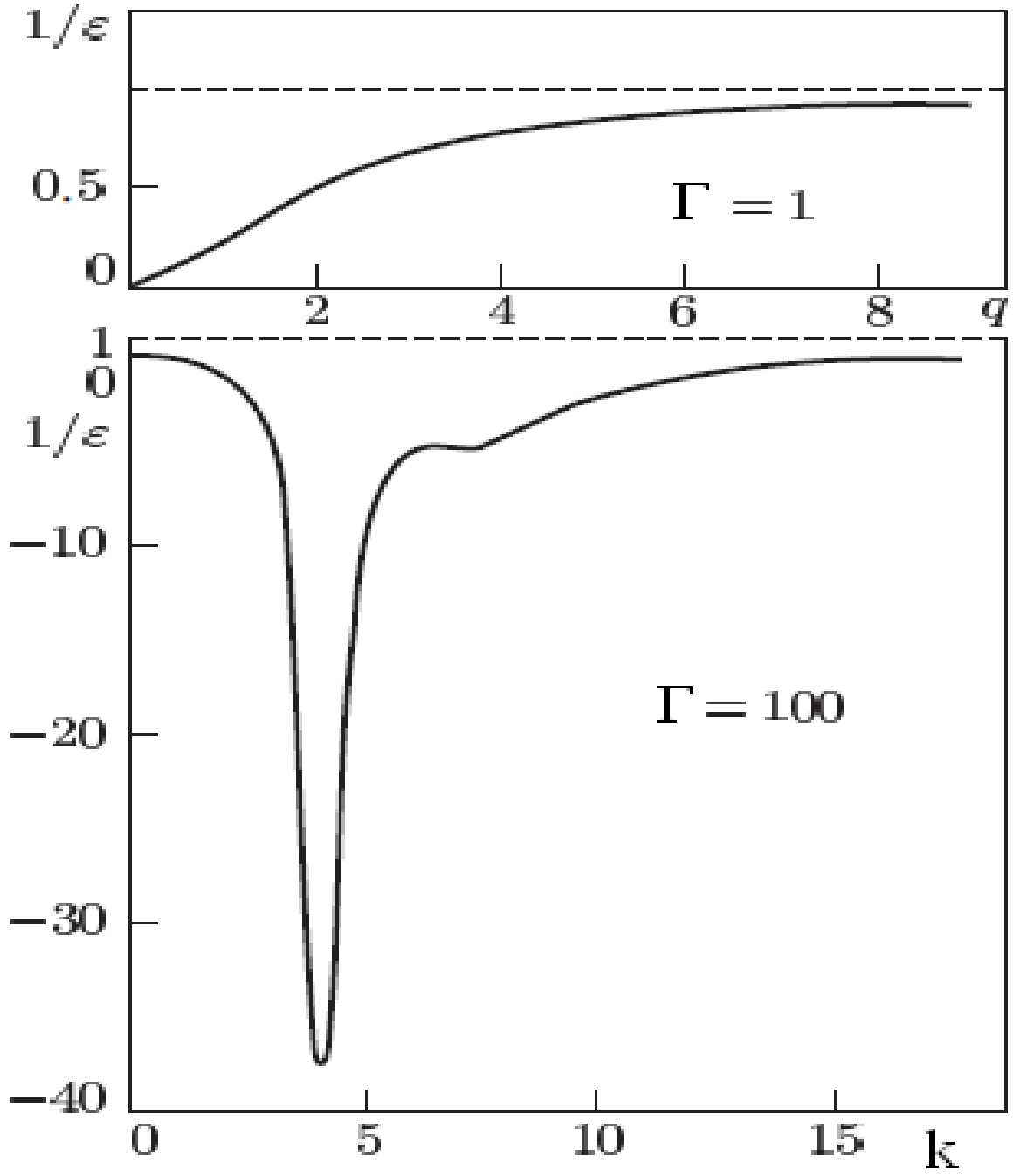

Figure 4.3 - The static dielectric functions of the OCP for different values of the coupling parameter Γ.

Knowing static structure factors the static dielectric permeability $\varepsilon(k,0)$ can be determined as follows:

$$\varepsilon(k,0) = \left[1 - \kappa_D^2 / k^2 S(k)\right]^{-1}, \qquad (4.2)$$

where $\kappa_D^2 = 4\pi n_i (Ze)^2 / k_B T$. In the case of almost ideal plasma ($\Gamma << 1$) these functions are monotonic and are described by the linearized Debye approximation:

$$S_D = k^2\left(k^2 + \kappa_D^2\right)^{-1}, \tag{4.3}$$

$$\varepsilon(k,0) = \left(k^2 + \kappa_D^2\right)/k^2. \tag{4.4}$$

The radial distribution (pair correlation) functions are monotonic up to $\Gamma \approx 3$ and can be described by the linearized Debye approximation:

$$g(r) = 1 - \frac{\gamma}{r}\cdot r_D \cdot \exp\left(-r/r_D\right), \tag{4.5}$$

where $\gamma = (eZ)^2/(r_D k_B T)$ is the nonideality parameter and $r_D = (4\pi Z^2 e^2 n_i / k_B T)^{-1/2}$ is the Debye radius of screening. At $\Gamma \geq 3$ functions $g(r)$ have oscillations due to the formation of short-range ordered structures. It means that the system changes from the ideal gas to a liquid state. With an increase in Γ the oscillations increase and an effective hard core is formed.

Knowing the pair correlation functions and static structure factors the thermodynamic properties can be calculated. Here we will briefly discuss these results. Let us consider the regions of weak ($\Gamma << 1$) and moderate ($0{,}1 \leq \Gamma \leq 1$) nonideality. On the basis of Mayer's diagrams for the excess part of free energy we have the following expression:

$$\frac{F_{ex}}{Nk_BT} = -\frac{\sqrt{3}}{3}\Gamma^{3/2} + S_2(\Gamma) + S_3(\Gamma) + \ldots, \tag{4.6}$$

where the first term corresponds to the summation of the "ring" diagrams (the Debye approximation), $S_2(\Gamma)$ and $S_3(\Gamma)$ are contributions to the free energy on the basis of the screened Coulomb potential:

$$\Phi(r) = \frac{e^2}{r}\exp\left(-r/r_{TF}\right), \tag{4.7}$$

where r_{TF} is the Tomas-Fermi radius. The expression for $S_2(\Gamma)$ is given by

$$S_2 = \frac{N}{2}\int\left[e^{-\Phi(r)/k_BT} - 1 + \Phi(r)/k_BT - \frac{1}{2}(\Phi(r)/k_BT)^2 \ldots\right]d\vec{r} \tag{4.8}$$

and has the value $O(\Gamma^3 \ln\Gamma)$ at $\Gamma \to 0$. On the basis of the relations between thermodynamic functions we can write the following expressions for the internal energy and thermal capacity:

$$\frac{U_{ex}}{Nk_BT} = -\frac{\sqrt{3}}{2}\Gamma^{3/2} + \frac{3}{2}\Gamma\frac{d}{d\Gamma}\left[S_2(\Gamma) + S_3(\Gamma) + ...\right], \quad (4.9)$$

$$\frac{c_V}{Nk_BT} = \frac{\sqrt{3}}{4}\Gamma^{3/2} - \frac{3}{2}\Gamma^2\frac{d^2}{d\Gamma^2}\left[S_2(\Gamma) + S_3(\Gamma) + ...\right]. \quad (4.10)$$

For the case of weakly nonideal regime ($\Gamma << 1$) we have the following simple relations according to the well-known Debye theory:

$$\frac{F_{ex}}{Nk_BT} = -\frac{1}{3}E; \qquad \frac{U_{ex}}{Nk_BT} = -\frac{1}{2}E;$$
$$\frac{c_V}{Nk_BT} = \frac{1}{4}E; \qquad E = \sqrt{3}\Gamma^{3/2} \quad . \quad (4.11)$$

In the opposite case ($\Gamma >> 1$) the asymptotic expression for internal energy can be written as:

$$\frac{U_{ex}}{Nk_BT} = -\frac{9}{10}\Gamma. \quad (4.12)$$

In order to obtain the formula for a wide range of the coupling parameter we have to approximate the computer simulated Monte Carlo data:

$$\frac{U_{ex}}{Nk_BT} = a\Gamma + b\Gamma^{1/4} + c\Gamma^{-1/4} + d, \quad (4.13)$$

where $a = -0{,}897; b = 0{,}945; c = 0{,}179; d = -0{,}801$ and expression (4.13) describes the OCP internal energy at $1 \le \Gamma \le 160$.

Multicomponent Plasma (MCP)

It is known that OCP model does not take into account the structure of opposite compensating background and basic quantum mechanical effects. Neglect of quantum–mechanical features can lead to major difficulties with the classical description of the particle motion at small distances (at $a \square \lambda_e$). It should be noted

that taking into account quantum mechanical effects leads to the formation of bound states (that is, molecules, atoms and ions). These quantum mechanical effects should be taken into account on the basis of the Boltzmann factor and the Slater sum (see Lecture No. 1).

Confined atom model (V. Fortov and V. Gryaznov, 1980).

Let us consider three–component plasma consisting of atoms, single-charged ions and electrons. We assume that the atoms are spheres with variable radius r_c. For simplicity the sizes of electrons and ions are ignored. We will consider the subsystem of finite–size atoms as a set of hard spheres, which do not interact when the distance between them exceeds $2r_c$. In this case it is necessary to take into account plasma effect on discrete spectrum of atoms and ions in dense plasma. These effects can be described in the framework of the confined atom model:

$$\Phi(r) = \begin{cases} -\dfrac{Ze^2}{r}, r < r_c \\ \infty \ , \ r > r_c \end{cases}. \qquad (4.14)$$

The free energy of such model can be written as:

$$F(N_a, N_i, N_e, V, T) = F_{id} + F_{hs} + \Delta F_{coul}, \qquad (4.15)$$

where the first term is the free energy of the ideal plasma, but the atomic partition function depends on the radius, the second term is the contribution of the hard sphere repulsion which also depends on r_c. In order to include this contribution, the computer simulation of molecular dynamic results for the hard-sphere systems is used:

$$\Delta F_{hs} = n_a k_B T \frac{3y-4}{(y-1)^2} y, \qquad (4.16)$$

where $y = n_a(4\pi r_c^3/3)$. The equilibrium value of atomic radius can be determined from the condition of minimum of the free energy:

$$\frac{\partial F}{\partial r_c} = 0. \qquad (4.17)$$

In order to determine the dependencies of partition functions on atomic radius r_c, it is necessary to numerically solve a set of nonlinear integral-differential equations according to the Hartree-Fock method.

Questions:
1. One component plasma (OCP).
2. Structural properties of OCP.
3. Thermodynamic properties of OCP.
4. Multicomponent plasma (MCP).
5. Confined atom model.

LECTURE 5

Structural and Thermodynamic Properties of Nonideal Plasma by Monte Carlo method

Pair Correlation Functions (Radial Distribution Functions)

A pair correlation function (PCF) $g(r)$ plays an important role in the investigation of structural and thermodynamic (equilibrium) properties of a plasma. This function measures the time-independent correlations between the particles. More precisely, $g(r)$ is the probability that a particle is found at a distance r from any given (test) particle. In the spherical symmetric case when the function $g(r)$ depends on distance $r = \left|\vec{r}_i - \vec{r}_j\right|$ between particles, this function is called a radial distribution function (RDF). The pair correlation function for ideal and weakly nonideal plasma is easily calculated using well known integral equation methods (BBGKI chain, Ornstein-Zernike equation, etc.). In the case of nonideal (dense) plasma the approximate methods of theoretical physics are not effective due to the absence of small parameters in the system. Therefore the computer simulation by the Monte Carlo method is applied for investigation of structural and thermodynamic properties of a dense plasma.

Algorithm for calculation of $g(r)$.

1. For each particle its surrounding space is divided into spherical layers with thickness Δr. For simplicity $0 < r \le L/2$.
2. In each layer the number of particles $\Delta N(r)$ is calculated.
3. The obtained results are averaged over all particles in any configuration. In this case we use the normal (arithmetical mean) averaging.
4. The obtained results are averaged for all configurations of Markov's chain. In this case we use the weight function averaging with the Boltzmann factor.
5. Then the average number of particles $\overline{\Delta N}(r)$ located at a distance between r and $r + \Delta r$ from the given particle can be calculated by the following formula:

$$\overline{\Delta N}(r) = \sum_{i=1}^{M} \frac{1}{N} \sum_{j=1}^{N} (\Delta N)_{ij} \cdot \exp\left\{ -\frac{\bar{U}_i}{k_B T} \right\}, \qquad (5.1)$$

where $\overline{U}_i$ is the average potential energy of configuration; M is the number of equilibrium configurations from the "stationary" part of MC computer simulation "control card".

6. Finally, the pair correlation function (radial distribution function) is defined by the following expression:

$$g(r) = \frac{V}{N} \cdot \frac{1}{4\pi r^2} \cdot \frac{\overline{\Delta N}(r)}{\Delta r} . \qquad (5.2)$$

It should be noted that for the plasma we have a set of pair correlation functions $g_{\alpha\beta}(r)$, where α, β are the sorts of particles.

Discussion of results for $g(r)$.

The results for radial distribution function of dense semiclassical hydrogen plasma obtained by the Monte Carlo method are presented in Figures 5.1 – 5.5. At $\Gamma < 1$ we have a monotonic (Debye-like) character of $g(r)$. Fluctuations of $g_{ee}(r)$ at $\Gamma = 0,8$ do not have any physical meaning and are within the range of statistical errors (Figure 5.1).

In Figure 5.2 the electron-ion radial distribution functions $g_{ei}(r)$ at different values of coupling parameter are shown. Notice that the values of $g_{ei}(r)$ for $\Gamma = 0,8$ are located higher than the corresponding values at $\Gamma = 0,5$ and $\Gamma = 0,3$. From physical point of view this fact means that the probability of finding an electron-ion pair at the intermediate distance increases with increasing coupling parameter (increase in plasma density). In other words with increase in plasma density the probability of formation of electron-ion pair (probability of recombination) rapidly increases at intermediate and small interparticle distances.

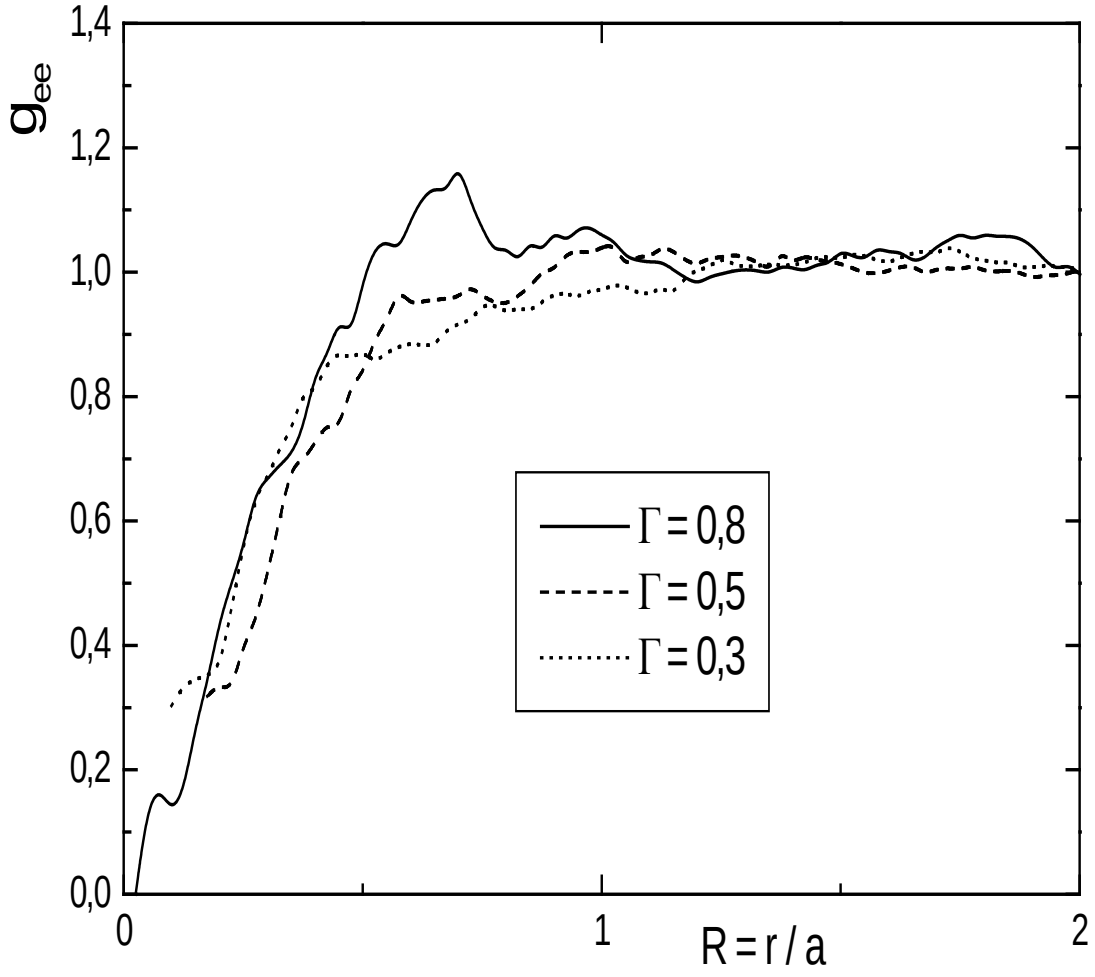

Figure 5.1 - Electron-electron radial distribution functions for dense semiclassical plasma at $r_s = 1$

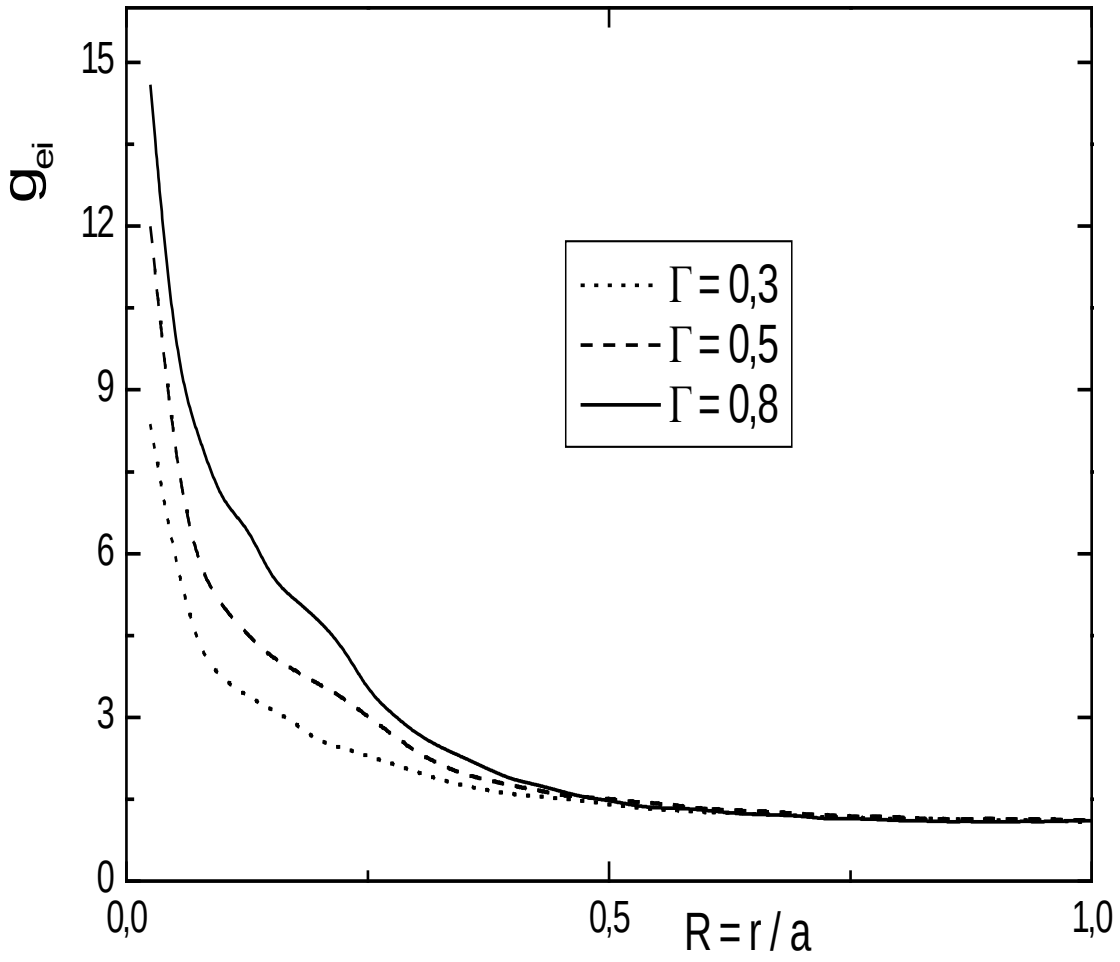

Figure 5.2 - Electron-ion radial distribution functions
for dense semiclassical plasma at $r_s = 1$

It should be noted that we have the opposite situation for ion-ion correlation functions $g_{ii}(r)$ (see, Figure 5.3). In this case the values of $g_{ii}(r)$ decrease with increasing coupling parameter (increasing of plasma density). This fact is connected with an increase in the probability of finding like (repulsive) particles with increasing plasma density (or coupling parameter).

It is seen from Figure 5.3 that minimal nonzero probability of finding an ion-ion pair is observed at relatively large values of interparticle distances with increasing Γ. This fact can be explained by a relative increase of average distances between ions (as repulsive particles) with increasing plasma density.

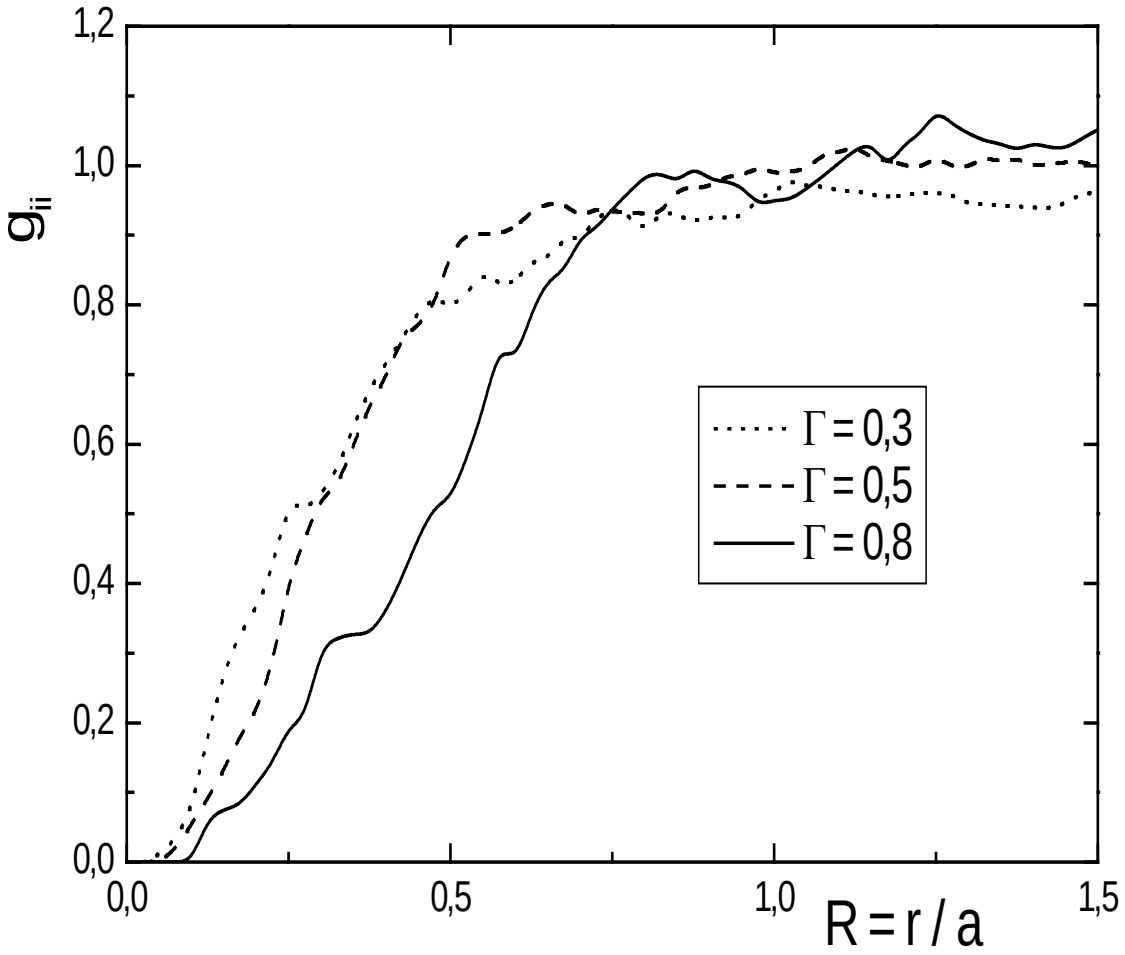

Figure 5.3 - Ion-ion radial distribution functions
for dense semiclassical plasma at $r_s = 1$.

Let us discuss the behavior of RDF at $\Gamma = (1 \div 10)$. For $\Gamma = 1$ we have a monotonic (Debye-like) character of $g_{ee}(r)$ (see Figure 5.4). It should be noted that at $\Gamma \geq 3$ $\lim_{r \to 0} g_{ee}(r)$ tends to a constant (non zero!) value. This fact can be explained as follows. With increasing coupling parameter it is necessary to take into account the interaction between electrons with anti-parallel spins due to the symmetry effect (the Pauli exclusion principle). The extremums of $g_{ee}(r)$ are related to the formation of quazi-bound states in the dense plasma.

The ion-ion radial distribution functions are presented in Figure 5.5. It is seen that these functions have pronounced peaks at $\Gamma > 5$. This fact can be explained by formation of ordered structures in dense plasma (see Figure 5.6).

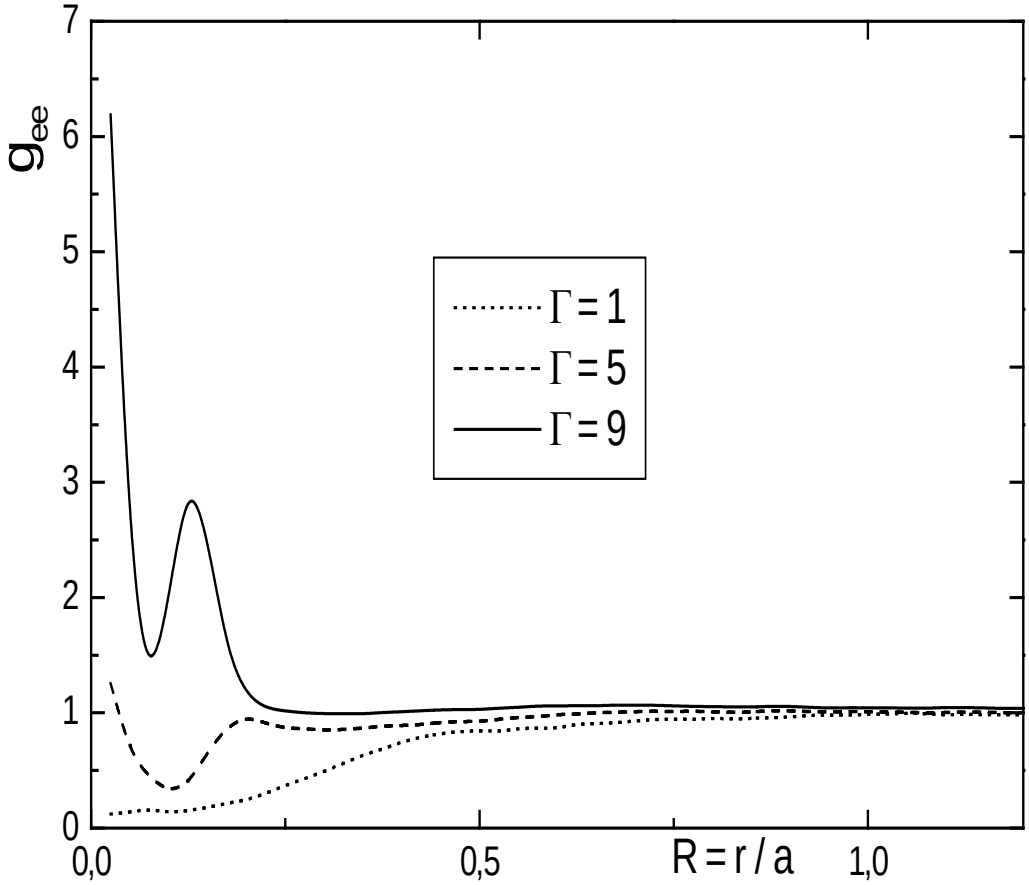

Figure 5.4 - Electron-electron radial distribution functions for dense semiclassical plasma at $r_s = 1$.

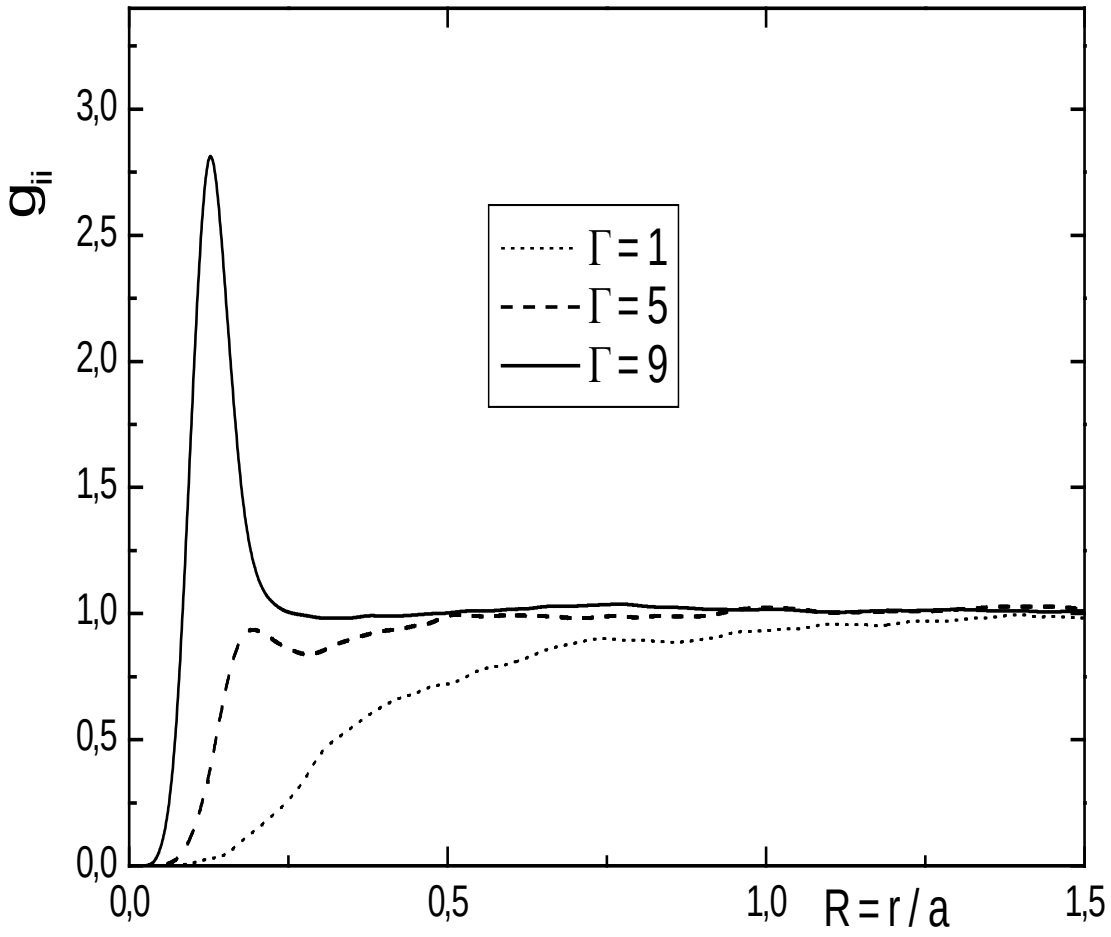

Figure 5.5 - Ion-ion radial distribution functions
for dense semiclassical plasma at $r_s = 1$.

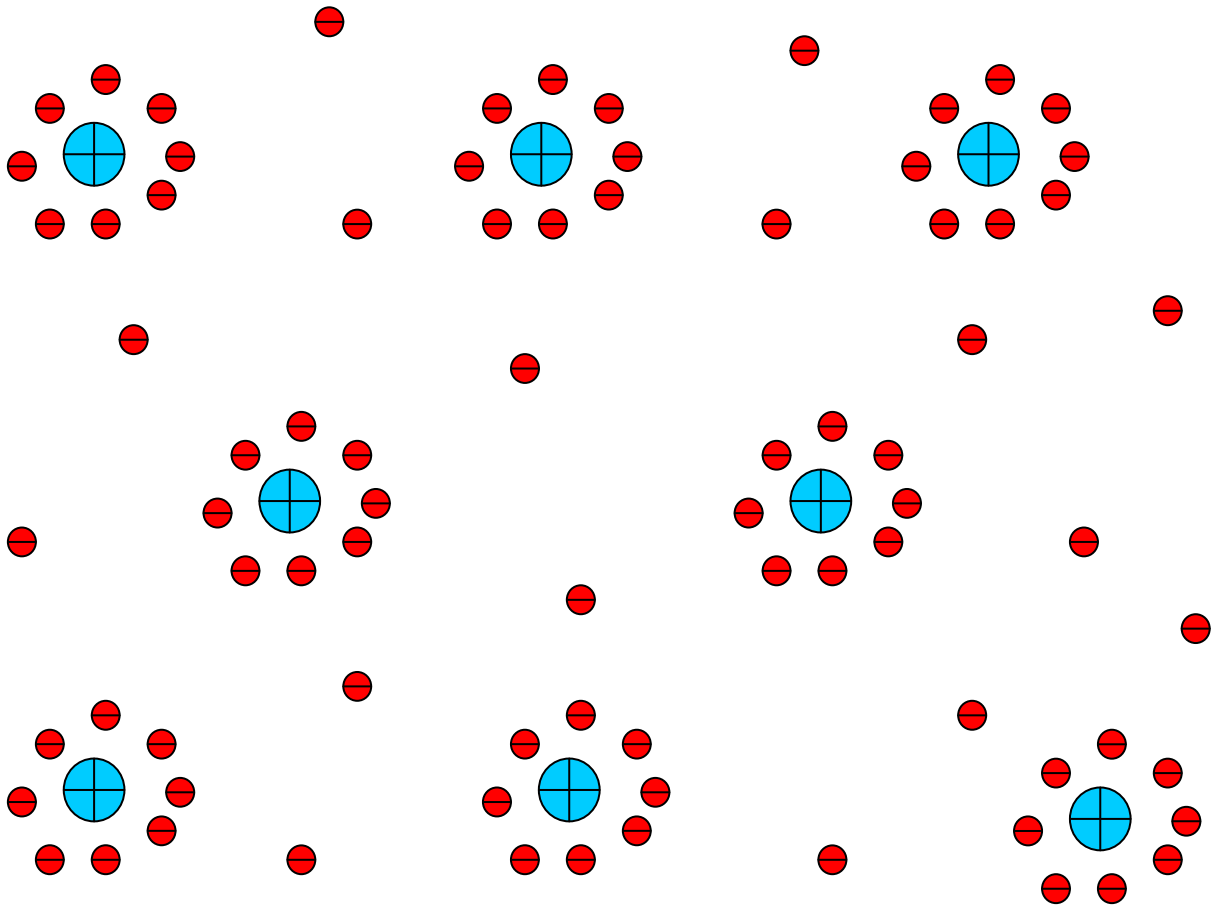

Figure 5.6 - Formation of ordered structures in dense semiclassical plasma.

Static Structural Factors of the System

The static structural factor (SSF) also plays an important role in the investigation of microscopic properties of plasma. Knowing the radial distribution functions, SSF can be defined in the following form:

$$S_{\alpha\beta}(k) = 1 + n\int d\vec{r}\left[g_{\alpha\beta}(r) - 1\right]\exp(-i\vec{k}\cdot\vec{r}), \qquad (5.3)$$

where k is the wave vector; $n = n_e = n_i$ is the density number. As an example, SSF for dense semiclassical plasma is presented in Figure 5.7.

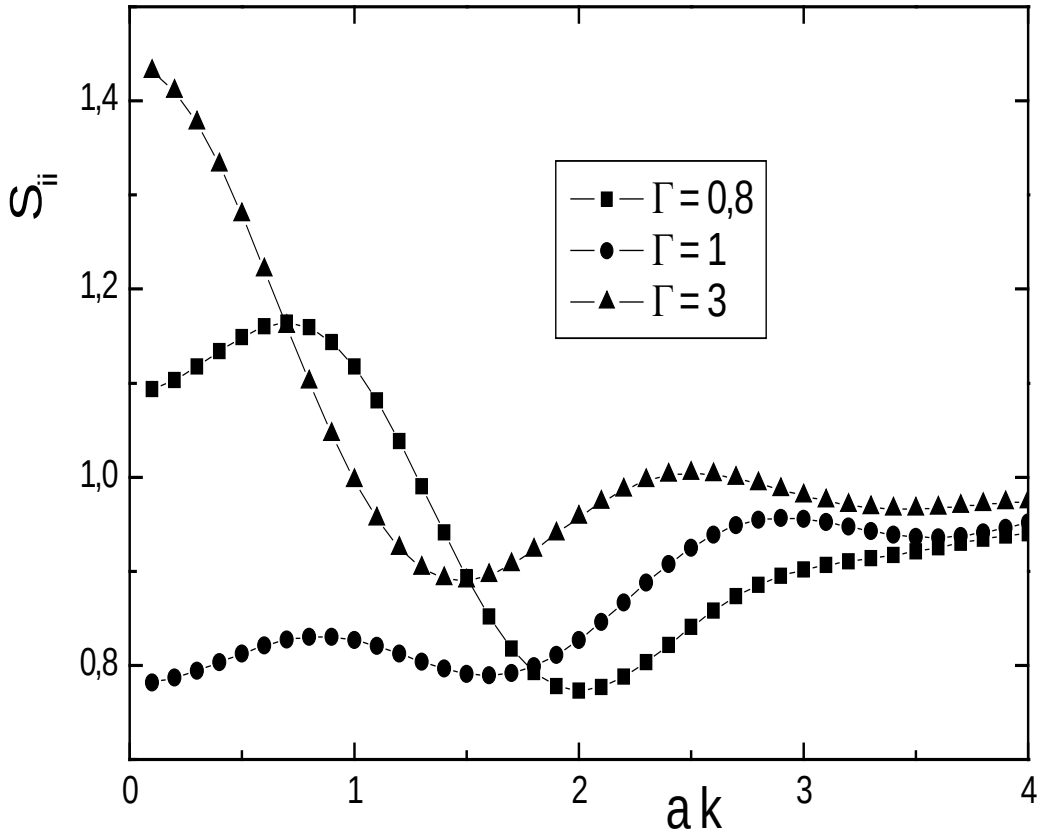

Figure 5.7 - Static structural factors for a dense semiclassical plasma.

Thermodynamic Properties of Plasma

We can define all thermodynamic properties of the plasma on the basis of the radial distribution functions. For instance, the equation of state $P = F(V,T) = f(\Gamma, r_s)$ can be calculated by the following formula:

$$P = nk_B T - \frac{2\pi}{3} n^2 \sum_{\alpha,\beta} \int_0^\infty \frac{d\Phi_{\alpha\beta}(r)}{dr} g_{\alpha\beta}(r) r_{\alpha\beta}^3 \, dr_{\alpha\beta} \,. \qquad (5.4)$$

The internal energy is calculated as follows:

$$E = \frac{3}{2} N k_B T + 2\pi n \sum_{\alpha,\beta} \int_0^\infty g_{\alpha\beta}(r) \Phi_{\alpha\beta}(r) r_{\alpha\beta}^2 \, dr_{\alpha\beta} \,. \qquad (5.5)$$

The excess part of the internal energy is given on the basis of the static structural factors by the following expression:

$$\frac{U_{\alpha\beta}}{Nk_BT} = \frac{1}{16\pi^3 k_B T}\int d\vec{k}\tilde{\Phi}_{\alpha\beta}(k)\left[S_{\alpha\beta}(k)-1\right], \qquad (5.6)$$

where $\tilde{\Phi}_{\alpha\beta}(k)$ is the Fourier transform of the potential.

In Figures 5.8 and 5.9 the results for excess internal energy and equation of state of dense semiclassical plasma are presented. The MC simulation results have a reasonable agreement with the Debye's asymptotic theory at $\Gamma \sim 1$ and the data of Ishimaru et al. [16], and Pierleoni et al. [17] at at the other values of the coupling parameter.

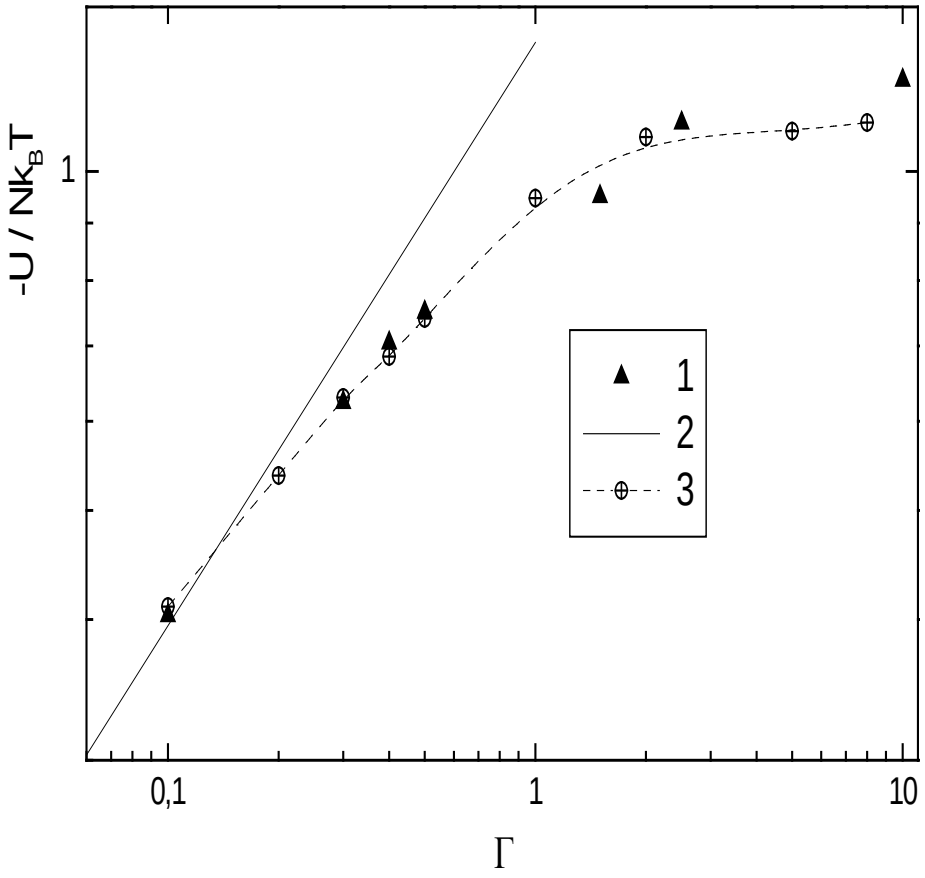

Figure 5.8 - Excess internal energy of a dense semiclassical plasma.

1 – Pierleoni et al. [17]; 2 – the Debye's asymptotic dependence; 3- MC simulation of Ramazanov et al. [18].

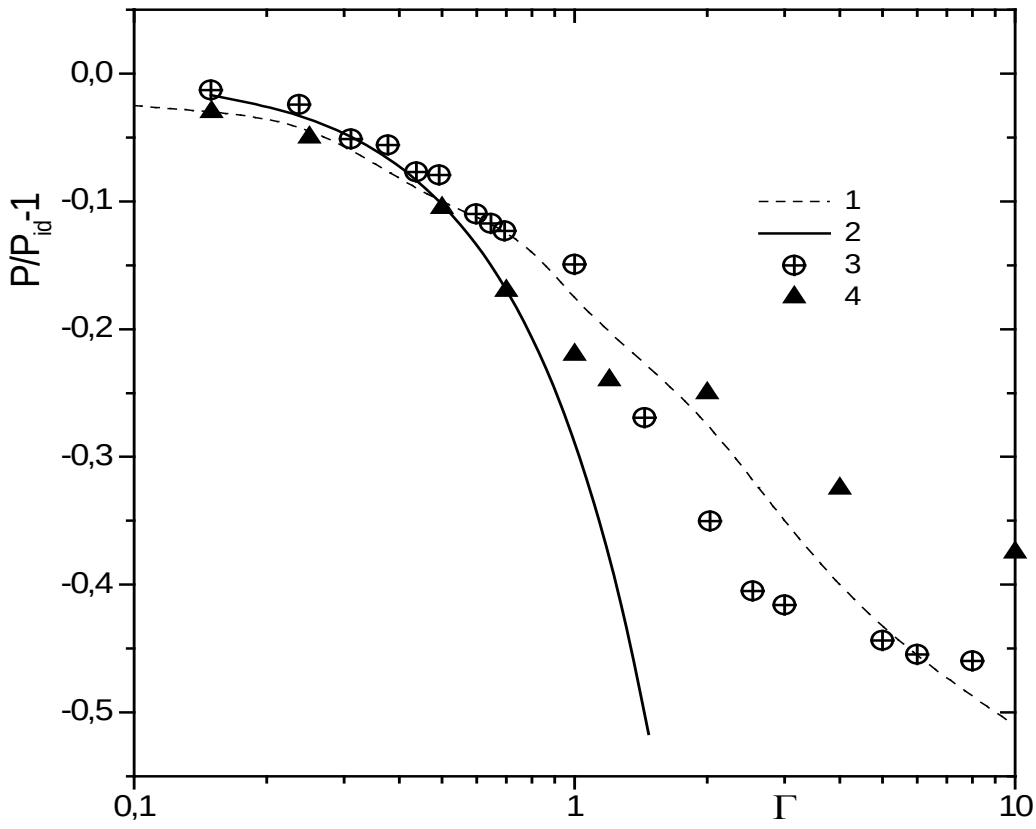

Figure 5.9 - Equation of state of a dense semiclassical plasma.
1 –interpolation formula of Ishimaru et al. [15]; 2 – the Debye's asymptotic dependence; 3- MC simulation of Ramazanov e.a. [17]; 4 - Pierleoni et al. [16].

Questions:

1. Pair correlation functions (PCF).
2. Integral equation methods for calculating PCF.
3. Algorithm for calculation of PCF.
4. Static structural factors of the system.
5. Thermodynamic properties of plasma.

LECTURE 6

Plasma composition in equilibrium state

The most natural way of plasma creation is heating of a gas to a high temperature. In collisions with neutral atoms gas particles, possessing high kinetic energy, knock out electrons from their nuclear orbits, the gas is ionized and a mixture of neutral particles, ions of different charges and electrons arises. It is clear that the degree of ionization of the plasma depends on temperature and concentration of the initial gas, but how? It is possible to give a universal answer if we assume that warm ionized gas is in the thermodynamic equilibrium. Thus, it is possible to use the methods of statistical physics and to consider the ionization process as a chemical reaction, using a minimum of thermodynamic potential in the equilibrium state [8].

Let's consider a system of electrons, ions and atoms of hydrogen in which there are ionization reactions by the electron impact:

$$H \Leftrightarrow H^+ + e^- . \qquad (6.1)$$

Free energy as well as other thermodynamic values is a function of the number of particles of each type:

$$F = F(T, V, N_i^*, N_e^*, N_0^*) . \qquad (6.2)$$

Here N_i^*, N_e^*, N_0^* are numbers of free ions, free electrons and free atoms, respectively. The total number of electrons (ions), both free and bounded, we will denote as $N_e(N_i)$. These values are connected by the following expressions:

$$N_e = N_e^* + N_0^*, \quad N_i = N_i^* + N_0^*, \quad N^*{}_e = N_i^*; \quad N_0 = N_i \quad . \qquad (6.3)$$

The total numbers N_e, N_i in the given system are constants and N_0^*, N_i^*, N_e^* are variables.

In the thermodynamic equilibrium free energy as a function of the numbers of particles must have a minimum, i.e.:

$$\frac{\partial F}{\partial N_i^*}\delta N_i^* + \frac{\partial F}{\partial N_e^*}\delta N_e^* + \frac{\partial F}{\partial N_0^*}\delta N_0^* = 0 . \qquad (6.4)$$

From (6.3) it follows that $\delta N_0^* = -\delta N_e^* = -\delta N_i^*$, therefore

$$\frac{\partial F}{\partial N_i^*} + \frac{\partial F}{\partial N_e^*} = \frac{\partial F}{\partial N_0^*}. \qquad (6.5)$$

Using the chemical potential

$$\mu_k^* = \left(\frac{\partial F}{\partial N_k^*} \right)_{T,V}, \qquad (6.6)$$

one can obtain the equation which presents the equilibrium condition:

$$\mu_i^* + \mu_e^* = \mu_0^*. \qquad (6.7)$$

For the ideal system of particles the chemical potential has the following form:

$$\mu_k^* = \mu_k^*(T) + k_B T \ln n_k^*, \qquad (6.8)$$

here n_k^* -is concentration of k-th component.

Substituting (6.8) in the equation (6.7), we obtain the so-called equation of acting masses:

$$\frac{n_0^*}{n_e^* n_i^*} = \exp\left[\frac{1}{k_B T} (\mu_i^{(0)} + \mu_e^{(0)} - \mu_0^{(0)}) \right] = K(T). \qquad (6.9)$$

The quantity *K(T)* is called the ionization constant. From elementary Boltzman statistics it is known that $\mu_k^{(0)}$ is connected with the statistical sum U_k as follows:

$$\mu_k^{(0)} = -k_B T \left(\ln U_k(T,V) \frac{1}{\Lambda_k^3} \right), \qquad (6.10)$$

$$U_k = \sum_s \exp\left[-\frac{E_s}{k_B T} \right] g_s, \qquad (6.11)$$

$$\Lambda_k = h / \sqrt{2\pi m k_B T}. \qquad (6.12)$$

Here summation is extended to all spectrum of internal power conditions of a particle of k-th type, and g_s characterizes the degeneration degree of the s-th energy level (statistical weight).

The condition with full moment *J* has a statistical weight:

$$g = 2J + 1 \tag{6.13}$$

So, for a free electron with quantum number *l=0* and *s=1/2* the statistical sum is $U_e=2$. Then the equation (6.9) has the following form:

$$\frac{n_0^*}{n_e^* n_i^*} = \Lambda^3 \frac{U_0(T)}{2U_i(T)}, \tag{6.14}$$

$$\Lambda = h / \sqrt{2\pi m_e k_B T} \sqrt{\frac{m_0}{m_i}} \approx h / \sqrt{2\pi m_e k_B T}\,. \tag{6.15}$$

In most cases the ion is in the ground state and division of the nuclear statistical sum is possible. If we assume full degeneration of levels of energy into spin and magnetic quantum numbers, we will have

$$U_0(T) = 2U_i(T)\sigma(T), \tag{6.16}$$

$$\sigma(T) = \sum_{sl} (2l+1) \exp(-E_{sl} / k_B T)\,. \tag{6.17}$$

In this case

$$\frac{n_0^*}{n_e^* n_i^*} = \Lambda^3 \sigma(T) = K(T)\,. \tag{6.18}$$

Expression (6.14) can be generalized for the case of multiple ionization of atoms in non-hydrogen plasma.

For the plasma in the condition of thermodynamic equilibrium the concentrations of any i - and (i+1) -ionized atoms (ions) of the same element are obtained from the equation (6.9):

$$\frac{n_i^*}{n_e^* n_{i+1}^*} = \Lambda^3 \frac{U_i(T)}{2U_{i+1}(T)}, \tag{6.19}$$

where:

n_e^* is the number density of free electrons,

n_i^* is the number density of *i*- times ionized atoms, for example $i=0$ for neutral atoms, $i=1$ for singly ionized particles,

n^*_{i+1} is the number density of *(i+1)* –times ionized atoms,

$U_i\ (T)$ is the statistical sum of *i-times* ionized atoms,

$U_{i+1}(T)$ is the statistical sum of (*i*+1)-times ionized atoms.

Let us note that all energies are counted from zero energy E=0 of the free electron, i.e. all bounded energies are negative. We will consider now the states sum σ for hydrogen plasma.

$$E_s = -\frac{I}{s^2}, \quad I = \frac{me^4}{2\hbar^2},$$
$$\sigma(T) = \sum_{s=1}^{\infty} s^2 \exp(I/(k_b T s^2)) \quad . \tag{6.20}$$

It is obvious that the sum disperses. It also disperses in case of alkaline metals:

$$\sigma(T) = \sum_{sl} (2l+1) \exp(-E_{sl} / k_B T), \tag{6.21}$$

If we limit by the first term in the statistical sum (2.21), we will obtain the so-called Saha equation. We can write down a system of ionization equations for hydrogen, including the Saha equation and the equations following conditions of a quasi-neutrality and preservation of the number of nuclei:

$$\begin{cases} \dfrac{n^*_0}{n^*_e n^*_i} = \Lambda^3 \exp(I / k_B T) \\ n^*_i = n^*_e \\ n^*_0 + n^*_i = n_0 \end{cases} \quad . \tag{6.22}$$

The Saha equation (6.22) can be applied to calculation of composition of high-temperature ideal plasma of hydrogen. We can define the ionization degree as the relation of the number of free electrons to the total number of electrons:

$$\alpha = n^*_e / n_e \, . \tag{6.23}$$

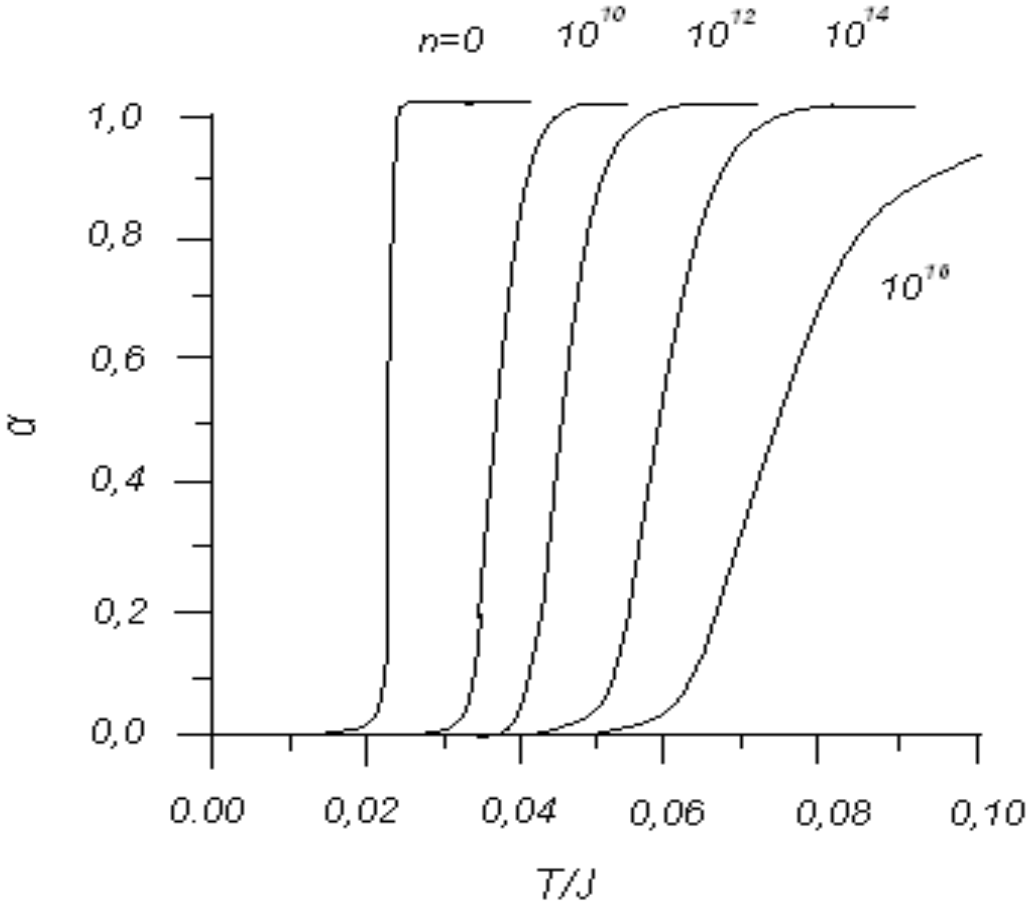

Figure 6.1 - Ionization degree of hydrogen plasma at different values of the number density (in the Figure in units of cm^{-3}).

The qualitative dependence $\alpha(T)$ is shown in Figure 6.1. At small temperatures α equals to zero, at high – to 1t, with smooth transition at intermediate temperatures.

In the nonideal plasma it is necessary to consider the collective effects which lead to a decrease in the potential of ionization (ionization by pressure). We consider the basic concepts of the thermodynamic theory of ionization equilibrium taking into account interactions between particles.

The chemical potential in any nonideal plasma also contains an additional contribution caused by interaction, i.e.

$$\mu_K^* = \mu_K^0(T) + k_B T \ln n_K^* + (\mu_K^*)^{\text{int}}. \qquad (6.24)$$

The elementary approach is the Debye approach, in which

$$(\mu_K^*)^{\text{int}} = -\frac{Ze^2}{2r_D}. \qquad (6.25)$$

Let us define now the ionization decrease as

$$\Delta I = -\frac{Ze^2}{2r_D}. \tag{6.26}$$

We can also find the Saha equation for nonideal plasma

$$\frac{n_0^*}{n_e^* n_i^*} = K(T)\exp(\Delta I / k_B T) = K_{eff}. \tag{6.27}$$

It is obvious that the system has the bounded states while there are negative eigenvalues of the Schrödinger equation. In systems with Coulomb interaction the existence of bounded states is limited by screening. Under the condition

$$r_D \le a_0. \tag{6.28}$$

The bounded states do not exist, i.e. K_{eff} is zero at $r_D < a_0$. Then we have a system of the Saha equations for hydrogen in the following form:

$$\begin{cases} \dfrac{n_0^*}{n_e^* n_i^*} = K_{eff} \\ n^*_i = n^*_e \\ n^*_0 + n^*_i = n_0 \end{cases}, \tag{6.29}$$

where

$$K_{eff} = \begin{cases} K(T)\exp(-\beta e^2/(2r_D)), & r_D \ge a_0, \\ 0, & r_D < a_{0.} \end{cases}. \tag{6.30}$$

In Figure 6.2 the concentrations of ions and free electrons of non-ideal Al plasma in the Debye approximation are presented [18].

Al plasma; Density: $n = 10^{20}$ cm^{-3};

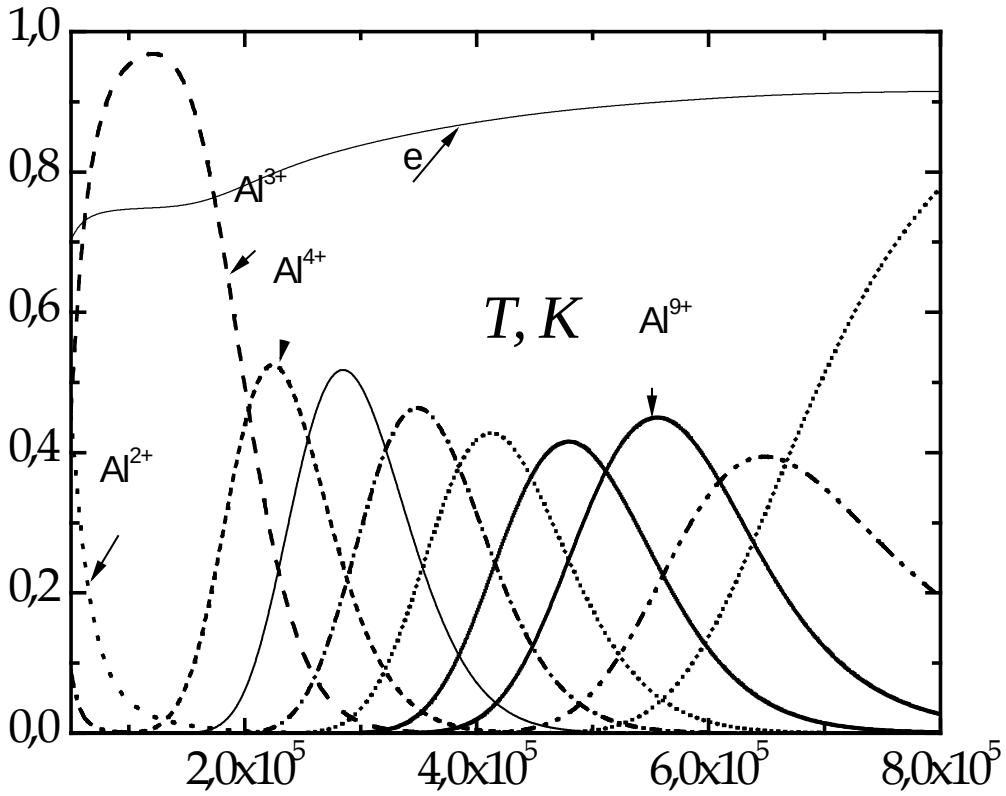

Figure 6.2 – Composition of Al plasma.

Questions:

1. Definition of the plasma composition in the equilibrium state.
2. The Saha equation for ideal plasma.
3. The Saha equation for nonideal plasma.
4. The decrease in the ionization potential.
5. Composition of nonideal plasma on the basis of Debye approximation.

LECTURE 7

Composition of dense Beryllium and Carbon Plasma

Effective potentials that take into account both collective effects at large distances and quantum diffraction effects at small distances were derived by means of the dielectric function [4, 5, 7]. All effective potentials introduced above can be used if $\lambda_{ei} < r_D / 2$.

Composition of partially ionized plasma

Partially ionized plasmas are multi-component systems that contain electrons, ions, and atoms. The interactions between the particles cause a decrease of the ionization potential compared with isolated atoms and ions; for details [8]. The composition of partially ionized non-ideal plasmas in thermodynamic equilibrium requires the evaluation of the chemical equilibrium for all relevant reactions in the system for a given density and temperature [6]. If the formation of molecules and higher neutral clusters can be neglected, the following ionization processes are taken into account [14]:

$$\begin{aligned} &Be \Leftrightarrow Be^{1+} + e; \quad Be^{1+} \Leftrightarrow Be^{2+} + e; \quad ..., \quad Be^{3+} \Leftrightarrow Be^{4+} + e; \\ &C \Leftrightarrow C^{1+} + e; \quad C^{1+} \Leftrightarrow C^{2+} + e; \quad ..., \quad C^{5+} \Leftrightarrow C^{6+} + e; \end{aligned} \quad . \qquad (7.1)$$

The system of Saha equations for the calculation of the plasma composition with maximal ionization state $k+$ can then be written in the following form:

$$n_0 = \frac{g_0}{g_{1+}} n_{1+} \exp\left[\beta(\mu_e^{id} + E_{ion}^{1+} + \Delta\mu_{1+}) \right]$$

$$\cdots\cdots\cdots\cdots\cdots\cdots\cdots\cdots\cdots\cdots \qquad (7.2)$$

$$n_{(k+)-1} = \frac{g_{(k+)-1}}{g_{k+}} n_{k+} \exp\left[\beta(\mu_e^{id} + E_{ion}^{k+} + \Delta\mu_{k+}) \right],$$

where $\beta = 1/k_B T$; $\mu_e^{id} = k_B T \ln(n_e \Lambda_e^3 / 2)$ is the ideal electron chemical potential, g_0=4, g_1=2, g_2=1, g_3=2, g_4=1 the spin factors for beryllium atom and ions, g_0=9, g_1=6, g_2=1, g_3=2, g_4=1, g_5=2, g_6=1 are the spin factors for carbon atom and ions. The values $\Delta\mu_{k+} = \mu_e^{nonid} + \mu_{k+}^{nonid} - \mu_{(k+)-1}^{nonid}$ are corrections due to the non-ideality of the plasma resulting in a shift of the chemical equilibrium relative to the ideal plasma.

These corrections to the chemical potentials are related to the free energy of the system. According to the usual relation:

$$\mu = \frac{\partial F}{\partial N_\alpha}, \ \Delta\mu_a = \left(\frac{\partial \Delta F}{\partial N_a}\right)_{T,V}. \tag{7.3}$$

The free energy is connected with the internal energy and the pressure. It is possible to determine the free energy F from well-known Clausius-Helmholtz relation:

$$\frac{E}{T^2} = -\frac{\partial}{\partial T}\frac{F}{T}, \ \frac{\Delta E}{T^2} = -\frac{\partial}{\partial T}\frac{\Delta F}{T}, \tag{7.4}$$

where ΔE is the energy in the plasma caused by the interaction between the particles:

$$\Delta E = \frac{V}{2}\sum_\alpha eZ_\alpha n_\alpha \phi_\alpha, \tag{7.5}$$

and V is the volume of the plasma, $eZ_\alpha\phi_\alpha$ is the potential energy of every ion in the electron field around the probe ion; ϕ_α is the potential energy created by charges at the location of the probe ion. Based on the effective interaction potentials (1.16) and (1.17), the non-ideality corrections to the chemical potentials were calculated.

In order to solve the system of Saha equations, we have to consider two further equations, the conservation of the number of nuclei and the conservation of the total charge in the system,

$$\sum_{k+=1} n_{k+} + n_0 = const, \ \sum_{k+=1} k n_{k+} = n_e. \tag{7.12}$$

The contribution from the polarization of neutral atoms [8] was calculated via the linearized virial coefficient for the interaction of electrons with atoms (2.13):

$$\mu_{eAtom}^{nonid} = n_{Atom}^0 B^{PP}, \quad B^{PP} = \int d^3r \ \Phi_{eAtom}(r). \tag{7.13}$$

Composition of Be plasma

We have solved the system of equations (7.9)-(7.13) numerically and present the results in Figures 7.1-7.3. The corrections to the chemical potentials (a decrease in the ionization energy) for Be plasma are compared with the usual Debye shift in Figure 1 as a function of temperature at a fixed density of $n=10^{20}$ cm^{-3}. The present results show that the consideration of short-range quantum diffraction effects beyond the Debye model in moderately dense plasmas gives lower ionization potentials. Figure 7.2 presents the curves for the relative fractions of particles versus the temperature for dense Be plasma at $\rho = 0.1 g/cm^3$ in comparison to the data of Kerley [24] and results calculated with the program package COMPTRA04 [25] taking into account higher interaction corrections based on efficient interpolation formulas. As one can see from Figure 7.2, all results are in good agreement for high temperatures, i.e. for weak non-ideality. The differences between the curves are mainly due to the consideration of quantum diffraction effects via the effective potentials in the present study. In Figure 7.3 the degree of ionization for Be plasma is shown for different temperatures.

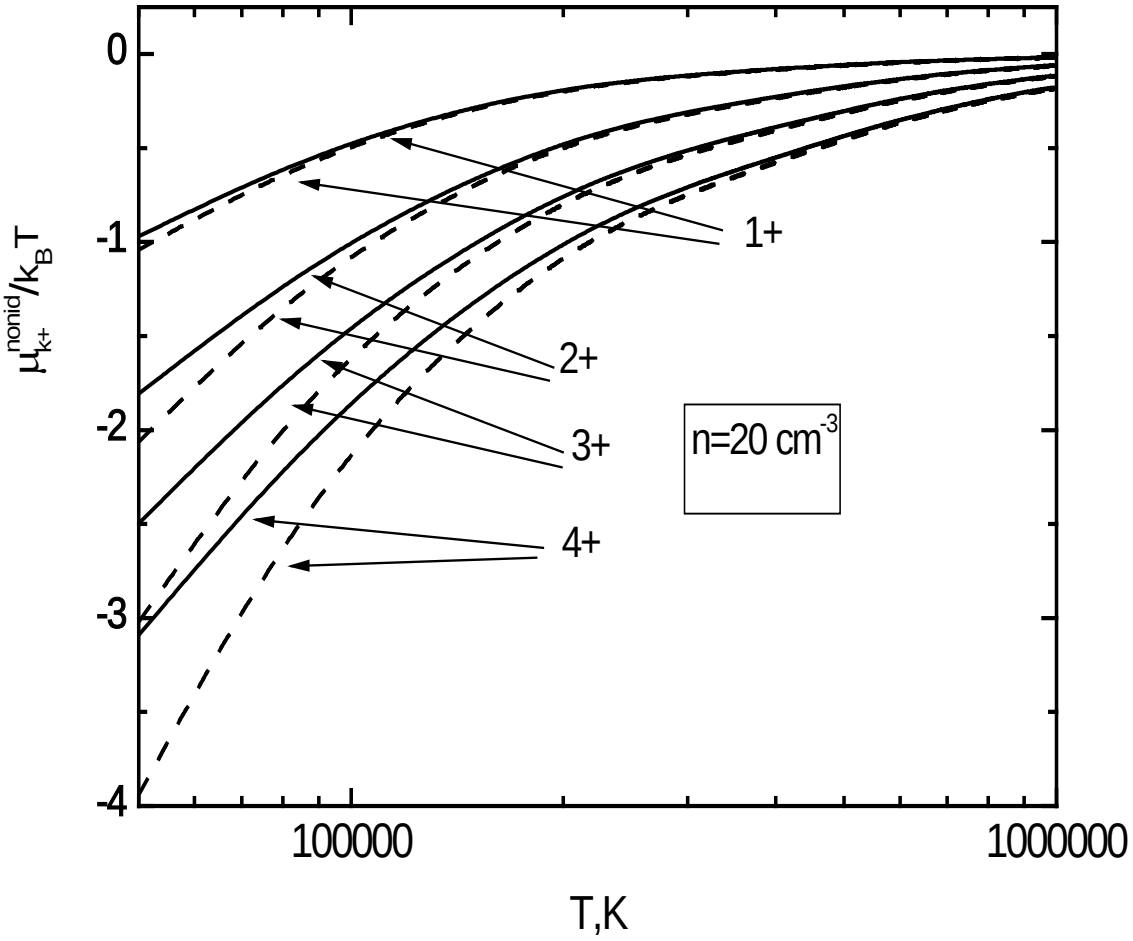

Figure 7.1 - Correction of the chemical potentials of non-ideal Be plasma: solid lines are the Debye approximation;
dashed lines are the results of the present work.

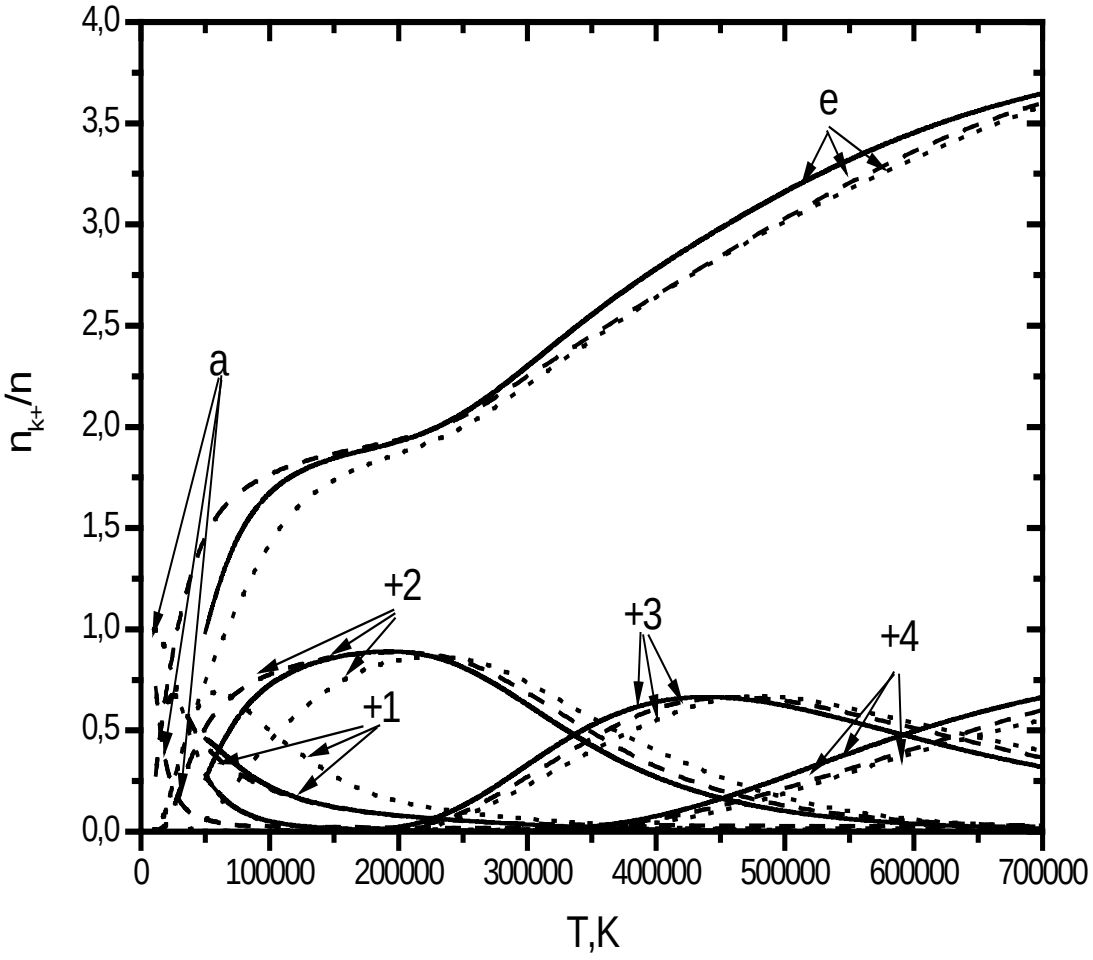

Figure 7.2 - Composition of Be plasma at $\rho = 0.1 g / cm^3$:
solid lines are the results of present woqsswrk; dashed lines are the results obtained by COMPTRA04; dotted lines are results of Ref.[20].

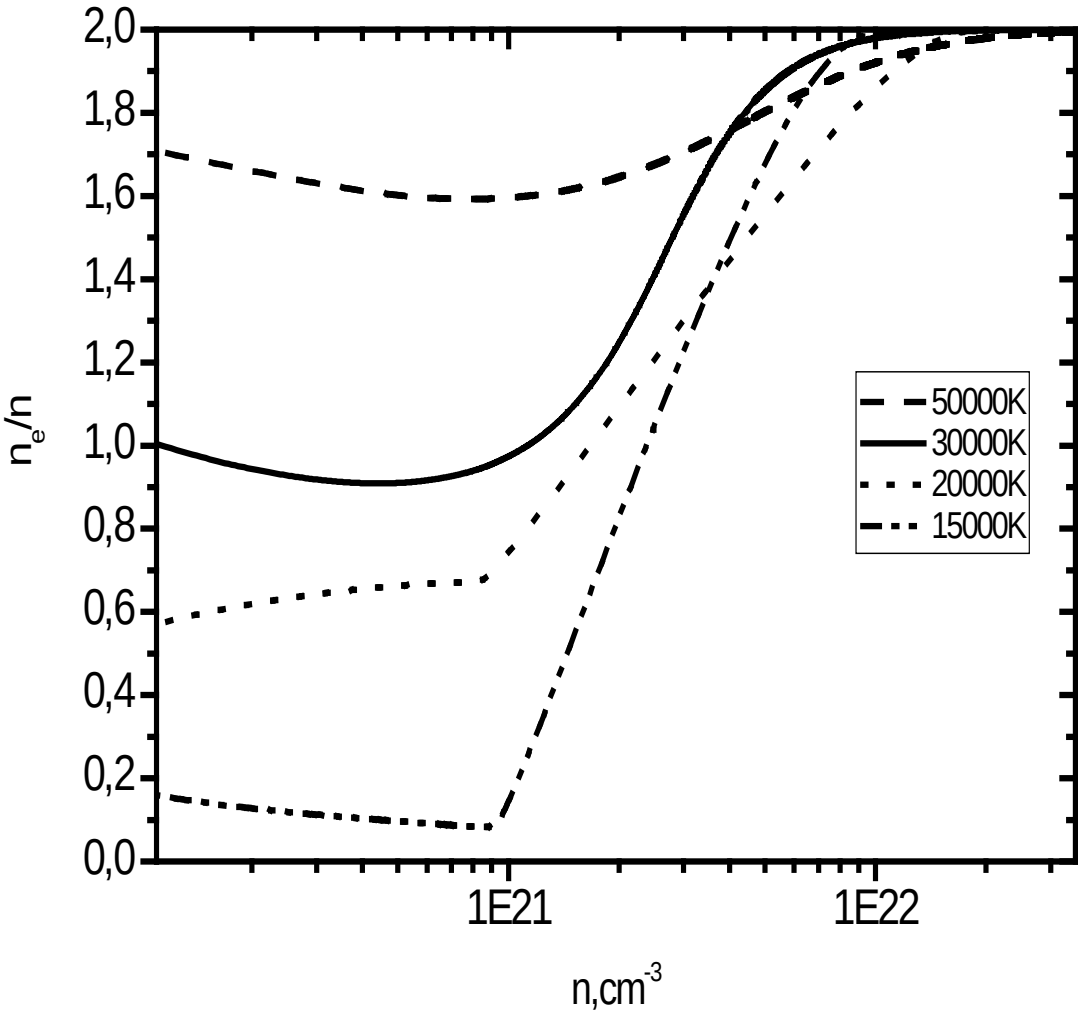

Figure 7.3 - Ionization degree of Be plasma
for different temperatures.

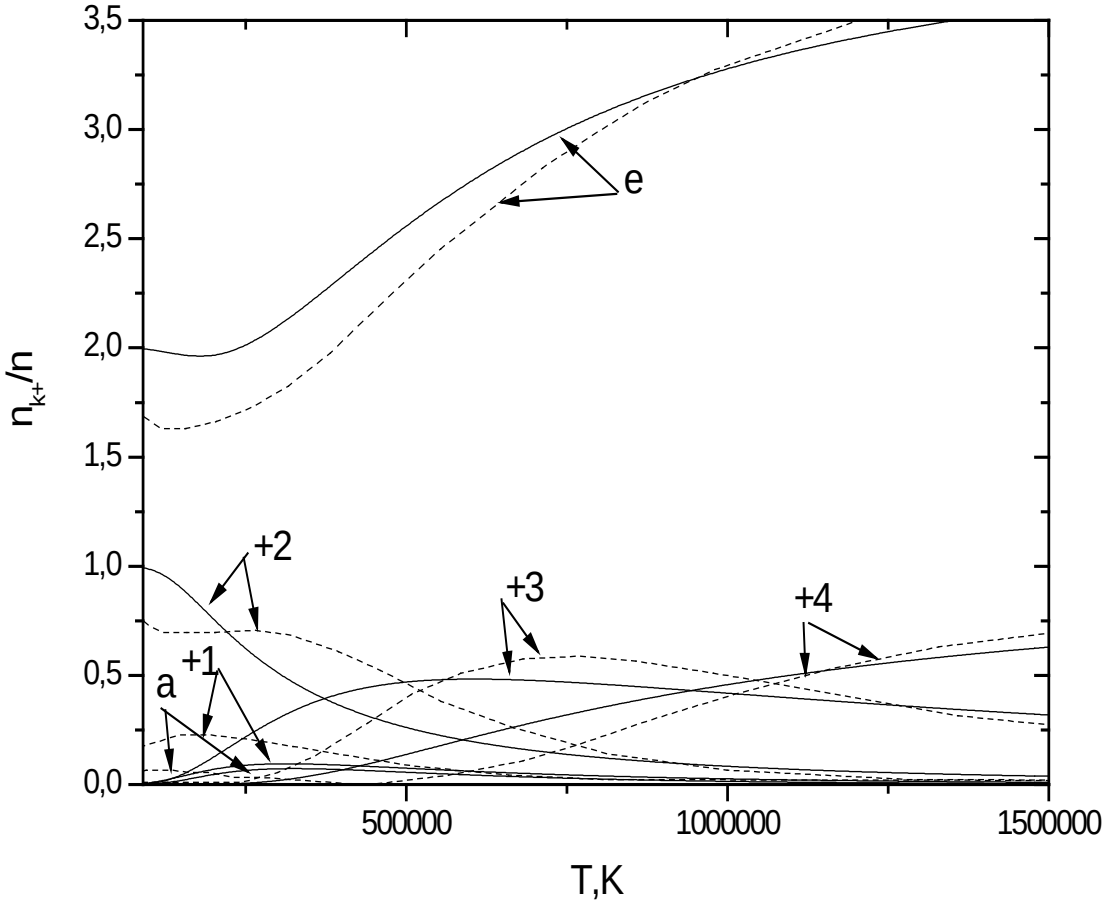

Figure 7.4 - Composition of Be plasma at $\rho = 1.85 g/cm^3$:
solid lines are the results of the present work; dashed lines are the results obtained by COMPTRA04.

Composition of C plasma

As for Be plasmas the composition of C plasma was derived by solving numerically the system of equations (7.9)-(7.13). The results are presented in Figures 7.5-7.6. The decrease in the ionization energies in C plasma was calculated on the basis of the effective potentials (7.1)-(7.3). Figure 7.4 shows the curves for the relative fractions of all particles versus temperature for dense C plasma at $\rho = 0.01 g/cm^3$ in comparison with results of Ref. [13]. Figure 7.5 shows the curves for the relative fractions of all particles versus temperature at a constant number density of $n = 1.4 \times 10^{22} / cm^3$ in comparison with results of Ref. [26]. The consideration of quantum diffraction effects in the interactions when calculating the composition of dense C plasma leads to the deviations in the curves.

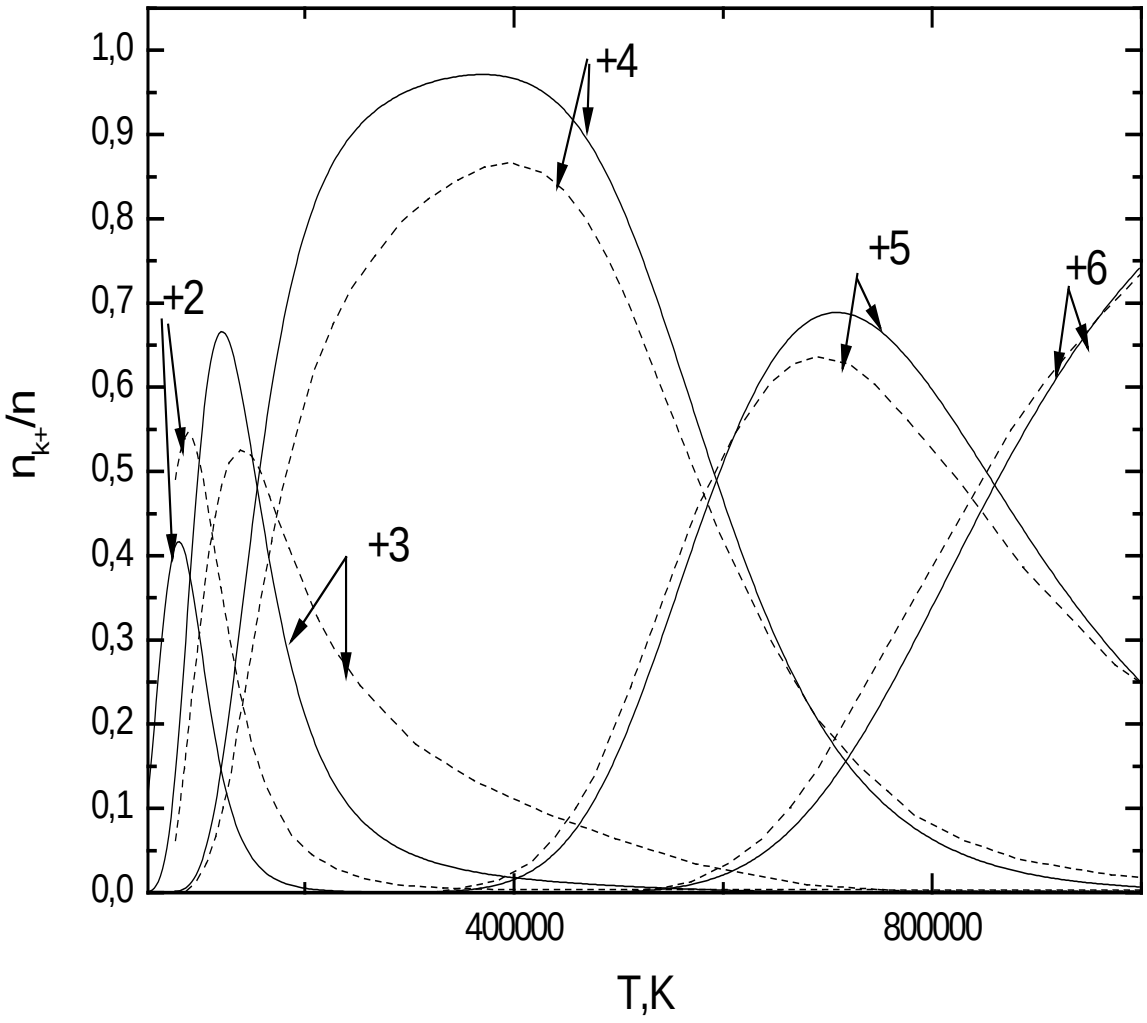

Figure 7.5 - Composition of non-ideal C plasma at a constant density of $\rho = 0.01 g / cm^3$ as function of temperature: solid lines are the results of the present work; dashed lines are the results of Ref. [21].

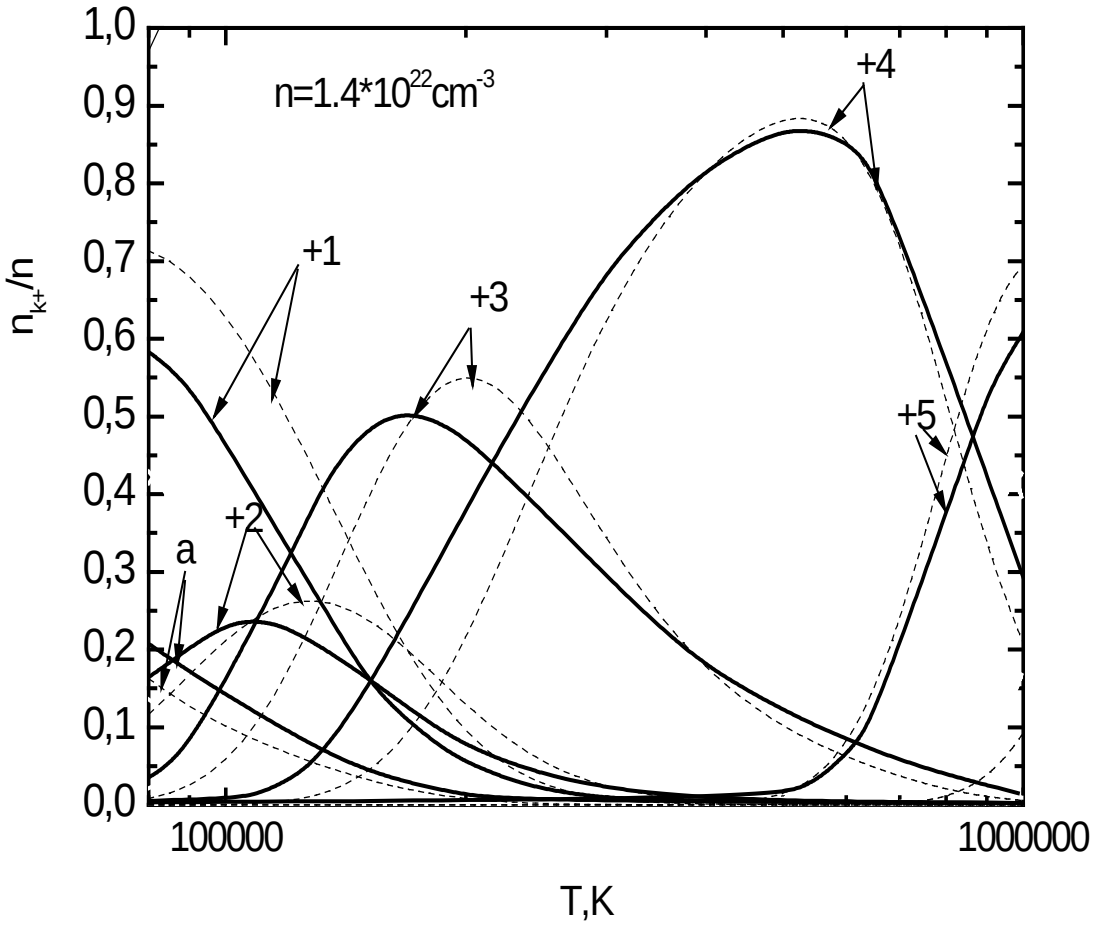

Figure 7.6 - Composition of non-ideal C plasma at a constant number density of $n = 1.4 \times 10^{22} / cm^3$ as a function of temperature: dashed lines are the results of the present work; solid lines are the results of Ref. Kundson.

Questions:

1. Composition of partially ionized plasma.
2. Composition of a semiclassical nonideal plasma.
3. Influence of non-ideality of the plasma in calculations of the plasma composition.
4. The corrections to the chemical potentials of Be and C plasma.
5. Quantum diffraction effects in calculations of the plasma composition.

LECTURE 8

Transport Properties of Nonideal Plasmas

Introduction

It is known that electrophysical properties of plasma are primarily determined by the electron component. Electrical conductivity of weakly nonideal plasma at $\Gamma << 1$ can be determined by well known Spitzer theory. For strongly coupled plasma ($\Gamma > 1$) we use a computer simulation molecular dynamic method. The transport properties of nonideal plasma at the moderate values of coupling parameter can be investigated by kinetic equation methods.

Electrical conductivity of weakly ionized plasma

The electrical conductivity σ is defined by the number density of electrons n_e and their mobility μ:

$$\sigma = e\mu n_e . \tag{8.1}$$

In the case of nonideal plasma, these quantities are connected by well known expressions from kinetic theory. The number densities of electrons n_e and ions n_i are related by the Saha formula (see Lecture No. 5):

$$\begin{cases} n_i \cdot n_e = K_1 n_a ; \\ K_1 = \dfrac{2\sum_i}{\sum} \left(\dfrac{m k_B T}{2\pi\hbar^2} \right)^{3/2} \cdot \exp(-I / k_B T) , \end{cases} \tag{8.2}$$

where n_a is the number density of atoms; $\sum$ and $\sum_i$ are statistical sums of atoms and ions, respectively; I is the ionization potential. Due to the absence of complex ions in the ideal plasma, we have $n_i = n_e$. At low temperatures the degree of ionization is low ($n_e << n_a$):

$$n_e = \sqrt{K_1 n_a} . \tag{8.3}$$

Electron–ion and electron–electron interactions can be ignored in weakly ionized plasma; therefore, we consider only interactions of electrons with atoms (molecules) of a neutral gas. Such a model of plasma is called the Lorentz gas model.

We will use the Boltzmann equation to derive the expression for mobility of electrons. In stationary and spatially homogeneous cases the Boltzmann kinetic equation for the distribution function of electrons $f(\upsilon)$ in the electric field $\vec{F}$ has the following form:

$$-\left(\frac{e\vec{F}}{m}\right)\partial f(\vec{\upsilon})/\partial\vec{\upsilon} = I_c(f)\,. \tag{8.4}$$

It should be noted that the left–hand side of this equation describes the field effect and the right–hand side is responsible for the variation of the number of electrons in an element of phase volume due to collisions; $I_c(f)$ is the collision integral. We assume small deviations of $f(\upsilon)$ from equilibrium due to the fact that the electron mass is much smaller than the atomic mass. Then, $f(\upsilon)$ should be close to spherically symmetric form and can be represented as follows:

$$f(\vec{\upsilon}) = f_0(\vec{\upsilon}) + \cos\vartheta\, f_1(\vec{\upsilon})\,, \tag{8.5}$$

where ϑ is the angle between the directions of the velocity and the electric field. Under conditions of thermodynamic equilibrium the symmetric part of the distribution function $f_0(\upsilon)$ is maxwellian. Notice that the nonsymmetric part $f_1(\upsilon)$ is important for calculation of the electron mobility and, consequently for investigation of plasma electrical conductivity.

Substituting the expression (8.5) for $f(\upsilon)$ in the kinetic equation (8.4) we obtain the following formula:

$$-\left(\frac{e\vec{F}}{m}\right)\partial f_0(\vec{\upsilon})/\partial\vec{\upsilon} = I_c(f_1)\,. \tag{8.6}$$

The direction of electron's velocity is strongly changed at each collisions and this direction does not depend on its velocity before collisions. Then

$$I_c(f_1) = -\nu(\vec{\upsilon})\, f_1(\vec{\upsilon})\,;\;\; \nu(\vec{\upsilon}) = n_a \upsilon q(\vec{\upsilon})\,, \tag{8.7}$$

where $q(\vec{\upsilon})$ is the transport cross section of electron–atom scattering and $\nu(\vec{\upsilon})$ is the corresponding electron–atom collision frequency. The electrons are mainly in chaotic thermal motion and drift in the direction opposite to the field $\vec{F}$. The drift velocity ($\vec{\omega} = -\mu\vec{F}$) is defined as the mean electron velocity over the time

considerably exceeding the time between individual collisions and given by the following expression:

$$\omega = \int \upsilon \cos\vartheta f(\vec{\upsilon}) d\vec{\upsilon} = \int \upsilon \cos^2\vartheta f_1(\vec{\upsilon}) d\vec{\upsilon}\,, \qquad (8.8)$$

because $f_0(\upsilon)$ does not make contribution to ω. Substituting the expression for $f_1(\upsilon)$ from kinetic equation in the formula for drift velocity ω we have the following relation for mobility of electrons $\mu = \omega / F$:

$$\mu = \frac{e}{m} \int \frac{\partial f_0}{\partial \vec{\upsilon}} \cos^2\vartheta \frac{\vec{\upsilon} d\vec{\upsilon}}{\nu(\vec{\upsilon})}\,. \qquad (8.9)$$

Integrating over the angles and substituting the maxwellian distribution for $f_0(\upsilon)$, and using the fact that $\partial f_0 / \partial \vec{\upsilon} = -f_0 \vec{\upsilon} / \upsilon_T^2$ we finally get:

$$\mu = \frac{1}{3}\sqrt{\frac{2}{\pi}} \frac{e}{m\upsilon_T^5} \int_0^\infty \frac{\upsilon^4}{\nu(\vec{\upsilon})} \exp\left(-\frac{\upsilon^2}{2\upsilon_T^2}\right) d\upsilon\,, \qquad (8.10)$$

where $\upsilon_T = \sqrt{k_B T / m}$ is the thermal velocity of electrons. Expressions (8.9) and (8.10) describe the mobility of electrons in the Lorentz plasma approximation. It should be noted that formula (8.10) is useful for calculation of electron's mobility in the real plasma. But in this case we should know electron-atom collision frequency $\nu(\upsilon)$.

The expressions (8.9) and (8.10) are valid at the following conditions:

1) The binary collision approximation is valid and the neutral gas must be sufficiently rarefied, i.e. $n_a q^{3/2} << 1$.

2) The temperature must be sufficiently high and the thermal wavelength of the electron sufficiently small, so that we can ignore the interference of the electron on atoms, i.e. $n_a q \lambda_e << 1$.

3) The potential energy of the Coulomb interaction between electrons must be much smaller than their kinetic energy, i.e. $e^2 n_e^{1/3} / k_B T << 1$.

4) The plasma must be nondegenerate, i.e. $\hbar^2 n_e^{2/3} / m k_B T << 1$.

5) The correlation between atoms can be neglected, i.e. $n_a b << 1$; $n_a a / k_B T << 1$ (a and b are the coefficients of the van der Waals equation of state for the neutral gas).

It is convenient to integrate over the electron energy $E = m\upsilon^2 / 2$ instead of velocity. Then, we have for mobility the following expression for mobility:

$$\mu = \frac{4}{3}\sqrt{\frac{1}{\pi}}\frac{e}{m(k_B T)^{5/2}}\int_0^\infty \frac{E^{3/2}}{\nu(E)}\exp\left(-\frac{E}{k_B T}\right)dE, \qquad (8.11)$$

where the collision frequency is $\nu(E) = n_a q(E)\sqrt{2E/m}$. Introducing the mean (effective) collision frequency $\overline{\nu}$ and cross section $\overline{q}$, one can write:

$$\begin{cases} \mu = \dfrac{e}{m\overline{\nu}}; \\ \overline{\nu} = \left(3\sqrt{2\pi}/4\right) n_a \overline{q}(T)\upsilon_T \end{cases}, \qquad (8.12)$$

where

$$\frac{1}{\overline{q}(T)} = \frac{1}{(k_B T)^2}\int_0^\infty \frac{E}{q(E)}\exp\left(-\frac{E}{k_B T}\right)dE. \qquad (8.13)$$

In the simplest case when the electron–neutral collision can be approximated as a scattering on a hard sphere of a diameter d, the transport cross section is independent of energy, i.e. $q(E) = \pi d^2 / 4$. In this case by averaging over energies we have the following values:

$$\begin{cases} \overline{q} = \pi d^2 / 4; \\ \overline{\nu} = (3\pi^{3/2} / 2^{7/2}) n_a d^2 \upsilon_T \end{cases}. \qquad (8.14)$$

In the case of real plasma the transport cross section is a function of energy. One can conclude that if the dependence $q(E)$ is known, the mean cross sections $\overline{q}(T)$ can also be easily calculated. A large number of reference data on electron–atom and electron–molecule scattering cross–sections is available from special books. As an example the data of averaged cross–sections for atoms of alkali metals are shown in the table 8.1.

Table 8.1

Averaged transport cross sections of electron scattering on atoms of alkali metals, $\overline{q}(T)$ in units of $10^2 a_0^2$

T, 10^3 K	Li	Na	K	Cs	T, 10^3 K	Li	Na	K	Cs
1.0	16.5	15.0	15.3	14.1	2.6	6.88	7.31	7.00	8.98
1.2	14.4	14.0	13.6	12.8	2.8	6.41	6.73	6.52	7.63
1.4	12.6	12.9	12.1	11.7	3.0	5.99	6.23	6.10	7.32
1.6	11.1	11.7	10.9	10.8	3.2	5.63	5.79	5.73	7.04
1.8	9.91	10.6	9.84	10.1	3.4	5.32	5.41	5.41	6.79
2.0	8.93	8.73	8.96	9.42	3.6	5.05	5.07	5.12	6.57
2.2	8.11	8.73	8.20	8.89	3.8	4.80	4.77	4.87	6.37
2.4	7.46	7.97	7.56	8.41	4.0	4.59	4.51	4.64	6.20

The electrical conductivity of plasma can be estimated by the following expression:

$$\sigma \cong 3.8 \cdot 10^6 \frac{n_e}{n_a} \frac{1}{\bar{q}\sqrt{T}} \; ohm^{-1} cm^{-1}, \tag{8.15}$$

where $\bar{q}$ is the average cross section in units of $10^{-16}\ cm^2$ and T is the temperature in K.

Questions:
1. Electrical conductivity of weakly ionized plasma.
2. Electrical conductivity of weakly ionized plasma in the Lorentz approximation.
3. Mobility of electrons in the Lorentz plasma approximation.
4. Validity of expressions (8.9) and (8.10) for mobility of electrons.
5. Collision frequency and cross-sections.

LECTURE 9

Transport Properties of Nonideal Plasmas (continuation)

Introduction

The equation derived in the previous lecture describes the electron mobility on the basis of electron-atom collision frequency and is not valid for the case when the electron–atom collision frequency ν becomes comparable with the electron–ion collision frequency ν_i.

Electrical conductivity of strongly ionized plasma

The above mentioned situation was considered by Spitzer (1962) [1]. It is known that due to the long–range character of the Coulomb interaction a small-angle scattering is important in strongly ionized plasma. The small-angle scattering can be taken into account by the so-called "Coulomb logarithm" $\ln\Lambda$. This quantity in a classical plasma is defined as the ratio between the Debye radius r_D and the Landau length Ze^2/k_BT. More information can be found in the Table 9.1 (see below).

According to Spitzer we can write the expression for electron-ion collision frequency in the following form:

$$\nu_i(E) = 2\pi e^4 Z^2 E^{-3/2} (2m)^{-1/2} n_i \ln\Lambda \ . \qquad (9.1)$$

If we assume that $\ln\Lambda$ does not depend on energy, then averaging over energies gives the following formula for the electron-ion collision frequency:

$$\nu_i = \frac{\pi^{3/2}}{4\sqrt{2}} n_i \sqrt{\frac{k_BT}{m}} \left(\frac{Ze^2}{k_BT}\right)^2 \ln\Lambda \ . \qquad (9.2)$$

Using the condition of electro-neutrality $n_e = Zn_i$ we get the expression for electrical conductivity:

$$\sigma = \frac{2(2k_BT)^{3/2}}{\pi^{3/2} Ze^2 m^{1/2}} \frac{1}{\ln\Lambda}, \qquad (9.3)$$

where $\ln\Lambda = \ln\frac{3}{\gamma}$; $\gamma = Ze^2/(r_D k_B T)$ is the nonideality parameter; $r_D = (4\pi n_e e^2 / k_B T)^{-1/2}$ is the Debye radius of electrons. In plasma due to the Coulomb long–range interaction the electron–electron correlations have influence on the electrical conductivity even at small values of nonideality parameter. In order to take into account these correlations, the term which is responsible for electron–electron collisions must be added to the right–hand side of the kinetic equation.

It should be noted that the electron–electron interactions cause a decrease in electrical conductivity. Initially, the velocity distribution function of electrons is spherically symmetric. The applied field disturbs this symmetrical distribution and the electron–electron interactions oppose this disturbance, consequently, the mobility of electrons decreases. Thus, the resulting expression for the electrical conductivity of fully ionized plasma (Spitzer's formula) is

$$\sigma_{Sp} = C(Z)\cdot\frac{2(2k_B T)^{3/2}}{\pi^{3/2} Z e^2 m^{1/2}}\frac{1}{\ln\Lambda}, \tag{9.4}$$

where $C(Z) = 0,582 \div 1,0$ at different values of charge number Z, i.e. $C(1)=0,582$ and $C(\infty) = 1,0$. For singly charged ions ($Z = 1$) we have

$$\sigma_{Sp} = 1,53\cdot 10^{-4}\cdot\frac{T^{3/2}}{\ln\Lambda}\ Ohm^{-1}\cdot cm^{-1}, \tag{9.5}$$

where T is the temperature in K. The Spitzer theory is valid for classical weakly nonideal plasma.

The Coulomb logarithm for plasma

As it was mentioned above the Coulomb logarithm is an important factor in the kinetic theory of plasma. In the general case it can be defined as a ratio between maximal and minimal values of impact parameter, i.e. $\Lambda = b_{\max}/b_{\min}$. It should be noted that the Coulomb logarithm has different expressions in the cases of classical and quantum plasmas (see Table 9.1).

Table 9.1

Classical and quantum expressions for the Coulomb logarithm

Typical lengths of Coulomb interactions	Classical plasma		Quantum plasma	
	$r_D > n_e^{-1/3}$	$r_D < n_e^{-1/3}$	$r_D > n_e^{-1/3}$	$r_D < n_e^{-1/3}$

$b_{\max}$	$\sim r_D$	$\sim a \approx n_e^{-1/3}$	$\sim r_D$	$\sim a \approx n_e^{-1/3}$
$b_{\min}$	$\sim e^2 / k_B T$	$\sim e^2 / k_B T$	$\sim \lambda\!\!\!^{-}_e$	$\sim \lambda\!\!\!^{-}_e$
Λ	$\sim \Gamma^{-3/2}$	$\sim \Gamma^{-1}$	$\sim \Gamma^{-3/2} \cdot T^{-1/2}$	$\sim \Gamma^{-1} \cdot T^{-1/2}$

According to Table 9.1 we can make the following conclusions:

- For the classical plasma, when $e^2 / k_B T >> \lambda\!\!\!^{-}_e$, then $\Lambda = f(\Gamma)$ and we have $\sigma^* = f(\Gamma)$, where $\sigma^* = e^2 m^{1/2} (k_B T)^{-3/2} \cdot \sigma$. Consequently, in the classical regime the isobars and isotherms for different matters are described by the universal curve $\sigma^*(\Gamma)$ on the coordinate plane $\sigma^* - \Gamma$. Therefore, we can conclude that the Coulomb properties of plasma have a similarity in this case.
- The similarity is not realized when the quantum effects become significant at $b_{\min} \sim \lambda\!\!\!^{-}_e$ and in this case we have the additional dependence of the Coulomb logarithm on temperature. This fact can explain layering (stratification) of isotherms on $\sigma^* - \Gamma$ diagram observed experimentally.

Electrical conductivity of nonideal plasma.
The Chapman-Enskog method

The transport properties of plasma can be calculated by kinetic equation method. In this case it is necessary to know the data of scattering processes of particles or the interaction potential between particles. For instance, the electrical conductivity of plasma is defined as follows:

$$\sigma = \frac{3e^2}{8m\Omega^{(1)}(1)}, \tag{9.6}$$

where

$$\Omega^{(l)}(r) = \sqrt{\pi}\int_0^\infty \exp(-\vec{g}^2)\vec{g}^{(2r+2)}\Phi^{(l)}(\vec{g})d\vec{g};$$

$$\Phi^{(l)}(\vec{g}) = 2(k_B T / m)^{1/2}\vec{g}\int_0^\infty b\left[1-\cos^l \vartheta(b,\vec{g})\right]db; \tag{9.7}$$

b is the impact parameter; $\vec{g} = \vec{u} / 2(k_B T / m)^{-1/2}$ is the dimensionless relative velocity.

The resulting isotherms of the electrical conductivity are shown in Figure 9.1 as a function of the total electron density. Comparison with the fully ionized case shows that partial ionization leads to a decrease in the electrical conductivity, especially at low temperatures. This may lead to a pronounced minimum in the conductivity isotherms.

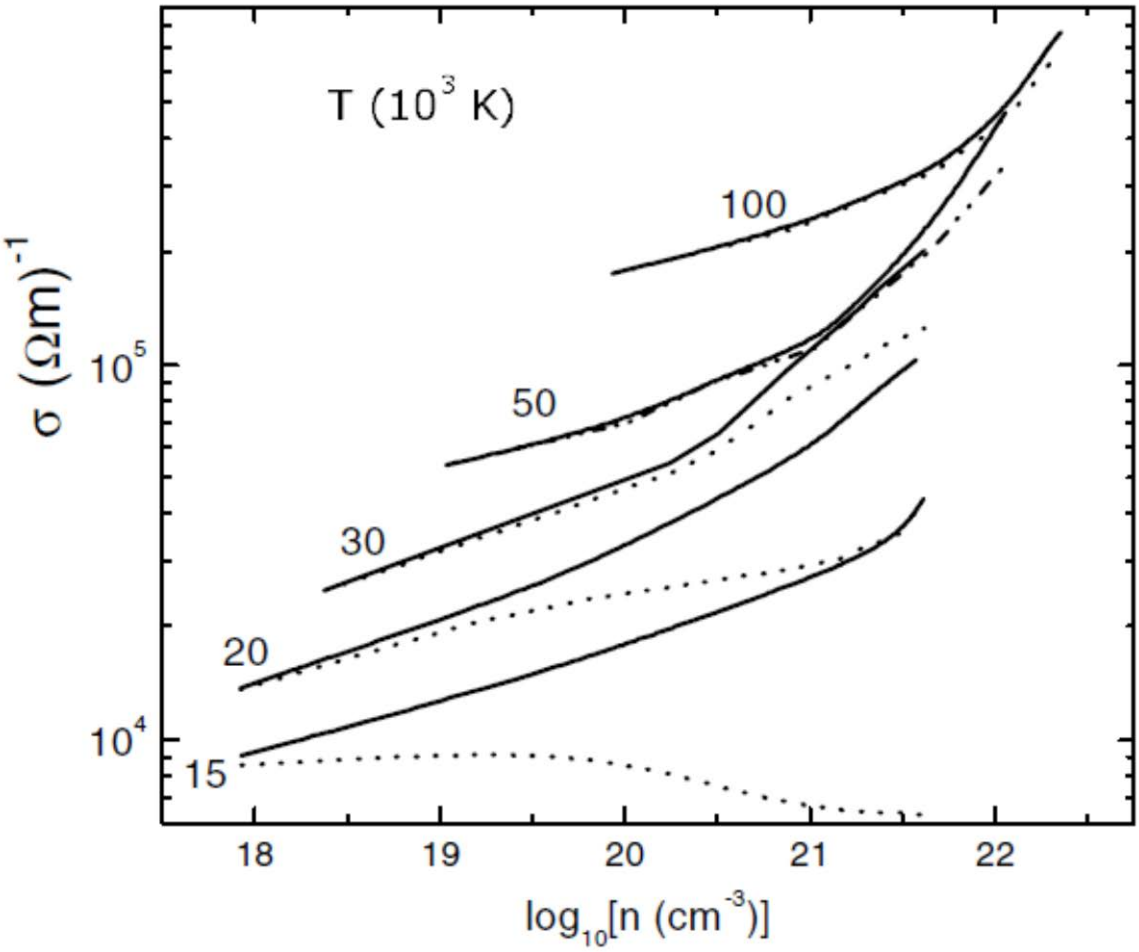

Figure 9.1 - Electrical conductivity of partially ionized hydrogen plasma (broken lines) in comparison with the results for the fully ionized case (solid lines) for various temperatures as a function of the total electron density.

The dimensionless electrical conductivity σ^* is shown in Figure 9.2 as a function of the nonideality parameter γ. For ideal plasmas $\gamma \ll 1$, we have good agreement with the Spitzer theory. The results for the fully ionized case agree well with the data for the partially ionized plasma for $\gamma \leq 0{,}1$. For higher nonideality parameters, the electrical conductivity of the partially ionized plasma is substantially lower. In the strong coupling regime $\gamma \sim 1$ we have good agreement with the experimental data.

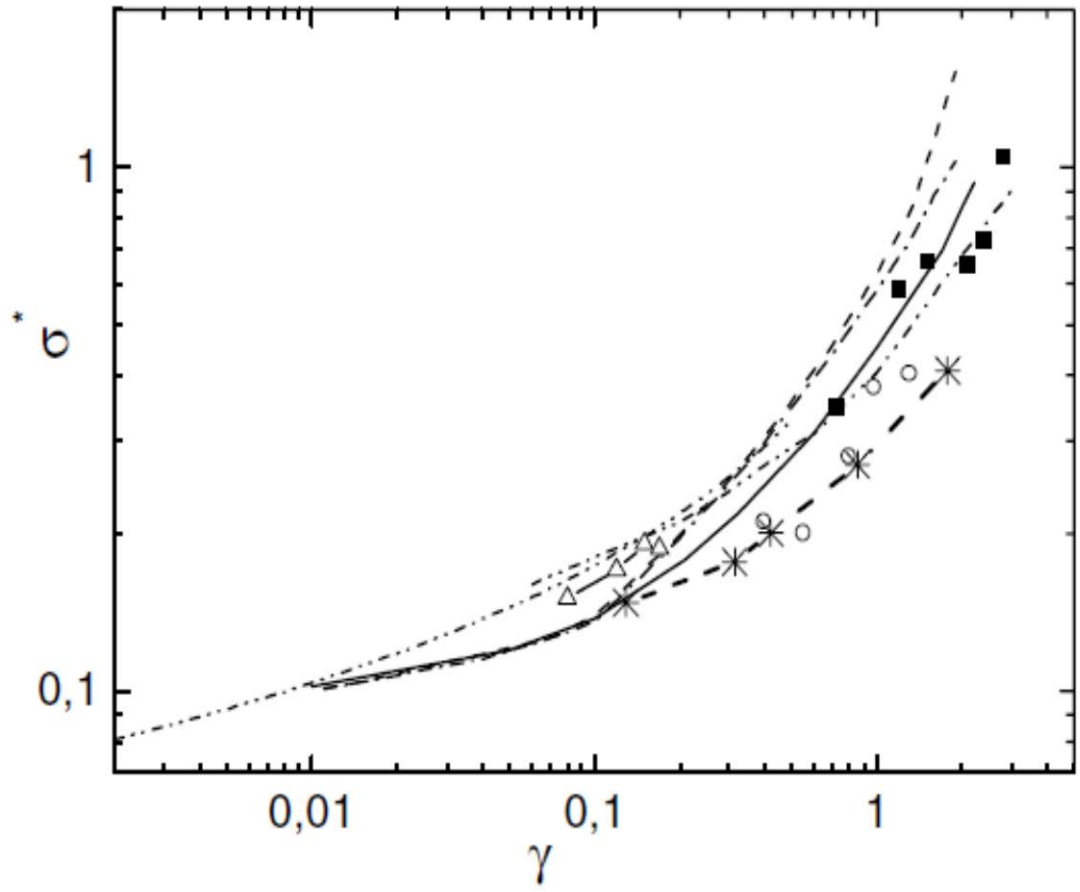

Figure 9.2 - Reduced electrical conductivity as a function of the nonideality parameter. Solid line represents the results for partially ionized plasma (T. Ramazanov et al.); dashed and dash-dotted lines denote the data for fully ionized plasma (Kh. Nurekenov & S. Kodanova); dotted line is the Spitzer theory; asterisks are Ichimaru's results; triangles, boxes and circles represent the experimental data (Radtke, Ivanov et al.).

Questions:
1. Electrical conductivity of strongly ionized plasma.
2. The Spitzer formula.
3. The Coulomb logarithm for plasma.
4. The electrical conductivity of nonideal plasma.
5. The Chapman-Enskog method.

LECTURE 10

Transport Properties of Plasma by Molecular Dynamics Simulation

Introduction

In the previous lecture we have considered molecular dynamics method for computer simulation of equilibrium (thermodynamic) as well as non-equilibrium (transport) properties of plasma. Using this method the microscopic state (particle's coordinates, velocities etc.) can be obtained. But our final goal is the evaluation of transport properties of plasma such as diffusion, electrical conductivity, viscosity etc. For this purpose we will consider at first the autocorrelation functions of dynamical variables. Then we will show how we can calculate macroscopic transport properties of plasma on the basis of the autocorrelation functions of microscopic dynamical variables.

Autocorrelation functions (ACF) of microscopic quantities. Properties of ACF

Definition. An autocorrelation function of random variable $X(t)$ is defined as follows:

$$G(S) = \left\langle X(t) \cdot X(t+S) \right\rangle, \tag{10.1}$$

where $\langle \ldots \rangle$ denotes the ensemble averaging. For random variable we have $\langle X \rangle = 0$. Thus an autocorrelation function at $S = 0$ has the following dispersion $\left\langle X^2 \right\rangle = 0$.

Autocorrelation function means the correlations between current and previous (or initial) microscopic states of the system.

Properties of autocorrelation functions.

1) An autocorrelation function is the even one, i.e.

$$G(S) = G(-S)$$

2) An autocorrelation function has a maximum at $S = 0$. Actually,

$$\left\langle \left[X(t) \pm X(t+S) \right]^2 \right\rangle = \left\langle X^2(t) \right\rangle + \left\langle X^2(t+S) \right\rangle \pm 2 \left\langle X(t) X(t+S) \right\rangle \geq 0,$$

It follows that $G(0) \geq G(S)$.

3) Since $X(t)$ is a random quantity we can suppose that correlation between $X(t)$ and $X(t+S)$ is absent at large values of S, therefore:

$$\lim_{S\to\infty} G(S) = 0$$

There are the most important autocorrelation functions for investigation of plasma's properties.

Velocity autocorrelation functions (VAF):

$$\left\langle \vec{\upsilon}(0)\vec{\upsilon}(t)\right\rangle = \frac{1}{3N}\sum_{i=1}^{N}\vec{\upsilon}_i(t_n)\cdot\vec{\upsilon}_i(t_n+t)\,. \qquad (10.2)$$

Microscopic electrical current correlation function:

$$\left\langle \vec{j}(0)\,\vec{j}(t)\right\rangle = \left\langle \sum_i Z_i\vec{\upsilon}_i(t)\cdot\sum_j Z_j\vec{\upsilon}_j(0)\right\rangle. \qquad (10.3)$$

For simplicity, autocorrelation functions are considered in units of:

$$\sum_{i=1}^{N}\left\langle \vec{G}_i(0)\cdot\vec{G}_i(0)\right\rangle. \qquad (10.4)$$

In Figures 10.1 and 10.2 velocity autocorrelation functions and mean square displacements of coordinates of a dense semiclassical plasma are shown for different values of coupling parameter. It should be noted that fluctuations of these quantities lie within statistical errors $\sim 1/\sqrt{N}$. The convergence of velocity autocorrelation functions becomes weak (slow) with decreasing of coupling parameter. This fact may be connected with decreasing of particle's collision frequency in weakly non-ideal plasma. Mean square displacements increase linearly with dimensionless time (in units of the Longmuir frequency ω_e) $t \le 5$ according to the Einstein formula $\sim 6D(t-t_0)$. The saturation range ($t \ge 12$) indicates that particles are distributed uniformly and diffusion process reaches its stationary value.

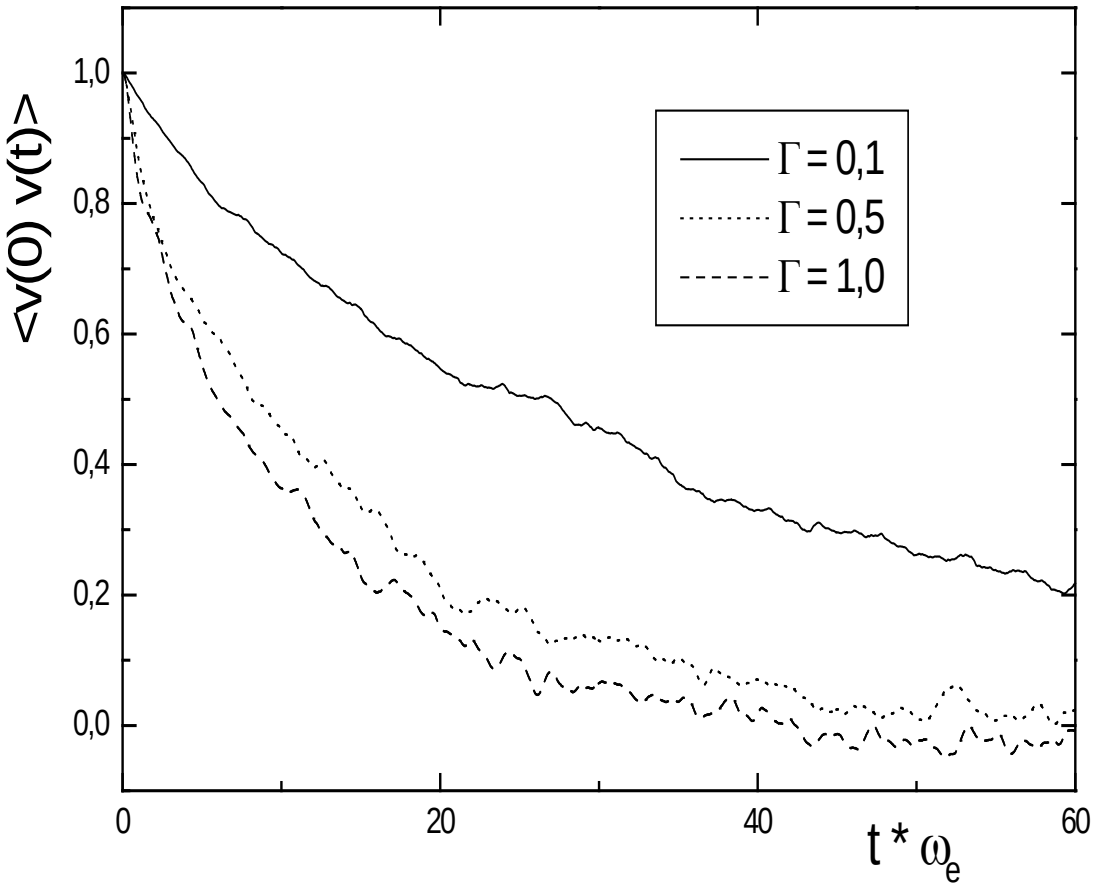

Figure 10.1 - Velocity autocorrelation as a function of dimensionless time at $r_S = 2$.

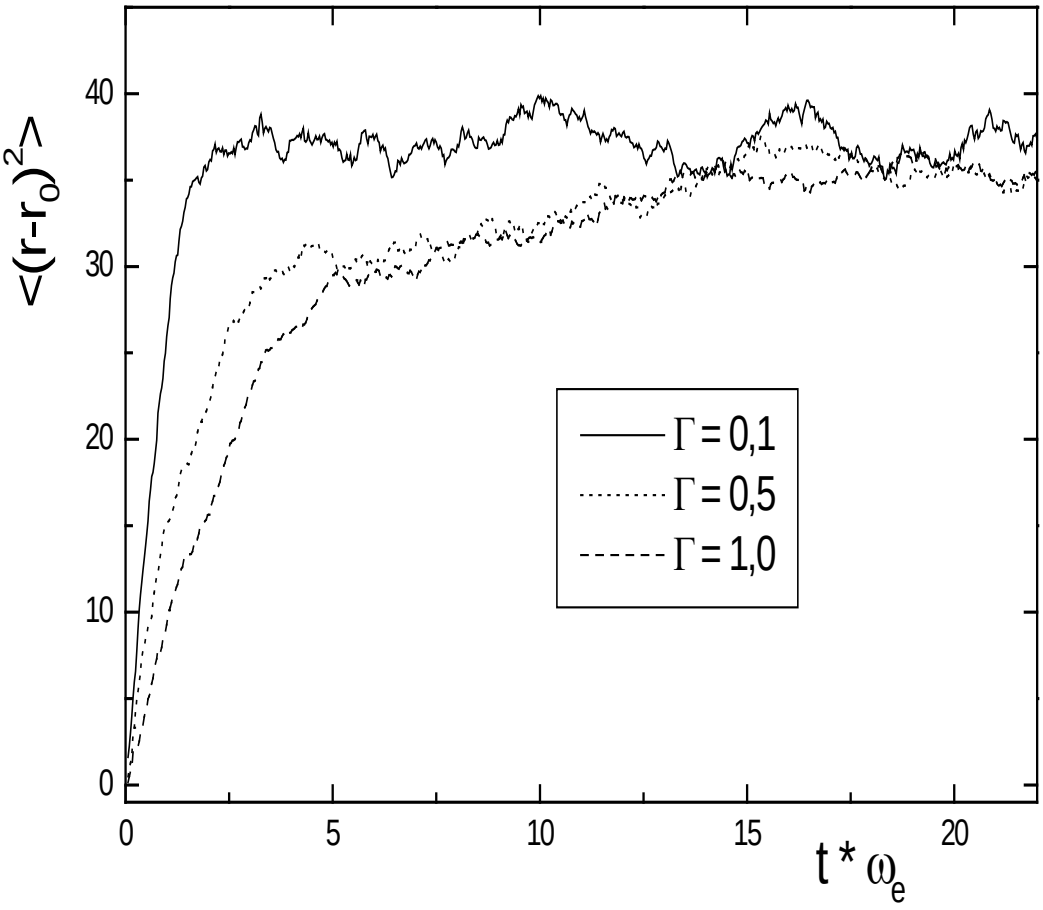

Figure 10.2 - Mean square displacements of coordinates as a function of dimensionless time at $r_S = 1$.

Relation between macroscopic (transport) coefficients and microscopic quantities in plasma. Basic principles of the Green-Kubo linear response theory

Using the microscopic states of the system we can estimate transport coefficients of plasma. For example, diffusion coefficient is calculated via mean square displacements of coordinates:

$$D = \lim_{t\to\infty} D(t) = \lim_{t\to\infty} \frac{\left\langle (\vec{r} - \vec{r}_0)^2 \right\rangle}{6(t - t_0)} \,. \tag{10.5}$$

In principal, knowing diffusion coefficient we can estimate another transport coefficients (for instance, by Onsager or Einstein relations).

Transport coefficients of plasma can be also obtained on the basis of the autocorrelation functions of microscopic dynamical variables. Relations between macroscopic (transport) coefficients and microscopic quantities in plasma are given by Green-Kubo linear response theory. According to this theory each macroscopic transport coefficient is defined by some microscopic dynamical variable (see, Table 10.1).

Table 10.1

The correspondence between microscopic dynamical variables and macroscopic transport coefficients of plasma

Dynamical variable	Transport coefficient
Velocity of particle - $\dot{\vec{r}}_i(t)$	Diffusion - D
Microscopic electric current $e\sum_i z_i \dot{\vec{r}}_i(t)$	Electrical conductivity - σ
Energy flux $\frac{d}{dt}\sum_i \vec{r}_i(t)E_i(t)$	Thermal conductivity - λ
Off-diagonal components of stress tensor $m\frac{d}{dt}\sum_i x_i(t)\dot{y}_i(t)$	Shear viscosity - η
Diagonal components of stress tensor $m\frac{d}{dt}\sum_i x_i(t)\dot{x}_i(t)$	Longitudinal viscosity $\frac{4\eta}{3}+\xi$

We can construct so-called Green-Kubo relations according to this table. For instance, diffusion coefficient is evaluated via velocity autocorrelation function as follows:

$$D = \frac{1}{3}\int_0^\infty \left\langle \vec{\upsilon}(0)\vec{\upsilon}(t)\right\rangle dt \,. \qquad (10.6)$$

An electrical conductivity is defined on the basis of the microscopic electrical current autocorrelation function by the following expression:

$$\sigma = const\int_0^\infty \left\langle \vec{j}(0)\vec{j}(t)\right\rangle dt \,. \qquad (10.7)$$

The basic principle of linear response theory for electrical conductivity of plasma can be explained as follows. Let plasma is located on the constant external electric field. Then in our system the electric current is induced, i.e. this current we can consider as a linear response to external perturbation (electric field). There is a direct proportionality between these quantities and they are related by well known Ohm's law:

$$\vec{j} = \sigma \vec{E}\,, \tag{10.8}$$

where the proportionality coefficient σ is the electrical conductivity [22].

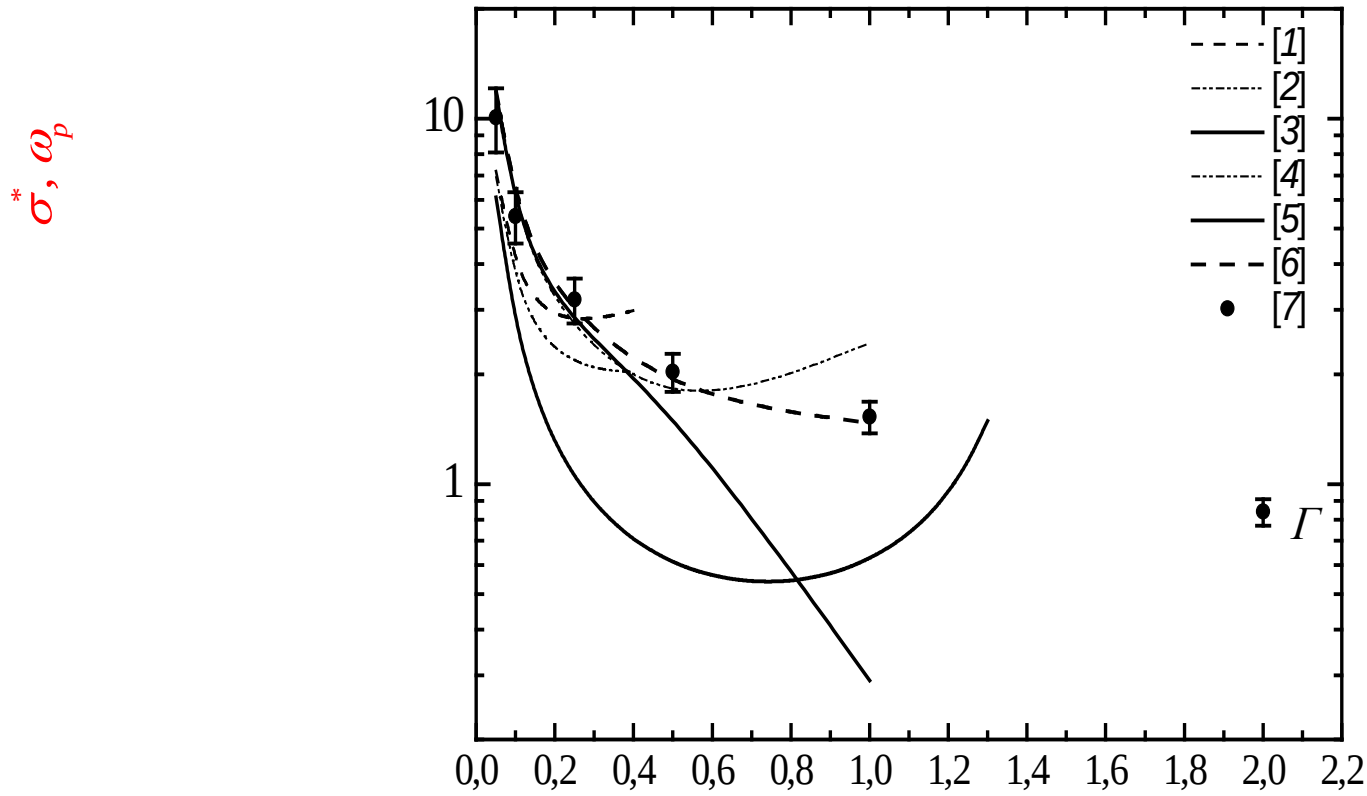

Figure 10.3 - Electrical conductivity of nonideal hydrogen plasma

1, 2 - T S Ramazanov, K N Dzhumagulova and A Zh Akbarov.//J. Phys. A: Math. Gen. **39** (2006) 4335.

3 - Spitzer theory

4 - Boercker D.B., Rogers F.J., DeWitt h.E.// Phys.Rev.A., 1982, v.25, p.1623.

5 - Baus Marc, Hansen Jean – Pierre, Sjogren Lenart. // Phys. Lett., V. 82A, № 4, 1980.

6 - Ishimaru S., Tanaka S.,// Phys. Rev., A.32, 1985, p. 1790.

7 – T.S.Ramazanov, G.Nigmetova, G.Roepke, R.Redmer. // J.Plasma Phys. 2006.

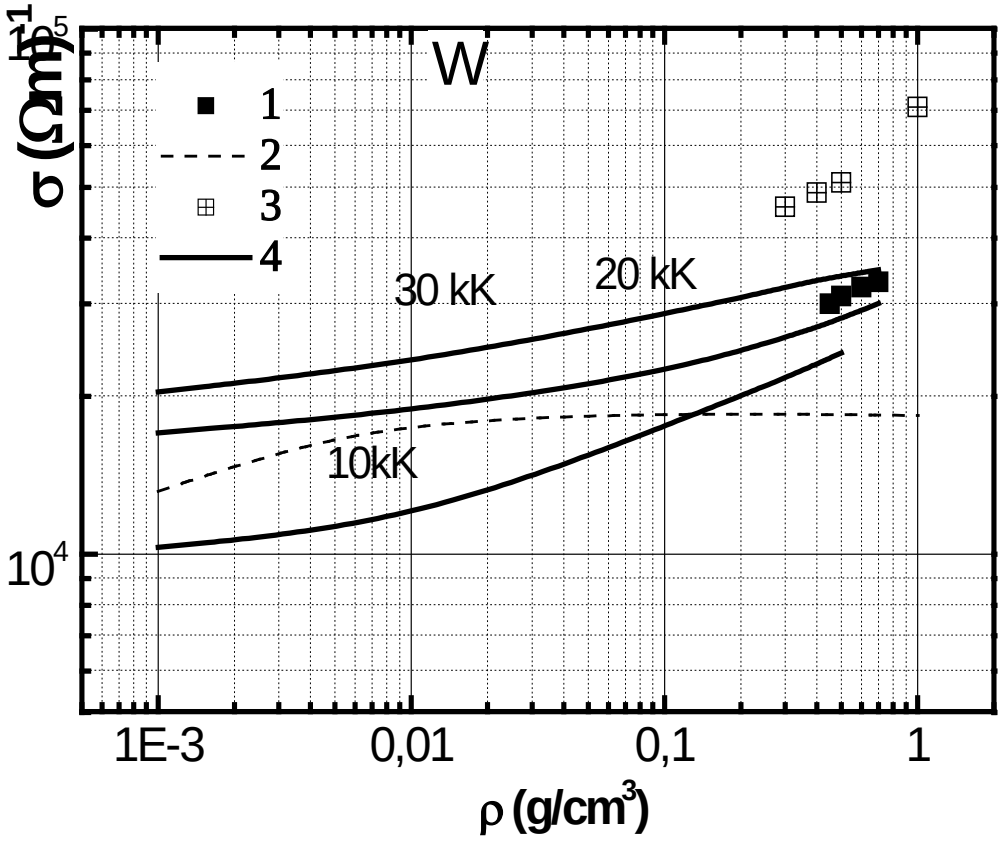

Figure 10.4 - Electrical conductivity of nonideal tungsten plasma

1 - Experiment: S. Saleem et al., Phys. Rev.E. Vol. 64. (056403)(2001) (for 20kK).
2 -Theoretical results for 20 kK of S. Kuhlbrodt, R. Redmer (Phys Rev. E – 2000. – vol. 62).
3 -Y.T. Lee and R.M. Moore.(Phys. Fluids 27, 1273 (1984)).
4 - Present work for different temperatures (T. Ramazanov, K. Galiyev, 2003).

Questions:
1. Autocorrelation functions (ACF) of microscopic quantities.
2. Properties of ACF.
3. Relation between macroscopic (transport) coefficients and microscopic quantities in plasma.
4. Basic principles of the Green-Kubo linear response theory.
5. Electrical conductivity on the basis of the microscopic electrical current autocorrelation function.

LECTURE 11

Optical Properties of Nonideal Plasmas

Introduction

The optical properties of plasma are also of great interest because the plasma radiation contains information concerning the temperature and concentration of particles, elastic and inelastic collisions, and ionization and recombination processes. Nowadays we have extensive data about optical properties of rarefied plasma where the elementary processes are easily separated. With increase of plasma density (at the weakly nonideal regime) we have such effects as a spectral line shift and broadening, as well as shift of photoionization continua. With a further increase of nonideality, these effects do not change in their behaviour but only increase quantitatively (we have so-called "spectroscopic stability"). At high density regime (in laser-condensed matter interaction, in pinched electric discharges, in dynamical experiments, etc.) the electron spectrum is deformed in highly compressed plasma.

Basic radiation processes in rarefied weakly ionized plasma

Let us introduce the basic concepts of the radiation theory. The spectral absorption coefficient κ_ν is determined in terms of the attenuation dI_ν which is experienced by the radiation intensity I_ν passing through a layer of matter of thickness dl:

$$dI_\nu = -\kappa_\nu I_\nu dl \tag{11.1}$$

In the case of thermodynamic equilibrium κ_ν is related to the radiation intensity I_ν by the following Kirchhoff's law:

$$I_\nu = \kappa_\nu B_\nu(T); \quad B_\nu(T) = 2h\nu^3 c^{-2}\left[\exp\left(\frac{h\nu}{k_B T}\right)-1\right]^{-1}, \tag{11.2}$$

where $B_\nu(T)$ is the Planck's function. The quantity $I_\nu d\nu$ is the energy emitted by volume dV per unit time in unit solid angle in the frequency interval $d\nu$.

The radiation processes in weakly nonideal plasma have been studied very well and can be divided into two groups:

1) Bound–bound transitions in atoms which provide a series of spectral lines. These lines converge at the photoionization thresholds.

2) Bound–free and free–free transitions which define the photoionization and bremsstrahlung processes with the continuous spectrum.

It should be noted that this division is not absolute, for instance, in strongly nonideal and high–pressure plasma the spectral lines are overlapped with the continuous spectrum.

The integrated intensity of the spectral line is defined by the oscillator strength $f_{nn'}$:

$$\int \kappa_\nu d\nu = \left(\pi e^2 / mc\right) f_{nn'} n_n , \qquad (11.3)$$

where κ_ν is the absorption coefficient in a spectral line due to the $n \to n'$ transition. n_n is the concentration of absorbing atoms.

According to (11.2) and (11.3) the integrated intensity of the spectral line is

$$I = \int I_\nu d\nu = \frac{2\pi h e^2}{m\lambda^3} \frac{g_n}{g_{n'}} \cdot n_{n'} f_{nn'} , \qquad (11.4)$$

where $n_{n'}$ is the concentration of radiating atoms; g_n and $g_{n'}$ are the statistical weights of the low–lying and high–lying states, respectively.

The oscillator strength of absorption line is defined by the Einstein probability of spontaneous transition:

$$f_{nn'} = \frac{g_{n'}}{g_n} \frac{mc^3}{8\pi^2 e^2 \nu^2} \cdot A_{n'n} \quad . \qquad (11.5)$$

The factor $A_{n'n}$ is equal to the inverse lifetime of an atom in the state n relative to the $n \to n'$ transition. The complete data for $f_{nn'}$ and $A_{n'n}$ are provided by special books (for instance, see Wiese W., et al. Atomic transitions probabilities. Washington, 1966).

For hydrogen–like atom we have the well known quaziclassical Kramers formula:

$$f_{n'n} = \frac{32}{3\pi\sqrt{3}} \frac{1}{(n')^5 n^3} \left[(n')^{-2} - n^{-2}\right]^{-3} = \frac{1{,}96}{(n')^5 n^3} \left(\frac{E_{n'} - E_n}{Z^2 Ry}\right)^{-3} , \qquad (11.6)$$

where $E_{n'}$ and E_n are the binding energies of the n'-th and n-th levels. In Kramers formula (11.6) the transition is considered between states with the main quantum numbers n' and n averaged over the remaining quantum numbers. The line spectral intensity fully depends on the absorption coefficient because the Planck function varies slightly within the line (see formula (11.2)). The dependence κ_ν on frequency ν is defined by the behaviour of the line broadening. In a rarefied (weakly nonideal) plasma, the line broadening is defined by radiation damping and the Doppler effect. The broadening in nonideal plasma is mainly defined due to the interparticle interactions.

Let us consider the bound–free and free–free transitions:

- Bound–free transitions in the field of an ion (recombination radiation):

$$A^+ + e \to A + h\nu\,. \tag{11.7}$$

- Free–free transitions in the field of the ion (bremsstrahlung in the field of the ion):

$$A^+ + e\left(\frac{m\upsilon_1^2}{2}\right) \to A^+ + e\left(\frac{m\upsilon_2^2}{2}\right) + h\nu\,. \tag{11.8}$$

- Free–free transitions in the field of the atom (bremsstrahlung in the field of the atom):

$$A + e\left(\frac{m\upsilon_1^2}{2}\right) \to A + e\left(\frac{m\upsilon_2^2}{2}\right) + h\nu\,. \tag{11.9}$$

In the case of absorption we distinguish the following transitions.

- Bound–free transitions in the field of ions (photoionization of atoms):

$$A + h\nu \to A^+ + e \tag{11.10}$$

- Free–free transitions in the field of the atom and ion (the expressions of (11.8) and (11.9)).
- Photodetachment of the electron (the absorption process):

$$A^- + h\nu \to A + e \tag{11.11}$$

- Photoattachment of the electron (the radiation process):

$$A + e \rightarrow A^{-} + h\nu \qquad (11.12)$$

It should be noted that the final (resultant) continuous spectra represent the superposition of several continua due to individual processes. Therefore, the determination and analysis of the resultant spectrum are a complicated problem.

In the case of plasma with developed ionization, the greatest contribution to the continuous spectrum intensity is made by free–free transitions of electrons in the fields of ions. The absorption coefficient, including the correction for stimulated radiation, is given by Kramers' formula:

$$\kappa_\nu = \frac{2\sqrt{2}e^6 Z^2}{3\sqrt{3\pi}c\hbar m^{3/2}\sqrt{k_B T}}\frac{g}{\nu^3} n_e n_i \left(1 - e^{-h\nu/k_B T}\right), \qquad (11.13)$$

where Z is the ion charge; g is the Gaunt factor.

L. Biberman and G. Norman (1967, UFN-Physics Uspekhi) developed an approximate calculation technique for the calculation of absorption and radiation coefficients in both free–free and bound–free transitions in the plasma of complex atoms and ions. This technique takes into account the following effects:

- The merging of spectral lines near the continuous spectrum boundary.
- The lowering of the ionization potential ΔI .
- The complex atoms are not hydrogen–like.

Optical properties of nonideal plasma

The influence of the interparticle interaction on the optical properties causes the well–known effects of spectral line broadening and shift. In the case of dense plasma, both broadening and shift effects are caused by the interaction between a radiating atom or ion and surrounding particles.

The scheme of calculating line broadening through the interaction of atoms with ions and electrons in weakly nonideal plasma is as follows (Baranger, 1962). The electric field generated by ions is assumed to be constant and the Stark broadening is determined for an atom in this field. The broadening of each Stark component is then calculated within the impact approximation. After that, the resultant distribution of intensity is averaged over all possible values of intensity of the ion microfield. In this case taking into account these effects for absorption coefficient we have the following expression:

$$\kappa_\nu = \kappa_0 \left[1 + \left((\nu - \nu_0) - \Delta^2\right) \Big/ \left(\delta/2\right)^2\right]^{-1}, \qquad (11.14)$$

where δ is the line width; Δ is the line shift; the absorption coefficient at the line center is $\kappa_0 = (8\pi)^{-1}\lambda^2(g_2/g_1)A_{21}n_1(2/\pi\delta)$; λ is the radiation wavelength; n_1 is the number density of absorbing atoms.

The shift and width of spectral line are expressed in terms of the amplitude of elastic forward scattering $f(0)$:

$$\Delta = -\frac{h}{m}n_e \,\mathrm{Re}\left[f(0)\right]_{av}; \quad \delta = \frac{h}{m}n_e \,\mathrm{Im}\left[f(0)\right]_{av} = \frac{1}{2}n_e(\upsilon_e q_{tot})_{av}, \quad (11.15)$$

where q_{tot} is the total scattering cross section.

As a rule the Holtsmark distribution of ion microfields is used for calculation of the absorption coefficient in lines. On the other hand it is known that the Holtsmark distribution is valid for rarefied weakly nonideal plasma. Therefore it should be noted that nowadays the systematic studies have not yet been performed with taking into account the effect of strong nonideality on the spectral lines. For this purpose it is necessary to use the adequate microfield distribution functions which take into account both quantum and screening effects in dense (nonideal) plasma and results of recent experiments (Griem, 2000).

Figure 11.1 represents the spectral absorption coefficient of air plasma. The broken line indicates the contribution made by continua. With increasing the density, the lines broaden considerably and merge to form quasi–continua, thus making significant contribution to the integral optical characteristics.

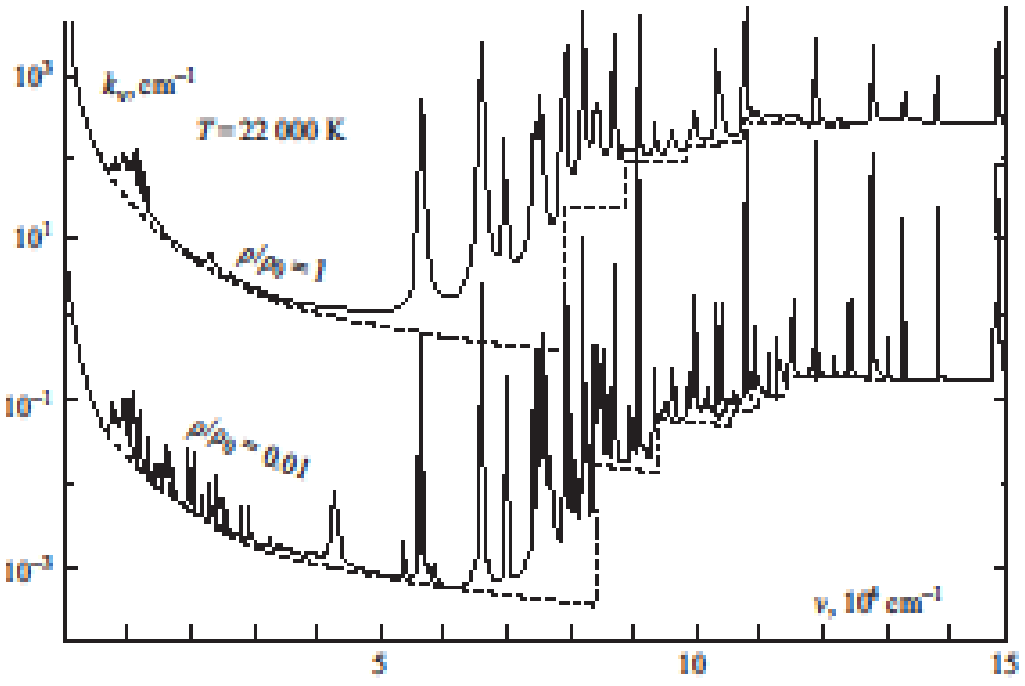

Figure 11.1 - The absorption coefficient of air plasma for $T = 2,2 \cdot 10^4 K$ at two values of relative density ρ / ρ_0; ρ_0 is the normal density of air.

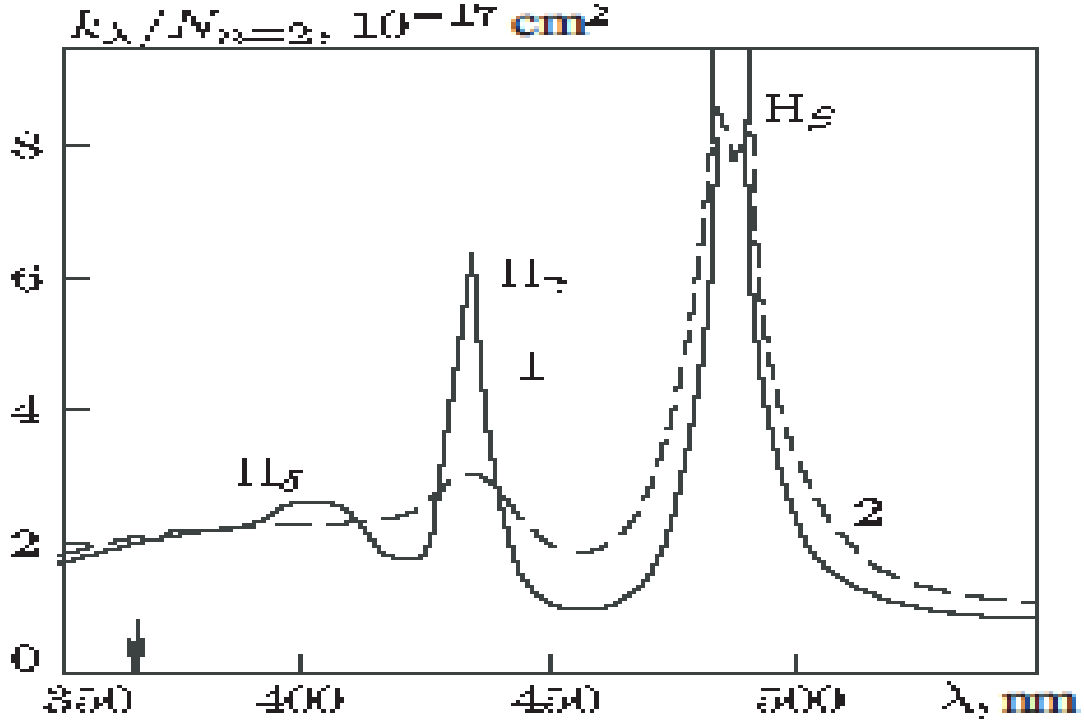

Figure 11.2 - The absorption coefficient of the Balmer series per single absorbing atom as a function of wavelength λ (Guenter et al. 1985). Experimental results: 1 - $n_e = 1,7 \cdot 10^{17} sm^{-3}$; $T = 1,6 \cdot 10^4 K$; 2 - $n_e = 8,4 \cdot 10^{17} sm^{-3}$; $T = 2,22 \cdot 10^4 K$.

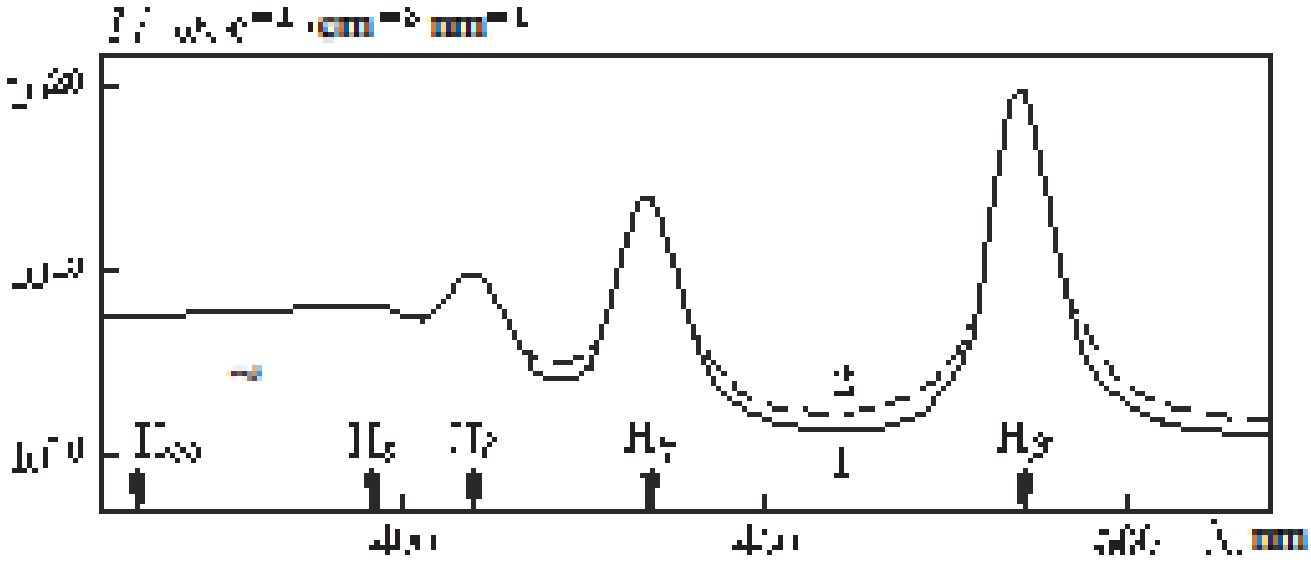

Figure 11.3 - The radiation spectrum of hydrogen plasma. $n_e = 9,3 \cdot 10^{16} sm^{-3}$; $T = 1,41 \cdot 10^4 K$. Solid line is the experimental data (Wiese et al., 1972). Dashed line represents the theoretical results of D'yachkov et al., 1987.

Questions:
1. Basic radiation processes in rarefied weakly ionized plasma.
2. Bound–bound transitions.
3. Bound–free.
4. Free–free transitions.
5. Optical properties of nonideal plasma.

LECTURE 12

Basic Concepts of Nonideal Dusty Plasma

Introduction

Dusty plasma is the system consisting of the plasma's particles as well as of macropaticles of condensed matter. Other terms used for such systems are "complex plasmas", "colloidal plasmas" and "plasmas with a condensed disperse phase". Such system is strongly coupled and forms liquid–like and crystal–like structures. Dusty plasma occurs in the nature and in many laboratory and technological devices.

Charging of dust particles in plasmas

It should be noted that dust particles immersed in plasma acquire an electric charge and can be considered as additional charged component (see Figure 12.1). Therefore, the properties of dusty plasmas are much more diverse in comparison with the ordinary multicomponent plasmas consisting of electrons and different types of ions. The dust particles can be considered as recombination centres for plasma electrons and ions and as sources of electrons (thermo-, photo-, and secondary electron emission). It means that the dust component can significantly influence the plasma ionization balance. It should be also added that the dust particle charge is not fixed, but is determined by the surrounding plasma parameters and can fluctuate even for constant plasma parameters.

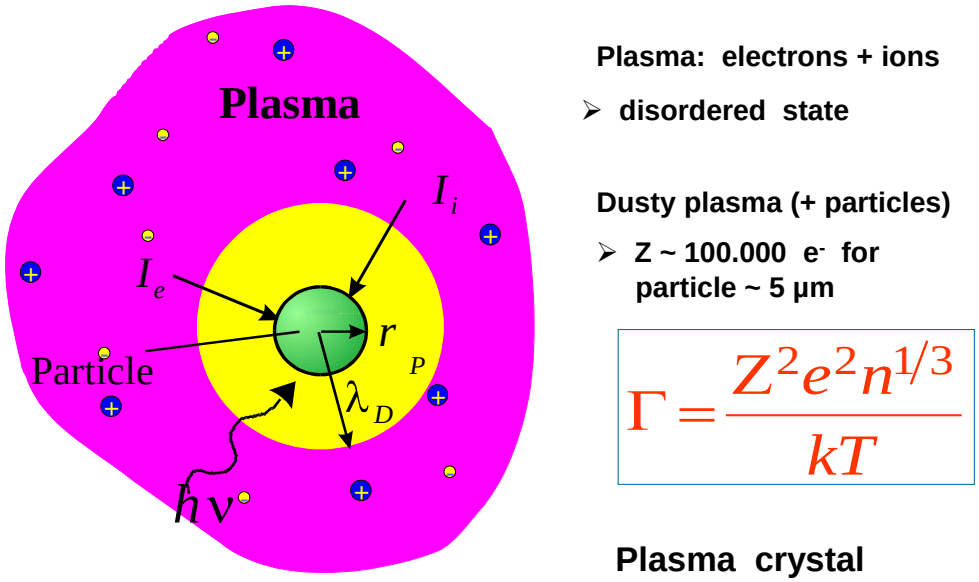

Figure 12.1 - The schematic representation of dusty plasma.

At the present time we can mention the following important directions in the study of dusty plasma properties:

- formation of ordered structures, including crystallization and phase transitions in the dust subsystem;
- elementary processes in dusty plasmas: charging of dust for different plasma and particle parameters;
- interactions between the particles, external forces acting on the particles;
- linear and nonlinear waves in dusty plasmas (solitons, shock waves, Mach cones), their dynamics, damping and instability.

There are four mechanisms for charging of dusty particles in plasma (see Figure 12.2):

1) Capturing of electrons. In this case we have the following plasma parameters: $P = 0,1 \div 2\, torr$ is the pressure; $T_e = (1 \div 8)10^4 K$ is the temperature of electrons; $T_i = 300K$ is the temperature of ions; $n_e = 10^8 \div 10^{10} cm^{-3}$ is the electron density number; $Z = (10^4 \div 10^5)e$ is the charge of dusty particles; $\Gamma = 10^4 \div 10^6$ is the coupling parameter.

2) Thermal-electron emission. The plasma parameters for this case are as follows: $n_e \sim n_i = 10^9 \div 10^{12} cm^{-3}$ is the density number of electrons and ions; $n_d = 10^4 \div 10^7 cm^{-3}$ is the density number of dusty particles; $Z = (10^2 \div 10^3)e$ is the charge of dusty particles; $\Gamma \le 120$.

3) Photo-electron emission. By this mechanism the following plasma parameters can be realized: $P = 0,01 \div 40\, torr$ is the pressure; $T_i \approx T_n = (300 \div 400)K$ is the temperature of ions; $n_d = 10^2 \div 10^3 cm^{-3}$ is the density number of dusty particles; $Z = (10^3 \div 10^4)e$ is the charge of dusty particles; $\Gamma \sim 10^4$.

4) Radioactive generated plasma. In this case we can reach the following plasma parameters: the fission energy is $E_f = (5 \div 100)MeV$; the energy of beta decay is $E_\beta = 100keV$; $Z = (10^2 \div 10^3)e$ is the charge of dusty particles; $\Gamma \sim 100$.

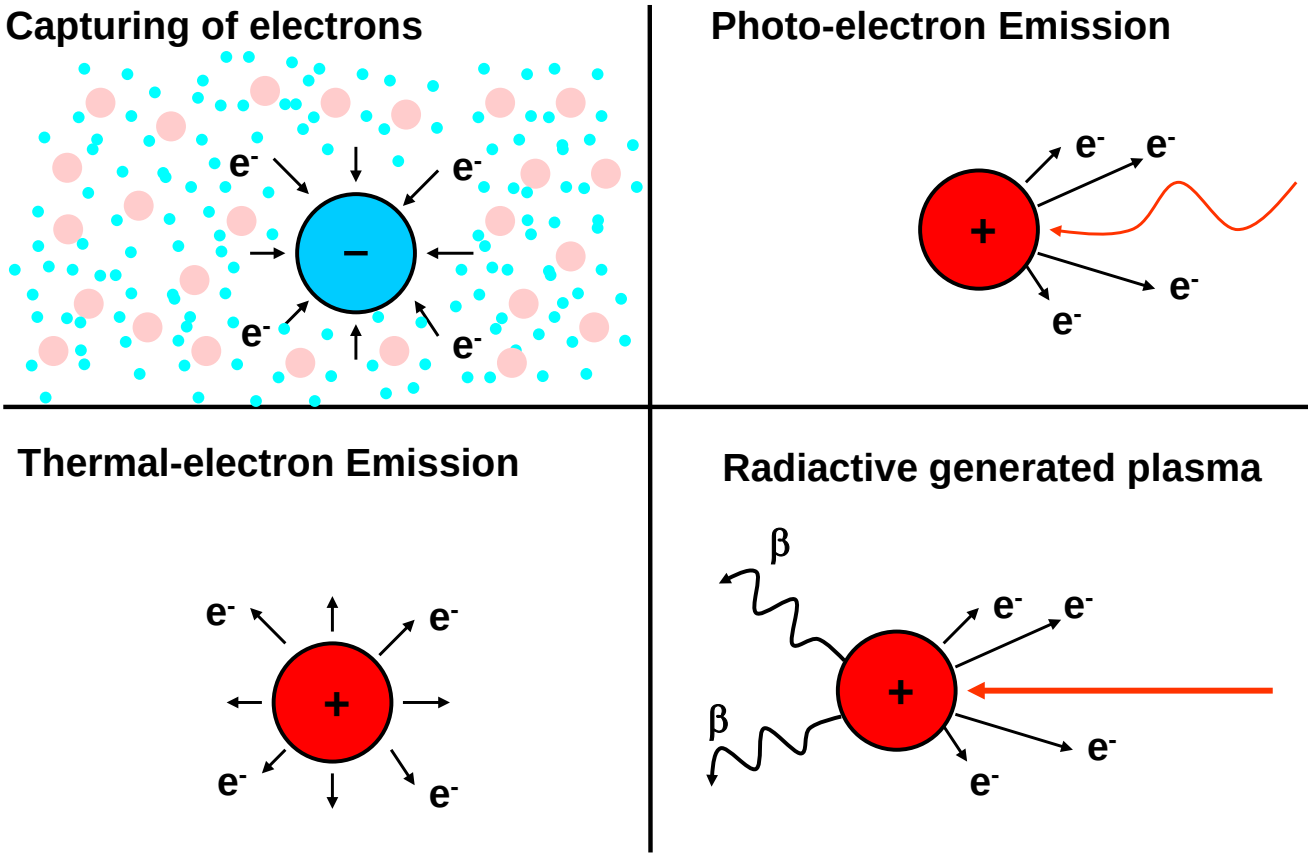

Figure 12.2 - The different charging mechanisms of dusty particles in plasma

The photo of dusty particles obtained by electronic micrography is presented in the Figure 12.3. As one can see it looks as "cauliflower".

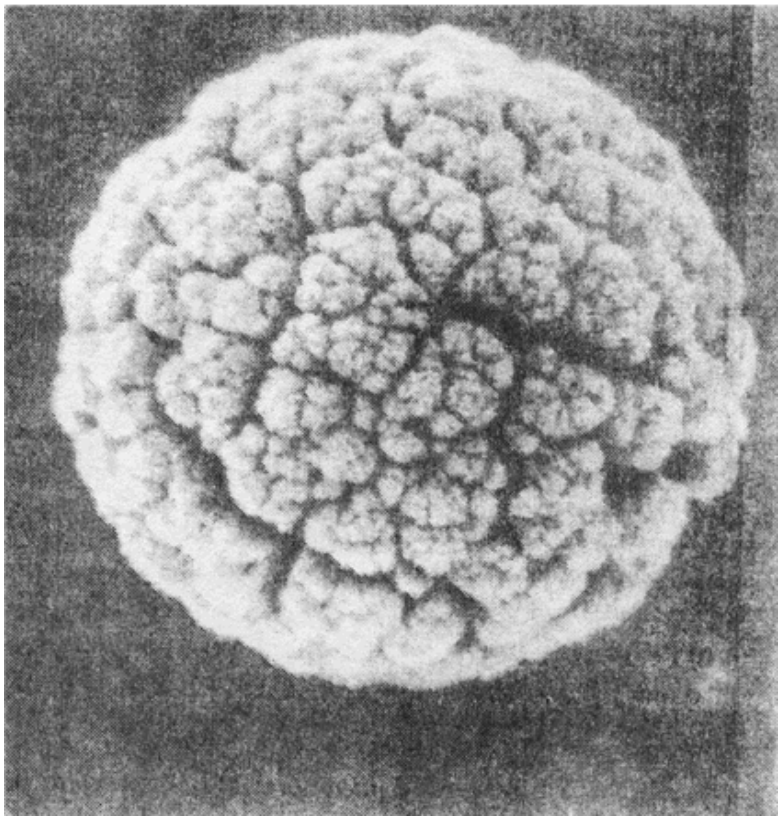

Figure 12.3 - Photo of dusty particle was formed in RF discharge (15 MHz, 1 Torr) and obtained by electronic micrography (A. Garscadden et al., 1994) ("Cauliflower")

Some peculiarities of dusty plasma. OML theory

Let us represent some peculiarities about specific processes in dusty plasma.

- If the dusty particle charge in the unit volume is more than the charge of free electrons, i.e. $n_d Z_d / n_e \geq 1$, then the collective influence of particle-grain interaction on plasma processes is significant.
- The charge of dusty particles is the variable quantity and depends on parameters of surrounding medium.
- The screening of electrical field of dusty particles is realized at the following Debye radius:

$$\frac{1}{D^2} = \frac{1}{d_e^2} + \frac{1}{d_i^2}, \qquad (12.1)$$

where d_e , d_i are the Debye radii of electrons and ions, respectively. Since in many experiments the condition $d_i << d_e$ is realized, then the screening process is

defined by the radius of ions and the linear size of dusty particles satisfies the following condition $a << D$.

- In order to consider the dust component as the additional component of plasma it is necessary to realize the following condition for particles in Debye's sphere of dusty particles.

$$N_d = \frac{4\pi}{3} n_d D^3 >> 1. \qquad (12.2)$$

In this case the resulting Debye's radius is defined as follows:

$$\frac{1}{r_D^2} = \frac{1}{d_e^2} + \frac{1}{d_i^2} + \frac{1}{D^2}. \qquad (12.3)$$

It should be noted that if the distance between dusty particles is more than r_D then the interaction between macroparticles is non-Coulomb.

- Due to the high rate of dissipation, the plasma particle's fluxes recombined on dusty particles must be supported by external sources. Since the dusty plasma is the open system the probability of ordered structures formation in such system is high.

Orbit motion limited (OML) approximation. In order to describe particle charging in gas discharge plasmas some methods are used. One of the most frequently used approaches is the orbit motion limited (OML) theory. According to this theory the cross–sections for electron and ion collection by the dust particle are determined only from the laws of conservation of energy and angular momentum. The conditions of applicability of the OML theory are formulated in the following form:

$$a >> r_D >> l_{i(e)}, \qquad (12.4)$$

where $l_{i(e)}$ is the mean free path of the ions (or electrons). It is also assumed that the dust particle is isolated and other dust particles do not affect the motion of electrons and ions in its vicinity.

In the OML theory it is assumed that the electrons and the ions are collected if their trajectories cross or graze the particle surface. In this case the corresponding velocity–dependent cross–sections are given by the following expressions:

$$\sigma_e(\upsilon)=\begin{cases}\pi a^2\left(1+\dfrac{2e\varphi_s}{m_e\upsilon^2}\right), & \dfrac{2e\varphi_s}{m_e\upsilon^2}>-1\\ 0, & \dfrac{2e\varphi_s}{m_e\upsilon^2}<-1,\end{cases}$$
$$\sigma_i(\upsilon)=\pi a^2\left(1-\frac{2e\varphi_s}{m_i\upsilon^2}\right) \qquad (12.5)$$

where m_e and m_i are the mass of electrons and ions, respectively; υ is the velocity of the electrons and ions relative to the dust particle; the surface potential φ_s of the dust particle is negative and the ions are singly charged.

Knowing the corresponding cross–sections and velocity distribution functions $f_{e(i)}(\upsilon)$ the electron and ion fluxes to the particle surface can be determined by the following integration:

$$I_{e(i)}=n_{e(i)}\int\upsilon\sigma_{e(i)}(\upsilon)f_{e(i)}(\upsilon)d^3\upsilon\,. \qquad (12.6)$$

If we use the Maxwellian velocity distribution of plasma particles:

$$f_{e(i)}=\left(2\pi\upsilon_{T_{e(i)}}^2\right)^{-3/2}\exp\left(-\frac{\upsilon^2}{2\upsilon_{T_{e(i)}}^2}\right), \qquad (12.7)$$

where $\upsilon_{T_{e(i)}}=\sqrt{k_BT_{e(i)}/m_{e(i)}}$ is the electron (ion) thermal velocity, then integration in equation (12.6) using (12.5) and (12.7) gives the following expressions for electron and ion fluxes:

$$I_e=\sqrt{8\pi}a^2n_e\upsilon_{T_e}\exp\left(e\varphi_s/k_BT_e\right),$$
$$I_i=\sqrt{8\pi}a^2n_i\upsilon_{T_i}\exp\left(1-e\varphi_s/k_BT_i\right). \qquad (12.8)$$

It should be noted that the stationary potential of the dust particle surface (floating potential) is determined by the balance of electron and ion fluxes collected by the particle:

$$I_e=I_i\,. \qquad (12.9)$$

The range of existence of nonideal dusty plasma (in nature, laboratory and technology)

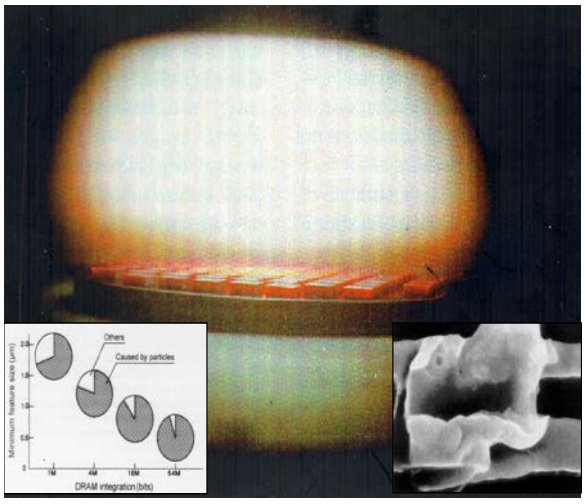

Microelectronic devices with plasma technology

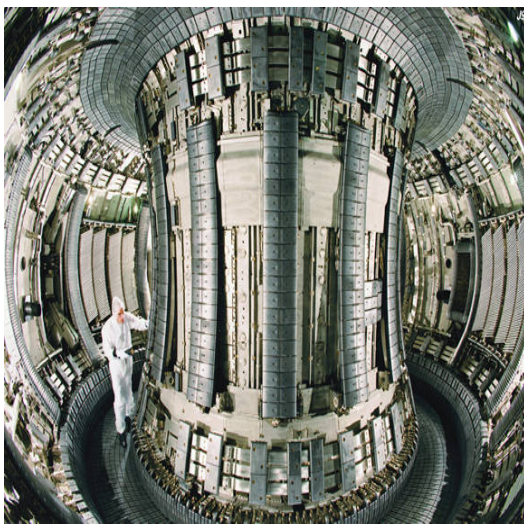

Thermonuclear devices

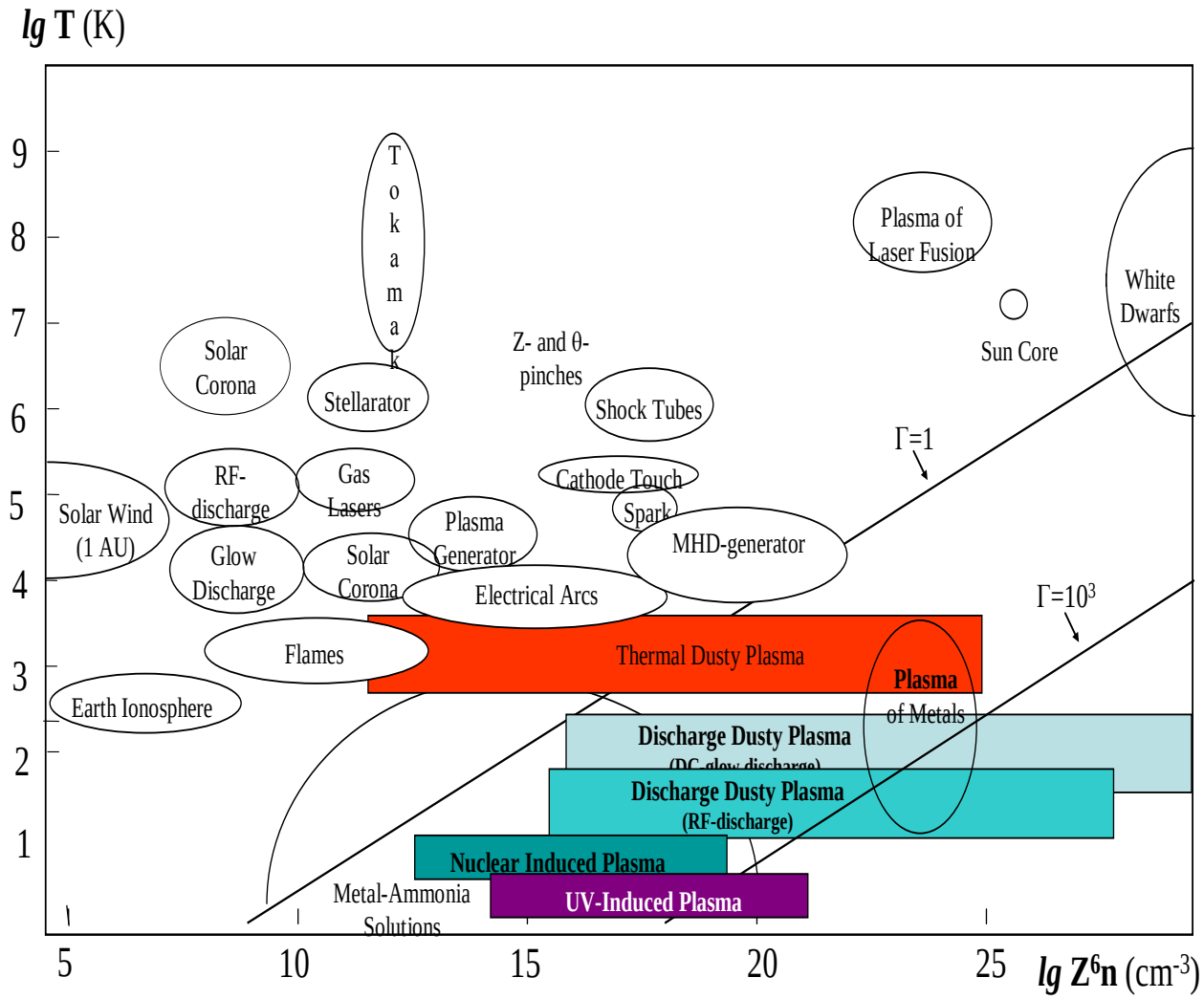

Questions:

1. Charging of dust particles in plasmas.
2. Mechanisms for charging of dust particles in plasma.
3. Some peculiarities of dusty plasma.
4. OML theory.
5. The range of existence of nonideal dusty plasma.

LECTURE 13

Basic Concepts of Nonideal Dusty Plasma (continuation)

Electrostatic potential around a dust particle

The distribution of the electrostatic potential $\varphi(r)$ around an isolated spherical dust particle of charge Z_d in isotropic plasma satisfies the Poisson equation:

$$\Delta\varphi = -4\pi e(n_i - n_e)\,. \tag{13.1}$$

with the boundary conditions $\varphi(\infty) = 0$ and $\varphi(a) = \varphi_s$. The potential is connected to the particle charge according to the following relation:

$$\left.\frac{d\varphi}{dr}\right|_{r=a} = -\frac{Z_d e}{a^2}\,. \tag{13.2}$$

In the case of plasma with a Boltzmann distribution of electrons and ions, where the condition $\left|e\varphi_s / k_B T_{e(i)}\right| < 1$ is satisfied, we can linearize the right–hand side of Eq. (13.1) and have the following expression for $\varphi(r)$:

$$\varphi(r) = \varphi_s \cdot \frac{a}{r}\exp\left(-\frac{r-a}{r_D}\right), \tag{13.3}$$

where in this case $r_D^{-2} = d_e^{-2} + d_i^{-2}$. The surface potential is connected to the charge through the formula $\varphi_s = \dfrac{Z_d e}{a}\left(1 + a / r_D\right)$. For the case $a << r_D$, the expression for the potential distribution can be written in the following form:

$$\varphi(r) = \frac{Z_d e}{r}\exp\left(-\frac{r}{r_D}\right). \tag{13.4}$$

It should be noted that the potential (13.4) is the screened Coulomb potential which is often applied to describe the electrostatic interaction between the particles in

dusty plasmas. In different physical systems this form of the potential is also known as the Debye–Hueckel or Yukawa potential.

Main forces acting on dust particles in plasmas

Notice that the main forces acting on dust particles in plasmas can be conveniently divided into two groups:

- the forces which do not depend on the particle charge (force of gravity, neutral drag force, thermophoretic force):
- the forces which depend directly on the particle charge (electrostatic force and the ion drag force).

The gravitational force. The gravitational force is determined by the following expression:

$$F_g = m_d g \,, \tag{13.5}$$

where g is the gravitational acceleration. The gravitational force is proportional to the particle volume, i.e. $F_g \sim a^3$.

The neutral drag (friction, resistance) force. In the case of weakly ionized plasma, the main contribution to this resistance force comes from the neutral component. The two regimes which are determined by the Knudsen number $Kn = l_n / a$ should be distinguished. Here l_n, a are the atomic or molecular free path and the size of dust particles, respectively. In the case $Kn << 1$ (the hydrodynamic regime) the resistance force is determined by the Stokes expression:

$$F_n = -6\pi\eta a u \,, \tag{13.6}$$

where η is the neutral gas viscosity and u is the particle velocity relative to the neutral gas. In the opposite limiting case of $Kn >> 1$ (the free molecular regime) and for sufficiently small relative velocities ($u \sim \upsilon_{T_n}$) we have the following formula:

$$F_n = -\frac{8\sqrt{2\pi}}{3}\delta a^2 n_n T_n \frac{u}{\upsilon_{T_n}} \,, \tag{13.7}$$

where n_n and T_n are the concentration and temperature of the neutrals; δ is a coefficient of the order of unity that depends on the exact processes proceeding on

the particle surface. In the case of high relative velocities ($u \sim \upsilon_{T_n}$) the neutral drag force is determined as follows:

$$F_n = -\pi a^2 n_n m_n u^2 , \tag{13.8}$$

where m_n is the mass of neutrals.

The thermophoretic force. If a temperature gradient takes place in a neutral gas, then the particle experiences a force directed opposite to this gradient, i.e. in the direction of lower temperatures. It is connected with the fact that the larger momentum is transferred from the neutrals coming from the higher temperature region.

$$F_{th} = -\frac{4\sqrt{2\pi}}{15}\frac{a^2}{\upsilon_{T_n}}\kappa_n \nabla T_n \ , \tag{13.9}$$

where κ_n is the thermal conductivity coefficient of the gas.

The electrostatic force. The electrostatic force acting on conducting charged particles is given by the following formula:

$$\vec{F}_{el} = Z_d e \vec{E}_{eff} \ , \tag{13.10}$$

where an effective electric field can be expressed as:

$$\vec{E}_{eff} = \vec{E}\left[1 + \frac{(a/r_D)^2}{3(1+a/r_D)}\right]. \tag{13.11}$$

Plasma polarization induces a dipole moment of dust particles $\vec{p} \approx a^3 \vec{E}_{eff}$ directed along the field. In the nonuniform electric field the force acting on dipole has the following form:

$$\vec{F}_{dp} = (\vec{p}\nabla)\vec{E} \ . \tag{13.12}$$

Ion drag force. If we have a drift of ions (electrons) relative to the dust particle, then there is a force connected with the momentum transfer from the plasma to the dust particle. Due to the larger ion mass, the effect associated with the ions typically

dominates; therefore, this force is called "ion drag force". The ion drag force is connected with two processes: momentum transfer from the ions that are collected by the particle (non-elastic scattering) and momentum transfer from the ions that are elastically scattered in the electric field of the particle.

In the general case the formula for the ion drag force is written as:

$$\vec{F}_I = m_i n_i \int \vec{v} f_i(\vec{v}) \sigma_i^{tr}(\upsilon) \upsilon d\vec{v} \,, \qquad (13.13)$$

where $f_i(\vec{v})$ is the ion velocity distribution function and $\sigma_i^{tr}(\upsilon)$ is the momentum transfer cross–section for ion collisions with the dust particle.

It should be noted that at the present time most of the results have been obtained for binary collision (BC) approximations, i.e. for the case **of collisionless ions** with "isolated" dust particles.

Questions:

1. Electrostatic potential around a dust particle.
2. Main forces acting on dust particles in plasmas.
3. Forces which do not depend on the particle charge.
4. Forces which depend directly on the particle charge.
5. Drift of ions (electrons).

REFERENCES

1 Spitzer L.F. Physics of full ionized gas. - M. IL, 1957. - P. 112.

2 N.H. March Bound-state Slater sum for a bare Coulomb field derived from s-states alone // Phys. Let. A. - 1985. - Vol. 111, № 1-2. - P. 47-48.

3 Deutsch C., Combert M.M. Diffraction corrections to equilibrium properties of the classical electron gas. Pair correlation function // J. Math. Phys. - 1976. - Vol. 17, № 7. - P. 1077-1090.

4 Ramazanov T.S., Dzhumagulova K.N., Effective screened potentials of strongly coupled semiclassical plasma // Phys. Plasmas. - 2002. - Vol. 9. - P. 3758.

5 Ramazanov T.S., Dzhumagulova K.N., Gabdullin M.T. Ion-ion interactions potential and potentials for partially ionized plasma // Phys.Plasmas. - 2010. - Vol. 17. - 042703.

6 Redmer, R. Electrical conductivity of dense metal plasmas // Phys. Rev. E. - 1999. - Vol. 59, № 1. - P. 1073-1081.

7 Ramazanov, T.S., Dzhumagulova, K.N., Omarbakiyeva, Yu.A. Effective polarization interaction potentials «charge-atom» for the partially ionized dense plasma // Phys.Plasmas. – 2005. - Vol.12. - 092702.

8 Ebeling W., Kraeft W. D., Kremp D. Theory of Bound States and Ionization Equilibrium. - Berlin: Akademie-Verlag, 1976. - P. 325.

9 Fortov V.Ye., Yakubov I.T. Physics of nonideal plasma. - M.: Atomenergoizdat, 1994. - P. 368.

10 Kulik P.P., Ryabyi V.A., Ermpkhin N.V. Nonideal plasma. - M.: Energoatomizdat, 1983. - P. 199.

11 Zeldovich Ya.B., Raizer Yu.P. Physics of shock-waves compressions and high temperature hydrodynamic phenomena. - M.: Scince, 1966. - P. 688.

12 Da Silva, L.B., Celliers, P., Collins, G.W., Budil, K.S., Holmes, N.C., Barbee, Jr.T.W., Hommel, B.A., Kilkenny, J.D., Wallance, R.J., Ross, M., Cauble, R., Ng, A., Chiu, G. Absolute Equation of State Measurements on Shocked Liquid Deuterium up to 200 GPa (2Mbar) // Phys. Rev. Lett. - 1997. - Vol. 78. - P. 483.

13 Mintsev, V.B., Fortov, V.E. Dense plasma properties from shock wave experiments // J. Phys. A: Math. Gen. - 2006. - Vol. 39. - P. 4319-4327.

14 Ramazanov, T.S., Dzhumagulova, K.N., Gabdullin, M.T. Microscopic and thermodynamic properties of dense semiclassical partially ionized hydrogen plasma // J. Phys. A: Math. Gen. - 2006. - Vol. 39. - P. 249-253.

15 Iyetomi, H., Utsumi, K., Ichimaru, S. Screening effects of degenerate electron background in high density plasmas. I: Tthermodynamic properties // J. Phys. Soc. Jap. - 1981. - Vol. 50. - P. 3769.

16 Pierleoni, C., Margo, W.R., Ceperley, D.M., Bernu, B. Path integral Monte-Carlo simulation of hydrogen plasma // Physics of Strongly Coupled Plasma / ed. W.D. Kraeft, M. Shlanges. - London: World Scientific NJ., 1996. - P. 11-26.

17 Ramazanov, T.S., Baimbetov, F.B., Bekenov, M.A., Redmer, R., Röpke, G. Correlation functions and equation of state of strongly coupled hydrogen plasma in HNC approximation // In: Strongly Coupled Coulomb Systems / ed. G. Kalman, M. Romel, K. Blagoev. - NY.: Plenum Press., 1998. - P.236.

18 Ramazanov T.S., Dzhumagulova K.N., Gabdullin M.T., Akbar A.Zh. and Redmer R., J. Phys. A: Math. Theor. - 2009. - Vol.42. - 214049.

19 Kuhlbrodt S., Redmer R., Phys. Rev. E. - 2000. - Vol.62. - P. 719.

20 Kerley G.I., J. Chem. Phys. – 1996. – Vol. 85, № 9. P. - 5228-5231 (1986).

21 Potekhin A.Y., Massacrier G., Chabrier G., Phys. Rev. E. – 2005. – Vol. 62. – P. 046402.

22 T S Ramazanov, K N Dzhumagulova and A Zh Akbarov.//J. Phys. A: Math. Gen. 39 (2006) 4335.

Questions

1. The definition of nonideal plasma and criteria of nonideality.
2. Existence of nonideal plasmas.
3. Interparticle interactions in the case of fully ionized plasma.
4. Screening and quantum effects.
5. The interaction between isolated classical atoms and charges in partially ionized nonideal plasma.
6. The screening and quantum effects in “charge-atom” interactions for partially ionized nonideal plasma. Neutral and compound particles in plasma.
7. The range of existence and the classification of states of nonideal plasma. Nonideal plasma in the nature and its scientific and technical applications.
8. Electrical methods of nonideal plasma generation.
9. Dynamical methods of nonideal plasma generation.
10. One component plasma (OCP). Structural and thermodynamic properties of OCP.
11. The confined atom model for multicomponent plasma.
12. Definition of the plasma composition in equilibrium state. The Saha equation for ideal plasma.
13. The Saha equation for nonideal plasma. The lowering of ionization potential.
14. Composition of a nonideal plasma on the basis Debye approximation.
15. Composition of a semiclassical nonideal plasma.
16. Ionization of plasma by pressure. Mott transition.
17. Chemical plasma model. Physical plasma model.
18. Structural and thermodynamic properties of nonideal plasma by Monte Carlo method.
19. Electrical conductivity of weakly ionized plasma in the Lorentz approximation.
20. Electrical conductivity of strongly ionized weakly nonideal plasma. The Spitzer formula. The Coulomb logarithm for a plasma.
21. The electrical conductivity of nonideal plasma. The Chapman-Enskog method.
22. Integral equations in statistical physics.
23. The Ornstein-Zernike equation for OCP. HNC and PI approximations.
24. The Ornstein-Zernike equation for multi-component plasma. The computational scheme.
25. Microscopic and transport properties of nonideal plasma by molecular dynamic method.
26. Optical properties of nonideal plasma. The basic radiation processes in plasma.

27. Nonideal dusty plasma. Basic principles and charging types of macroparticles.

28. The peculiarities of interaction between macroparticles in dusty plasma and formation of dust-plasma structures.

29. Basic forces acting on dusty particles in plasma. Phase diagram.

30. Determination of the basic parameters and structure characteristic of a dusty plasma.

Educational issue

Ramazanov T.S.
Gabdullin M.T.

PHYSICS OF NONIDEAL PLASMAS

Educational manual

Editor
Typesettingand
cover design*G. Kaliyeva*

IP №

Signed for publishing 15.03.2016.Format 60x84$^{1}/_{12}$. Offset paper.
Digital printing. Volume 6,62 printer's sheet. copies. Order №.
Publishing house «Kazakh University»
Al-Farabi Kazakh National University
KazNU, 71 Al-Farabi, 050040, Almaty

Printed in the printing office of the «Kazakh University» publishing house